PHYSICAL CONTROLS ON LAND-WATER LINKAGES: CARBON CYCLING AND FOOD WEBS IN BOREAL WATERSHEDS

Adrianne P. Smits

A dissertation submitted in partial fulfillment of the
requirements for the degree of
Doctor of Philosophy

University of Washington
2016

Reading Committee:
Daniel E. Schindler, Chair
Gordon W. Holtgrieve
Michael T. Brett

Program Authorized to Offer Degree:
School of Aquatic and Fishery Sciences

© 2016

Adrianne P. Smits

University of Washington

Abstract

Physical Controls on Land-Water Linkages:
Carbon Cycling and Food Webs in Boreal Watersheds

Adrianne P. Smits

Chair of the Supervisory Committee:
Professor Daniel E. Schindler
School of Aquatic and Fishery Sciences

Aquatic ecosystem responses to changing climate and land-use are often extremely heterogeneous across landscapes: studies than quantify relationships between watershed features and biogeochemical and food web processes at intermediate scales (e.g., watershed-scale) would provide a means to extrapolate local findings across landscapes, potentially aiding future management efforts. I investigated how watershed features influence the movement of materials and energy between aquatic and terrestrial environments. I worked in a nearly pristine boreal river system in southwest Alaska (Wood River), where a high level of physical heterogeneity, coupled with natural landscape gradients, provided an opportunity to explore watershed geomorphic controls on ecosystem processes in streams.

In Chapter 2 I used fatty acid biomarkers as novel tracers of food web pathways to assess how assimilation of heterotrophic bacteria and algae by stream insects varied across a landscape gradient in watershed features. I found that watershed features such as mean slope are correlated

with the energetic base of food webs in boreal streams, with algal resources more important in steep streams and bacterial resources more important in flat watersheds. In Chapter 3 I used fatty acid and stable isotope tracers, coupled with several years of growth data, to investigate how stream thermal regimes affected the ability of juvenile coho salmon (*Oncorhynchus kisutch*) to benefit from marine resource subsidies (sockeye salmon eggs). I found that local environmental conditions (mean summer stream temperature) were a stronger control on fish growth than the magnitude of the resource subsidy, but also that individuals varied substantially in their metabolic responses to an energy-rich food source.

In Chapter 4 I examined geomorphic controls on the magnitude and sources of stream CO_2 emissions from boreal streams. I found that watershed slope interacts with precipitation events to control terrestrial carbon fluxes into and out of streams. Watershed slope influences C loading and stream CO_2 fluxes by determining the amount of carbon accumulation in watersheds, and to a lesser extent by determining gas transfer velocity across the air-water interface. These patterns provide a way to extrapolate across boreal landscapes by constraining CO_2 concentration and flux estimates by local geomorphic features.

In this dissertation I demonstrated that interactions between geomorphology, climate, and organisms produce incredible variability in ecosystem processes (carbon cycling, food web pathways) within a single river system, but that geomorphic features of watersheds regulate that variability.

Table of Contents

ACKNOWLEDGEMENTS 7
CHAPTER 1: INTRODUCTION 10
References 16
CHAPTER 2: GEOMORPHOLOGY CONTROLS THE TROPHIC BASE OF STREAM FOOD WEBS IN A BOREAL WATERSHED* 20
Abstract 21
Introduction 22
Methods 24
Study sites 24
Field sampling 25
Fatty acid analysis 26
Data Analyses 26
Results 29
Do consumer taxa differ in FA composition? 29
Is variation in consumer FA composition associated with geomorphic features of watersheds? 29
Discussion 30
Supplementary Information 38
References 44
CHAPTER 3: THERMAL CONSTRAINTS ON STREAM CONSUMER RESPONSES TO A MARINE RESOURCE SUBSIDY* 50
Abstract 50
Introduction 51
Methods 54
Field sampling 54
Stable isotope analysis 56
Fatty acid analysis 57
Effect of temperature and subsidy magnitude on body size in juvenile coho salmon 58
Individual variation in physiological responses to salmon resource subsidies 59
Results 61
Effect of temperature and subsidy magnitude on body size in juvenile coho salmon 61
Effects of sockeye egg consumption on individual size, condition and FA composition 62
Discussion 64
Supplementary Information 78
References 87

CHAPTER 4: WATERSHED GEOMORPHOLOGY INTERACTS WITH PRECIPITATION TO INFLUENCE THE MAGNITUDE AND SOURCE OF CO_2 EMISSIONS FROM ALASKAN STREAMS 94
Abstract 94
Introduction 94
Methods and Analyses 99
Watershed Description 99
Sample Collection and Analysis 100
Estimating gas transfer velocity and CO_2 fluxes 103
Results 107
Landscape gradient in stream carbon chemistry 107
Gas transfer velocity and CO_2 evasion fluxes 107
Isotopic composition of DIC and stream consumers 110
Discussion 111
CO_2 fluxes and gas transfer velocity 111
Stream DIC sources and consumer isotopes 114
Conclusions 117
Tables 119
Figure Legends 120
Figures 123
Supplementary Information 130
References 134
APPENDIX 1. ACKNOWLEDGEMENTS AND COLLABORATORS 143

ACKNOWLEDGEMENTS

It takes a village to raise a child—but it is equally true that it takes a village to train a new scientist. I am so thankful for the support of an amazing 'village' during my years as a graduate student.

First I would like to thank my advisor, Daniel Schindler, for his support throughout the last five years to follow my curiosity, often in unexpected directions. He has also been a true role model for how to do good science: ask the right questions, keep the big picture in mind, and get your hands dirty in the field. I would like to thank Gordon Holtgrieve for his continued advice and assistance through my grad school years—the number of different ways he has helped me—figuring out sampling logistics, interpreting confusing patterns in data, or suggesting new analyses to try when the old ones fail—are too many to count. I thank my other committee members, Michael Brett and David Butman, for their feedback on analyses and manuscript drafts, and for making sure my dissertation was the best in could be.

I have been surrounded by an incredible team of supportive, smart colleagues at UW, who were just as integral to my success as my PhD committee. Special thanks to all the members, past and present, of the Schindler and Holtgrieve labs for their excellent feedback and true friendship. I'm sure I'll be turning to you for advice for decades to come.

None of my dissertation research in remote boreal Alaska would have been possible without the hard work of the Alaska Salmon Program, specifically Jackie Carter, Chris Boatright, and Jason Ching, who manage everything from food shipments to data curation. I am truly grateful for their efforts, which allowed me to work in such spectacular landscapes. I would also like to thank the following technicians for their hard work doing often tedious field sampling with me: Mackenzie Consoer, Sydney Clark, Lindsy Ciepiela, Brendan Smith, and Dara Yiu.

I would like to thank the following people for their assistance with sample analysis: Sean Yeung, Dan Terracin, Arielle Tonus Ellis, Johnny Stutsman, Dongsen Xue, and Uggo Zoppi (in memorium). Finally, I am grateful for the people, programs, and funding sources that facilitated my research: the Brett Lab, the Quay Lab, Wood-Tikchik State Park, the National Science Foundation, and the Harriet Bullitt Professorship.

Last, but not least, are the friends and family who are the source of my creativity, strength, and happiness. You are the reason I made it this far, and the reason I will keep going. To Todd—you are, quite simply, the best.

DEDICATION

To Hillary Rodham Clinton, for being an inspiring model of strength, dignity, activism, and intelligence for women across the world. Also for showing that progress in not inevitable, but dearly won through the collective efforts of many brave individuals.

CHAPTER 1: INTRODUCTION

Freshwater ecosystems are essential for human society: they provide clean drinking water, irrigation and fertile soil for crop production, and nutritious food resources in the form of fisheries. Human civilizations rose from the floodplains of great rivers, and modern civilizations are no less dependent on them today. However, as a result of their importance, and as human population has increased exponentially, freshwaters are among the most altered and imperiled ecosystems on Earth. Eighty percent of the world's human population faces risks to their water supply, while over half the world's freshwater habitat (by discharge area) faces substantial risks to biodiversity (Vörösmarty et al. 2010). Most of the services humans derive from freshwater ecosystems depend on hydrological, biogeochemical, and ecological processes that are sensitive to anthropogenic activities (Foley et al. 2005). Aquatic ecologists are thus necessarily focused on understanding ecosystem functions and how these provide products and services in the face of intense exploitation and rapidly changing environmental conditions.

Understanding and managing threats to aquatic ecosystem function requires a landscape framework: there is no 'lake' or 'river' management without consideration for their watersheds. Early work established that aquatic systems are fundamentally integrated within their watersheds—they receive the majority of their chemical constituents and organic materials from surrounding uplands (Lindeman 1942). Human activities upslope, for example deforestation, often have negative impacts on stream water quality (Bormann et al. 1968). Aquatic-terrestrial connectivity has since emerged as central theme in aquatic ecology: classic frameworks such as the River Continuum Concept (RCC; Vannote et al. 1980) describe longitudinal changes in the strength of aquatic-terrestrial coupling along a river network, from small headwater catchments to large river floodplains. The concept of 'resource subsidies' across ecosystem boundaries provides a another useful way to describe movement of material and its effect on food webs

across multiple habitats (e.g. terrestrial and aquatic) within landscapes (Polis et al. 2004). However, given the different spatial and temporal scales at which climate, land-use change, and ecological processes operate, means that we need additional frameworks to understand watershed-level responses to stressors.

Stressors such as those imposed by changing climate are driven by global-scale forcing, but ecosystem responses will be heterogeneous at much smaller spatial scales, making prediction of local variation difficult (Levin 1992). Mitigating the effects of a changing environment on freshwater ecosystem function requires understanding interactions between drivers (e.g., climate and land-use) across different spatial and temporal scales (Soranno et al. 2014). How will local environment (e.g., geomorphology, soil characteristics) filter the effects of climate or land use to influence biogeochemical cycles and food web processes? What are the relevant attributes of stream and lakes that dictate their responses to changing air temperature, precipitation patterns, and land use?

Recent work has begun to quantify heterogeneous responses of aquatic ecosystems to large-scale drivers, as well as the landscape characteristics that produce them. A global synthesis of lake temperature data showed that while lakes are warming on average (0.34° C per decade), warming is not uniform within regions—lake characteristics and climate interact to produce greater variation in warming rates within regions than between regions (O'Reilly et al. 2015). In Alaskan streams, watershed geomorphology (slope and elevation) determines the sensitivity of stream thermal regimes to air temperature (Lisi et al. 2015), resulting in high thermal heterogeneity within a single river network that in turn influences a suite of ecosystem processes, from the run timing of salmon populations (Lisi et al. 2013), to ecosystem metabolism (Jankowski et al. 2014).

New frameworks for considering the role of watershed geomorphic features and river network topology in biogeochemical cycling and food web processes have emerged recently (stream hydrogeomorphology, Poole 2010; riverine macrosystems ecology, McCluney et al. 2014). However, empirical studies to establish relationships between watershed features and ecosystem processes are needed to inform and test these frameworks. Studies that quantify relationships between watershed features and biogeochemical and food web processes at intermediate scales (e.g., watershed-scale) provide a means to extrapolate local findings across landscapes, potentially aiding future management efforts. In my dissertation I investigated how broad scale watershed features influence the movement of materials and energy between aquatic and terrestrial environments. I worked in a nearly pristine boreal Alaskan river system (Wood River watershed, SW Alaska), where a high level of physical heterogeneity, coupled with natural landscape gradients, reveal underlying controls on ecosystem processes. Working within a study system that still exhibits considerable physical heterogeneity presents a unique opportunity to understand how landscape attributes regulate ecosystem function.

Physical attributes of rivers control the quantity and quality of energy sources available to consumers (Vannote et al. 1980, Marcarelli et al. 2011), but it remains untested whether geomorphic conditions of whole watersheds affect the assimilation of different resources by stream organisms. In Chapter 2 I used fatty acid biomarkers as novel tracers of energy flow through food webs: I compared the fatty acid (FA) compositions of two invertebrate consumer taxa (caddisflies, mayflies) collected from streams in the Wood River system to assess how assimilation of terrestrial organic matter (OM) and algae varied across a landscape gradient in watershed features. I found that by controlling the accumulation rate and processing of terrestrial OM, watershed features such as mean slope influence the energetic base of food webs

in boreal streams. I found relatively higher assimilation of algae in high-gradient streams compared with low-gradient streams, and the opposite pattern for assimilation of terrestrial OM and microbes. Invertebrates from low-gradient watersheds had FA markers unique to methane-oxidizing bacteria and sulfate-reducing microbes, indicating a contribution of anaerobic microbial pathways to primary consumers. The features that created conditions conducive to anaerobic respiration of OM (stagnant water, accumulation of terrestrial OM, anoxic sediments) resulted in alternative energy sources for higher consumers. That watershed slope, easily calculated from a digital elevation model, provided real information on food web pathways in a highly complex landscape suggests that similar approaches could be used to understand food web responses to anthropogenic stressors. Finally, these results also highlight that anthropogenic stressors to stream food webs will likely be modulated by the local geomorphic context that regulate ecosystem processes.

In addition to influencing basal food web resources, watershed geomorphology controls stream thermal regimes in the Wood River system by determining the residence time of water in stream channels, and the relative contributions of rain and snow to discharge (Lisi et al. 2015), thereby creating a heterogeneous mosaic of stream temperatures across the landscape. Because temperature controls the metabolic rates of organisms across all levels of food webs, from microbes to fish, ecosystem processes and rates should also vary with stream temperature. In high latitude regions such as Alaska, cold temperatures constrain feeding and growth rates of aquatic consumers, limiting their ability to capitalize on abundant but ephemeral food resources (Armstrong et al. 2010). In Chapter 3 I used fatty acid and stable isotope tracers, coupled with multiple years of growth data, to investigate how stream thermal regimes affected the ability of juvenile coho salmon (*Oncorhynchus kisutch*) to benefit from marine resource subsidies

(sockeye salmon eggs). I found that fish in warm streams grew significantly larger with access to energy-rich salmon eggs, but fish in cold streams attained the same size at the end of the growing season regardless of the presence of eggs. Interestingly, more spawning sockeye salmon in a stream (i.e. greater egg abundance) did not result in higher growth for juvenile coho salmon—local environmental conditions (temperature) were a stronger control on growth than the magnitude of the resource subsidy. Individuals that consumed more salmon eggs (estimated from $\delta^{15}N$) were larger and had altered fatty acid composition but did not have higher relative body condition. As air and water temperatures increase in high latitude regions such as SW Alaska, these results highlight that consumer responses to climate change will vary according to complex interactions between local habitat conditions, food availability, and individual variation in metabolic traits.

In Chapter 4 I expanded from investigating geomorphic controls on food web processes to carbon cycling within the Wood River system. Boreal ecosystems such as those found in southwest Alaska sequester a large fraction of the world's soil carbon and are warming rapidly (McGuire et al. 2009), prompting efforts to understand the role of freshwaters in carbon export from these regions. Previous studies have mostly focused either on fluxes from large rivers (ex. *S*triegl et al., 2012), or on intense characterization of C sources and fluxes in individual streams or small catchments (ex. Garnett et al. 2012; Leith et al. 2014). However, variability in CO_2 concentrations and fluxes among streams within regions is high (Wallin et al. 2011, Crawford et al. 2013); thus, there is a need for studies conducted at intermediate scales to understand underlying drivers of differences in carbon inputs and export.

In Chapter 4 I examined geomorphic controls on the magnitude of stream CO_2 emissions and sources of stream dissolved inorganic carbon (DIC) in the same streams as in Chapter 2. I

found that watershed slope and precipitation interact to control terrestrial carbon fluxes into and out of streams. Watershed slope influences C loading and stream CO_2 fluxes by determining the amount of carbon accumulation in watersheds, and to a lesser extent by determining gas transfer velocity across the air-water interface. Low gas transfer velocity in low gradient streams offsets some of the effects of higher terrestrial C loading at those sites, resulting in lower than expected vertical CO_2 fluxes. While the isotopic composition of stream DIC ($\Delta^{14}C$ and $\delta^{13}C$) was highly variable across space and time, shifts towards younger, more terrestrial sources after rain events were most pronounced in low gradient watersheds. At base flow DIC was a mixture of modern and aged sources of biogenic and geologic origin. Aged C sources contributed to food webs via an indirect pathway from DIC to algae to invertebrate grazers. I observed coherent changes in stream carbon chemistry after rainstorms despite considerable physical heterogeneity among watersheds. These patterns provide a way to extrapolate across boreal landscapes by constraining CO_2 concentration and flux estimates by local geomorphic features.

In this dissertation I demonstrate that interactions between geomorphology, climate, and organisms produce remarkable variability in ecosystem processes (carbon cycling, food web pathways) within a single river system. Boreal systems such as the Wood River watershed are not unique in this regard: ecosystems worldwide probably operate according to a different but no less complex set of drivers and interactions. Given the magnitude of complexity inherent to any ecosystem, how are ecologists and resource managers to move forward when faced with increasingly severe threats to biodiversity and ecosystem services? Despite the increasing volume of ecological knowledge, we will never fully characterize every vulnerable ecosystem.

Diverse physical conditions create opportunities for local decoupling from large scale drivers, stabilizing overall ecosystem response to stressors (Schindler et al. 2015). For example,

the landscape position of northern Wisconsin lakes determined whether the concentration of conservative cations (Mg + Ca) increased or decreased in response to a regional drought: higher elevation rain-dominated lakes showed decreased mass of ions as groundwater inputs decreased, but low elevation groundwater-dominated lakes showed the opposite response as precipitation inputs decreased in proportion to groundwater inputs (Webster et al. 1996). Landscape-induced differences in hydrology maintained a diversity of responses in lake chemistry to drought, potentially maintaining more suitable habitat for aquatic organisms at the landscape scale. However, human activities rarely increase or maintain landscape heterogeneity. Rather, we often suppress natural disturbance regimes that maintain spatial and temporal variation (e.g. floods, fires; Poff et al. 1997), fragment habitats (urban development, forestry; Foley et al. 2005), decouple aquatic and terrestrial habitats (Schindler and Smits 2016), and replace species-rich communities with monocultures (agriculture; Foley et al. 2005). As a result of these homogenizing forces, ecologists are thus tasked with the impossible goal of perfectly predicting how current ecosystems will respond to unpredictable future conditions. Instead, by preserving or re-establishing ecologically-relevant heterogeneity within landscapes, we can maintain the ability of populations and processes to shift and adapt to changes. This presents a robust conservation strategy that does not rely on perfect knowledge of the state of nature.

References

Armstrong, J. B., D. E. Schindler, K. L. Omori, C. P. Ruff, and T. P. Quinn. 2010. Thermal heterogeneity mediates the effects of pulsed subsidies across a landscape. Ecology 91:1445–54.

Bormann, F.H., G.E. Likens, D.W. Fisher and R.S. Pierce. 1968. Nutrient loss accelerated by

clear-cutting of a forest ecosystem. Science 159(3817): 882-884.

Crawford, J. T., R. G. Striegl, K. P. Wickland, M. M. Dornblaser, and E. H. Stanley. 2013. Emissions of carbon dioxide and methane from a headwater stream network of interior Alaska. Journal of Geophysical Research: Biogeosciences 118:482–494.

Foley, J. A., R. DeFries, G. P. Asner, C. Barford, G. Bonan, S. R. Carpenter, F. S. Chapin, M. T. Coe, G. C. Daily, H. K. Gibbs, J. H. Helkowski, T. Holloway, E. A. Howard, C. J. Kucharik, C. Monfreda, J. A. Patz, C. Prentice, N. Ramankutty, and P. K. Snyder. 2005. Global Consequences of Land Use. Science 309:570–574.

Garnett, M. H., K. J. Dinsmore, and M. F. Billett. 2012. Annual variability in the radiocarbon age and source of dissolved CO 2 in a peatland stream. Science of the Total Environment 427–428:277–285.

Jankowski, K., D. E. Schindler, and P. J. Lisi. 2014. Temperature sensitivity of community respiration rates in streams is associated with watershed geomorphic features. Ecology 95:2707–2714.

Leith, F. I., M. H. Garnett, K. J. Dinsmore, M. F. Billett, and K. V. Heal. 2014. Source and age of dissolved and gaseous carbon in a peatland-riparian-stream continuum: A dual isotope (14C and d13C) analysis. Biogeochemistry 119:415–433.

Lindeman, R. L. 1942. The trophic-dynamic aspect of ecology. Ecology 23:399–417.

Lisi, P. J., D. E. Schindler, K. T. Bentley, and G. R. Pess. 2013. Association between geomorphic attributes of watersheds, water temperature, and salmon spawn timing in Alaskan streams. Geomorphology 185:78–86.

Lisi, P. J., D. E. Schindler, T. J. Cline, M. D. Scheuerell, and P. B. Walsh. 2015. Watershed geomorphology and snowmelt control stream thermal sensitivity to air temperature. Geophysical Research Letters 42:3380–3388.

Marcarelli, A. M., C. V Baxter, M. M. Mineau, and R. O. Hall. 2011. Quantity and quality: unifying food web and ecosystem perspectives on the role of resource subsidies in freshwaters. Ecology 92:1215–1225.

McCluney, K. E., N. L. Poff, M. A. Palmer, J. H. Thorp, G. C. Poole, B. S. Williams, M. R. Williams, and J. S. Baron. 2014. Riverine macrosystems ecology: Sensitivity, resistance, and resilience of whole river basins with human alterations. Frontiers in Ecology and the Environment 12:48–58.

McGuire, a. D., L. G. Anderson, T. R. Christensen, S. Dallimore, L. Guo, D. J. Hayes, M. Heimann, T. D. Lorenson, R. W. Macdonald, and N. Roulet. 2009. Sensitivity of the carbon cycle in the Arctic to climate change. Ecological Monographs 79:523–555.

O'Reilly, C. M., R. J. Rowley, P. Schneider, J. D. Lenters, P. B. Mcintyre, and B. M. Kraemer. 2015. Rapid and highly variable warming of lake surface waters around the globe. Geophysical research letters:1–9.

Poff, N. L., J. D. Allan, M. B. Bain, J. R. Karr, K. L. Prestegaard, B. D. Richter, R. E. Sparks, and J. C. Stromberg. 1997. The Natural Flow Regime: A paradigm for river conservation and restoration N. BioScience 47:769–784.

Polis GA, Power M, Huxel GR, Eds. 2004. Food webs at the landscape level. Chicago: University of Chicago Press.

Poole, G. C. 2010. Stream hydrogeomorphology as a physical science basis for advances in stream ecology. Journal of the North American Benthological Society 29:12–25.

Richey, J. E., J. M. Melack, A. K. Aufdenkampe, V. M. Ballester, and L. L. Hess. 2002. Outgassing from Amazonian rivers and wetlands as a large tropical source of atmospheric CO2. Nature 416:617–20.

Schindler, D. E., J. B. Armstrong, and T. E. Reed. 2015. The portfolio concept in ecology and evolution. Frontiers in Ecology and the Environment 13:257–263.

Schindler, D. E., and A. P. Smits. 2016. Subsidies of Aquatic Resources in Terrestrial Ecosystems. Ecosystems.

Soranno, P. A., K. S. Cheruvelil, E. G. Bissell, M. T. Bremigan, J. A. Downing, C. E. Fergus, C. T. Filstrup, E. N. Henry, N. R. Lottig, E. H. Stanley, C. A. Stow, P. N. Tan, T. Wagner, and K. E. Webster. 2014. Cross-scale interactions: Quantifying multi-scaled cause-effect relationships in macrosystems. Frontiers in Ecology and the Environment 12:65–73.

Striegl, R. G., M. M. Dornblaser, C. P. McDonald, J. R. Rover, and E. G. Stets. 2012. Carbon dioxide and methane emissions from the Yukon River system. Global Biogeochemical Cycles 26.

Vannote, R. L., G. W. Minshall, K. W. Cummins, J. R. Sedell, and C. E. Cushing. 1980. The river continuum concept. Canadian Journal of Fisheries and Aquatic Sciences 37:130–137.

Vörösmarty, C. J., P. B. McIntyre, M. O. Gessner, D. Dudgeon, and A. Prusevich. 2010. Global Threats to Human Water Security and River Biodiversity. Nature 467:555–561.

Wallin, M. B., M. G. Öquist, I. Buffam, M. F. Billett, J. Nisell, and K. H. Bishop. 2011.

Spatiotemporal variability of the gas transfer coefficient (KCO2) in boreal streams: Implications for large scale estimates of CO2 evasion. Global Biogeochemical Cycles 25:1–14.

Webster, K. E., T. K. Kratz, C. J. Bowser, J. J. Magnuson, and W. J. Rose. 1996. The influence of landscape position on lake chemical responses to drought in northern Wisconsin. Limnology and Oceanography 41:977–984.

CHAPTER 2: GEOMORPHOLOGY CONTROLS THE TROPHIC BASE OF STREAM FOOD WEBS IN A BOREAL WATERSHED*

Abstract

Physical attributes of rivers control the quantity and quality of energy sources available to consumers, but it remains untested whether geomorphic conditions of whole watersheds affect the assimilation of different resources by stream organisms. We compared the fatty acid (FA) compositions of two invertebrate taxa (caddisflies, mayflies) collected from 16 streams in southwest Alaska to assess how assimilation of terrestrial OM and algae varied across a landscape gradient in watershed features. We found relatively higher assimilation of algae in high-gradient streams compared with low gradient streams, and the opposite pattern for assimilation of terrestrial OM and microbes. The strength of these patterns was more pronounced for caddisflies than mayflies. Invertebrates from low gradient watersheds had FA markers unique to methane-oxidizing bacteria and sulfate-reducing microbes, indicating a contribution of anaerobic pathways to primary consumers. Diversity of FA composition was highest in watersheds of intermediate slopes that contain both significant terrestrial inputs as well as high algal biomass. By controlling the accumulation rate and processing of terrestrial OM, watershed features influence the energetic base of food webs in boreal streams.

***Full Citation:** *Adrianne P. Smits, Daniel E. Schindler, and Michael T. Brett. 2015. Geomorphology controls the trophic base of stream food webs in a boreal watershed. Ecology 96: 1775-1782.*

Introduction

Much ecological research has focused on the relative importance of terrestrial subsidies versus in situ primary production for supporting higher trophic levels in freshwater systems (Cole et al. 2006; Brett et al. 2009), with growing realization that landscape features constrain the availability and assimilation of these energy sources. For example, the importance of terrestrial carbon to lake food webs depends strongly on lake size (Wetzel 1990). The dominant conceptual model describing how physical attributes of lotic systems control the relative contributions of autochthonous and allochthonous sources to food webs is the River Continuum Concept (RCC, Vannote et al. 1980). In forested watersheds, channel width controls canopy cover and therefore light availability and potential for detrital inputs from riparian forests. Under the RCC, consumers in small, forested headwater streams depend primarily on terrestrial organic sources of energy, whereas consumers in wider rivers are supported mainly by algal production. However, additional physical properties of watersheds beyond channel width and network position can exert controls on both algal production and terrestrial inputs. For example, in temperate and boreal ecosystems, watershed slope strongly determines the accumulation rate of terrestrial organic matter (OM) such as peat on the landscape, which in turn influences stream chemistry and the composition of invertebrate and fish communities (Walker et al. 2012, King et al. 2012). However, there has been little effort to directly assess how geomorphic conditions set by landform affect the transport and assimilation of different carbon sources in aquatic food webs.

While terrestrial inputs comprise the bulk of organic carbon transported in high latitude streams (Spencer *et al.* 2008), the molecular composition of this material often makes it a low-

quality energy source for invertebrate consumers compared to algae (Thorp and Delong 2002, Brett et al. 2009). Therefore, despite the higher quantities of terrestrial OM present in low gradient watersheds, consumer diets may not reflect this abundance if alternative resources such as algae are also available. There are multiple pathways by which terrestrial OM can become available to benthic consumers in streams, the two most studied being direct consumption of particulate OM (Cummins 1974), and heterotrophic processing of particulate and dissolved terrestrial OM (i.e., consumers grazing microbial biofilms; France 2011). In addition, invertebrate consumption of methanogenic and sulfate-reducing microbes, which perform anaerobic metabolism within inundated soils and leaf litter (Xu et al. 2013) is increasingly recognized as an alternative pathway by which terrestrial OM can enter freshwater food webs (Jones and Grey 2011). Previous studies have used stable isotope ratios of invertebrates and their food sources to compare carbon pathways between stream reaches (Finlay *et al.* 2002), or between shaded headwaters and exposed, higher order streams (McNeely *et al.* 2006), but no ecosystem scale study has explicitly examined the relationship between watershed geomorphology and the carbon sources assimilated by stream consumers. Thus, it remains untested whether geomorphic conditions of watersheds control the consumption of terrestrial and autochthonous resources by stream organisms.

In this study, we asked 1) how do the carbon sources assimilated by stream invertebrates vary across a landscape gradient in geomorphic conditions such as watershed slope, substrate size, and stream temperature, and 2) does this relationship differ between dominant groups of primary consumers? To test these questions we compared the fatty acid composition of two ubiquitous invertebrate groups (Trichoptera, Ephemeroptera) collected from 16 streams arranged across a watershed geomorphic gradient in southwest Alaska. Fatty acids are useful trophic

markers because most of the fatty acids from an organism's diet are stored in its tissues without modification, and certain fatty acids are indicative of specific groups of primary producers or bacteria (Dalsgaard et al. 2003). Much of the relevant geomorphic variation in this system is strongly associated with mean watershed slope (Lisi et al. 2013); our primary hypothesis was that by constraining the accumulation rate of terrestrial OM, in the form of debris and organic soils, geomorphic conditions such as watershed slope would act as an ultimate control over the proximate processes that influence the carbon sources assimilated by stream consumers. We predicted that invertebrates in streams draining high gradient watersheds would have higher concentrations of algal biomarkers in their tissues than those from low gradient watersheds due to lower availability of terrestrial carbon relative to OM fixed in situ. We also predicted that invertebrates from low gradient watersheds, which in this region typically drain peat bogs, would have higher concentrations of biomarkers associated with terrestrial OM and associated heterotrophic bacteria, reflecting higher abundance of both terrestrial carbon and microbial biomass.

Methods

Study sites

We sampled 16 streams within the Wood River basin in the Bristol Bay region of Alaska (59°20′ N, 158°40′W), which has a total drainage area of 3,950 km^2. The Wood River basin contains a series of large interconnected lakes—all the study streams but two flow directly into Lake Nerka or Lake Beverley. Streams within this system vary widely in their geomorphic characteristics (Pess 2009, Lisi et al. 2013); there is a general longitudinal gradient of peat accumulation across the basin, associated with a shift from high gradient, mountainous terrain on the western side to low gradient, wetland dominated terrain in the east. Temperature and flow regimes also generally reflect this gradient, wherein steep, high elevation streams are colder and snow-melt dominated,

and low gradient, low elevation streams are warmer and primarily rain-fed (Lisi *et al.* 2013). The mean watershed slope of sampled streams, calculated in ArcGIS from a digital elevation map, ranges from 0.5 to 29 degrees (Lisi *et al.* 2013). Mean watershed elevation ranges from 32 to 502 m above mean sea level. Vegetation at lower elevations (<150m) is dominated by a white spruce (*Picea glauca*) and paper birch (*Betula papyrifera*) mixed forest, interspersed with areas of moist tundra and sphagnum bog. Stands of green alder (*Alnus crispa*) cover steep, high elevation hill slopes. Riparian areas are dominated by feltleaf willow (*Salix alexensis*), as well as alder and cottonwood in steeper watersheds (Bartz and Naiman 2005). Higher gradient streams tend to have higher canopy cover presumably due to water-saturated soils hindering riparian tree growth at low gradient sites.

Field sampling

Benthic invertebrates (Trichoptera, Ephemeroptera) were collected by hand and with a Surber sampler in June and July of 2012 and 2013 prior to the spawning migrations of salmon, which produce a seasonal pulse of alternative food resources and drastically reduce invertebrate density via substrate disturbance (Moore and Schindler 2008). We collected larval case-building caddisflies and mayflies because they were the most ubiquitous basal consumers present in the study streams. The invertebrate communities of these streams have been previously described by Moore and Schindler (2008): caddisflies were primarily Brachycentridae and Limnephilidae, while mayflies were primarily Heptageneidae, Baetidae, and Ephemerellidae. In eight streams we collected samples from both invertebrate groups, whereas four streams contained only caddisflies, and only mayfly samples were collected from four streams due to low caddisfly abundance. Five to twenty individuals per group were collected within 1000 meters of the stream mouth on each sampling date. Post collection, samples were frozen in water until further analysis.

Fatty acid analysis

For each unique sampling event (site and date), insects in the same family were combined into composite samples for further analysis. Samples were freeze-dried, homogenized, and analyzed for fatty acid composition to quantify the proportion of their lipids derived from organic matter sources such as terrestrial vegetation and stream algae. Fatty acid extraction and analysis was performed as described in Strandberg et al. (2014). Samples were weighed (1-2 mg dry mass), then extracted in in a chloroform/methanol/water solution (2:1:0.8, by volume). Lipids were dissolved in toluene and trans-methylated at 50° C for 16 h, using an acidic catalyst (1% H2SO4 in methanol). The resulting fatty acid methyl esters (FAME) were analyzed at the University of Washington, with a HP6890 gas chromatograph (GC), equipped with flame ionization detection, using a DB-23 capillary column (length 30 m, ID 0.25 mm, film thickness 0.25 lm, Agilent) with helium as carrier gas (1 mL min^{-1}) and splitless injection. FAME peaks were tentatively identified by comparison of retention times with known standards (37-component FAME mix, Supelco). For final determination of peak identities, a subset of the samples was analyzed by gas chromatography/mass spectrometry (Shimadzu GCMS QP2010 plus; Agilent DB-23 column) with splitless injection. Double-bond configuration of C_{16} and C_{18} mono-unsaturated fatty acids (MUFA) was determined by analysis of their dimethyl disulphide adducts (Nichols et al. 1986) . In all, 25 fatty acid peaks were identified, and all data were mass corrected as well as converted to proportion of total fatty acids ([g FA methyl ester/g total FA methyl ester]). Only these 25 peaks were included in data analyses.

Data Analyses

We compared the fatty acid composition of caddisflies and mayflies using analysis of similarity (ANOSIM), a non-parametric multivariate analog to ANOVA, and principal component analysis (PCA). ANOSIM compares the average rank of similarity among objects within groups against

the average rank of similarity among objects between groups. Significance of the R-statistic was tested using Monte Carlo randomization (1000 permutations). We also tested for multivariate homogeneity of group dispersions (variances) between caddisfly and mayfly FA composition by calculating the average Euclidean distance of each sample to the group centroid and performing ANOVA on these distances. In the PCA, functionally similar fatty acids were summed to form 11 fatty acid variables (see Supplementary Information). A PCA using all 25 FA yielded similar results. Significance of the resulting eigenvalues was tested using Monte Carlo randomization (1000 permutations).

We examined relationships between watershed geomorphic features and specific fatty acid concentrations in individual invertebrate samples using simple linear regression (significance level of $p < 0.05$). Separate regressions were performed for caddisflies and mayflies. We used mean watershed slope as the sole geomorphic predictor variable, as slope correlates strongly with other geomorphic variables such as substrate size and elevation in Wood River watersheds (Lisi *et al.* 2013; see Supplementary Information). An important caveat when using FA biomarkers in diet studies is that most FA are not strictly diagnostic (that is, associated with only one resource type) and can be synthesized by a range of basal resources. For example, C_{18} PUFA are produced by both terrestrial plants and algae, and many SAFA and MUFA are ubiquitous in algae, terrestrial plants and bacteria (e.g., 16:0, 18:0, and 18:1n9). In addition, stream insects most likely synthesize some FA de novo (ex. 18:1n9) or modify ingested FA, however the lipid metabolism of most stream invertebrates is at present poorly characterized.

We used only FA known to be diagnostic or highly characteristic of specific carbon sources as response variables in regressions. Linoleic acid (LIN, 18:2n6), α-linoleic acid (ALA, 18:3n3), eicosapentaenoic acid (EPA, 20:5n3), and C_{16} PUFA are highly abundant in green algae

and diatoms compared with terrestrial vegetation (Torres-Ruiz *et al.* 2007), and were thus considered algal biomarkers. Conversely, terrestrial vegetation is much higher in SAFA than algae, and is particularly characterized by long-chain SAFA (i.e., 20:0, 22:0, 24:0, and 26:0; Brett et al. 2009; Taipale et al. 2014). Branched FA are considered bacterial biomarkers (Kharlamenko *et al.* 1995). The FA 16:1n8 and 18:1n8 are diagnostic of Type I methane-oxidizing bacteria (MOB) (18:1n8 was not detected in our samples; Sundh *et al.* 2005; Taipale et al. 2012), and 16:1n5 is synthesized by sulfate-reducing bacteria (Elvert *et al.* 2003).

Additionally, we examined whether diversity in invertebrate FA varied with watershed slope. To quantify FA diversity within each stream, we calculated the Shannon-Weiner diversity index as described in Krebs (1999) for each sample using proportional FA composition (all 25 identified FA were included): values were then averaged by stream for caddisflies and mayflies separately. Linear and 2nd order polynomial regression was used to test the relationship between watershed slope and the average diversity index for each stream, with the most parsimonious model chosen using AIC. Since the detection of rare (low proportion) FA in a sample can depend on overall sample FA concentration rather than the FA ingested by an individual, we regressed total FA peak area (from chromatograms) against the Shannon Index for each sample. Because there was no significant relationship here ($p=0.58$), we assume that the Shannon Index represents the diversity of resources assimilated by consumers.

All analyses were conducted in R version 2.15.2 (R Core Development Team 2012), using the Vegan (Oksanen et al. 2012) package.

Results

Do consumer taxa differ in FA composition?

ANOSIM showed that caddisflies and mayflies were significantly different in overall FA composition ($R=0.51$, $p = 0.001$). Caddisfly FA composition also varied more among samples (mean distance to centroid = 0.12, $p < 0.05$) than did mayfly FA composition (mean distance = 0.09).

PCA accounted for about half the variation in fatty acid composition among samples on two primary axes (54%, $p < 0.001$), with the two invertebrate taxa separating strongly along PC axis 1 (Figure 1A). Branched FA, SAFA, and C_{18} MUFA were negatively correlated with PC1, whereas algal FA (LIN, ALA, EPA, C_{16} PUFA) were positively correlated with this axis. SDA, C_{16} MUFA, and C_{14} MUFA loaded significantly onto PC2. Only PC 1 and PC2 explained a significant proportion of the variance in the data.

FA characteristic of algae made up on average 24% (±7.9%, 1 SD) of total FA in caddisflies, and 10% (±4.5%) in mayflies. Caddisflies had significantly higher proportions of algal FA than mayflies (Wilcoxon Rank Sum Test, $W=1479$, $p < 0.0001$, $n = 81$), but lower proportions of branched FA ($0.6 \pm 0.35\%$, $W = 437$, $p < 0.001$) and SAFA ($30.7 \pm 4.9\%$, $W = 82$, $p < 0.0001$) than mayflies ($0.8 \pm 0.24\%$; $44.3\% \pm 6.2$, for branched FA and SAFA, respectively).

Is variation in consumer FA composition associated with geomorphic features of watersheds?

Diversity of FA composition (Shannon-Weiner index) in both taxa was highest in watersheds of intermediate slope (Fig. 1B). For caddisflies, a second-order polynomial regression ($R^2 = 0.34$, $p = 0.09$, $n=10$) fit the relationship between FA diversity and watershed slope significantly better than a linear model ($\Delta AIC=3.44$). For mayflies, a second-order polynomial regression ($R^2 = 0.31$, $p = 0.09$, $n=10$) also fit significantly better than a linear model ($\Delta AIC=3.62$).

Total FA concentration (μg/mg dry mass) was a positive linear function of watershed slope for caddisflies (R^2=0.18, p=0.003, n=45, Fig. 2A), but not for mayflies (p=0.47). The proportion of algal fatty acids in caddisflies was also positively related with watershed slope (R^2= 0.37, p < 0.001, n= 45, Fig. 2B) but this relationship was not significant in mayflies (R^2=0.07, p=0.09, n=28, Fig. 2B). The proportion of SAFA was a positive, but marginally significant linear function of watershed slope for caddisflies (p = 0.054, R^2 = 0.067, Fig. 3C), and not at all for mayflies (p = 0.19, Fig. 2C). Caddisflies in low gradient watersheds had higher proportions of branched (i.e., bacterial) FA than those in steep watersheds (R^2= 0.25, p<0.001, n=45, Fig. 2D), whereas mayflies did not exhibit this pattern (p=0.65, n=28, Fig. 2D).

Mayflies had higher proportions of MOB FA (i.e. 16:1n8) in low gradient watersheds (R^2= 0.32, p=0.001, n=28), however, this relationship was not significant for caddisflies (R^2=0.05, p=0.07, n=45, Fig. 2E). The proportion of 16:1n5, a marker for sulfate-reducing bacteria, was negatively related with slope for both caddisflies (R^2 = 0.33, p < 0.0001, Fig. 2F) and mayflies (R^2 = 0.18, p = 0.016, Fig. 2F). One mayfly sample was an outlier (16:1n5 was > 4 standard deviations above the mean) and thus omitted from the regression. Doing so did not change the direction of the regression line, only the regression coefficients.

Discussion

Our data indicate that there are geomorphic constraints on the carbon sources assimilated by consumers in boreal streams, with relatively greater assimilation of algae in streams draining steep watersheds compared with relatively greater assimilation of terrestrially-derived carbon in low gradient streams. However, the relationship between watershed slope and carbon source assimilation by invertebrates was mediated by feeding differences among taxa. Caddisfly larvae had higher proportions of algal FA in steeper watersheds and higher proportions of microbial

biomarkers in low gradient watersheds. Mayfly nymphs, on the other hand, showed little variation in FA composition across the landscape, except for an increase in certain bacterial biomarkers (MOB FA, 16:1n5) in low gradient watersheds (average slope < 14 degrees).

That both invertebrate groups had higher proportions of microbial FA in low gradient watersheds is not surprising as these streams are generally warmer (Lisi et al. 2013) and DOC-rich (Jankowski et al. 2014), providing conditions conducive to high bacterial biomass. While a review of stream and lake food web studies showed that invertebrate consumers select for autochthonous food sources in a large majority of systems (Marcarelli *et al.* 2011), bacterial conditioning of recalcitrant terrestrial carbon particles is known to enhance assimilation by invertebrates (France 2011), and in some streams insects derive high fractions (> 20%) of their mass from bacterial carbon (Hall and Meyer 1998). In our system, both microbial priming of terrestrial OM, as well as direct consumption of bacterial carbon likely provide substantial energy sources to invertebrate consumers. Though both caddisflies and mayflies had low proportions of microbial biomarkers (< 5%), this does not necessarily reflect the absolute contribution of heterotrophic processing of terrestrial OM to the food web. Unlike long-chain PUFA, certain microbial FA such as branched FA serve no structural function in invertebrates, and would therefore be preferentially catabolized for energy rather than retained in cells (Taipale et al. 2012). In addition, bacteria and terrestrial plants synthesize ubiquitous FA such as 16:0, 18:0, and 18:1n9, making calculations of absolute diet contributions impossible using only the proportional FA profiles of consumers, unless extensive feeding trials are conducted. Finally, without estimates of biomass and turnover rates, our inference is limited to descriptions of relative differences in resource assimilation among sites, rather than magnitudes of energy flow (Benke and Wallace 1997). Nevertheless, the negative relationship between watershed slope and

proportion of microbial FA in insects demonstrates how geomorphology regulates the proximate stream conditions (terrestrial OM accumulation, temperature, microbial production) that control the types of resources assimilated by consumers.

There are multiple possible explanations for the higher algal FA (LIN, ALA, EPA) content of caddisflies in high-gradient watersheds. If algae are proportionally more abundant in steep streams than in low gradient ones, caddisfly FA composition may simply reflect this pattern, without change in feeding behavior across the landscape gradient. Alternatively, caddisflies may increase their selectivity towards algal carbon in steeper watersheds, especially if lower microbial biomass results in less priming of terrestrial OM. In lakes, zooplankton can increase PUFA retention at colder temperatures to maintain cell-membrane fluidity (Schlechtriem et al. 2006), however this capability has not been tested in benthic stream invertebrates, nor would it explain why mayflies did not have higher PUFA content in cold, steep streams. Water temperature can also affect the production and retention of long chain PUFA in algae— PUFA rich autotrophs (e.g., diatoms) are associated with colder water temperatures, whereas PUFA depauperate autotrophs (e.g., cyanobacteria) are associated with warm temperatures (Taipale et al. 2013). If benthic algae composition in Wood River streams is similarly influenced by temperature, higher PUFA content in caddisflies in steep, snow-fed streams, which tend to be colder than low gradient streams (Lisi et al. 2013), may reflect the higher PUFA content of algae, rather than greater feeding selectivity. However, because we did not analyze food sources for FA composition or conduct feeding trials, we cannot explicitly test this hypothesis.

Our FA results indicate that caddisflies rely more heavily on algal carbon than mayflies. There is some evidence that caddisflies may be more competitive grazers on algae than mayflies:

in a study in a forested headwater stream, excluding caddisfly grazers from stream reaches caused mayfly nymphs to shift towards a more algal-based diet (McNeely *et al.* 2007). Alternatively, the differences in FA composition between caddisflies and mayflies could indicate taxon-specific variation in lipid metabolism and storage strategies, as has been observed among consumer groups in boreal lakes (Lau et al. 2012). Because we conducted our study at a coarse scale of taxonomic resolution, we cannot account for the effects of community composition change on the differences in FA composition among sites, for example if caddisfly species in cold streams simply have higher PUFA content than species inhabiting warmer streams, regardless of dietary inputs. However, since we see consistent patterns in multiple biomarkers across the landscape gradient, it is unlikely that these are entirely attributable to inherent metabolic differences among species, rather than reflecting changes in food resources.

Both mayflies and caddisflies showed higher assimilation of carbon derived from anaerobic pathways such as methanogenesis and sulfate reduction in low gradient watersheds, where inundated, anoxic soils are most common. Stable isotopes and FA biomarkers suggest that anaerobic pathways support benthic invertebrate consumers in lakes and temperate rivers (Trimmer et al. 2009, Jones and Grey 2011), but our study is the first to show this pathway in boreal streams. Anaerobic processing of soil carbon and leaf litter is currently an under-studied alternative pathway by which terrestrial OM can support stream consumers, and merits further investigation.

Consumer fatty acid composition was most diverse in watersheds of intermediate gradient. In the Wood River system, low gradient streams drain peat bogs and are thus DOC-rich and likely strongly heterotrophic, whereas the steepest streams drain rocky mountain slopes without significant organic soils (Jankowski et al. 2014). Our results indicate that intermediate

levels of terrestrial resources increase the diversity of metabolic pathways contributing to stream food webs. In their synthesis, Moore et al. (2004) hypothesized that the structural and chemical diversity of detritus (mainly terrestrial inputs) supports a more diverse set of consumers in aquatic food webs than would algal production alone, and it is reasonable to hypothesize a similar effect on the diversity of trophic resources assimilated by consumers.

Our results suggest that there are clear yet poorly described geomorphic controls on the resource base of lotic food webs beyond those described in the RCC (i.e. channel width as a function of river network position). All study streams are first to third order, and many are located within several kilometers of one another, yet basal consumers differed markedly in FA composition. The underlying effects of watershed slope on food webs are likely expressed via a mixture of proximate processes such as organic soil and debris accumulation, riparian zone inundation, riparian shading of the stream channel, bacterial priming of OM, physical degradation of particles, and hydrologic transport from terrestrial to aquatic systems. Further exploration of these physical constraints on carbon pathways will be especially relevant in high latitude ecosystems, where rapid climate change is likely to alter carbon flux between terrestrial and aquatic systems as a result of changes in vegetation, hydrology, microbial production, and stream community composition. Improved understanding of geomorphic constraints on resource flows through food webs provides a means to extrapolate effects observed at local scales to entire landscapes, and will enhance our ability to develop scenarios that account for climate driven changes to aquatic landscapes and the organisms they support.

Figure Legends

Figure 1 (A) Ordination plot showing a PCA of fatty acid composition of caddisflies (black filled circles) and mayflies (open triangles) collected from Wood River streams. Labeled arrows show fatty acids driving significant variation between samples. PC axis 1 (horizontal) explained 33.7% of the variation among samples, and PC axis 2 (vertical) explained 20.63%.

(B) Second order polynomial regressions between mean watershed slope (x-axis) and mean Shannon-Weiner diversity index of caddisflies and mayflies. Bars show one standard deviation above and below the mean diversity index of invertebrates in each watershed**.**

Figure 2. Simple linear regressions between mean watershed slope (x-axis) and total FA content (ug/mg dry mass) (A), proportion algal FA out of total FA (B), proportion SAFA (C), proportion branched FA (D), proportion MOB FA (E), and proportion 16:1n5 in caddisflies (black filled circles) and mayflies (open triangles). Each symbol denotes the mean value for a stream. Bars show one standard error above and below the mean. Regression lines for caddisflies (black solid line) and mayflies (black dashed line) are shown for statistically significant relationships ($p < 0.05$).

Figures

Figure 1:

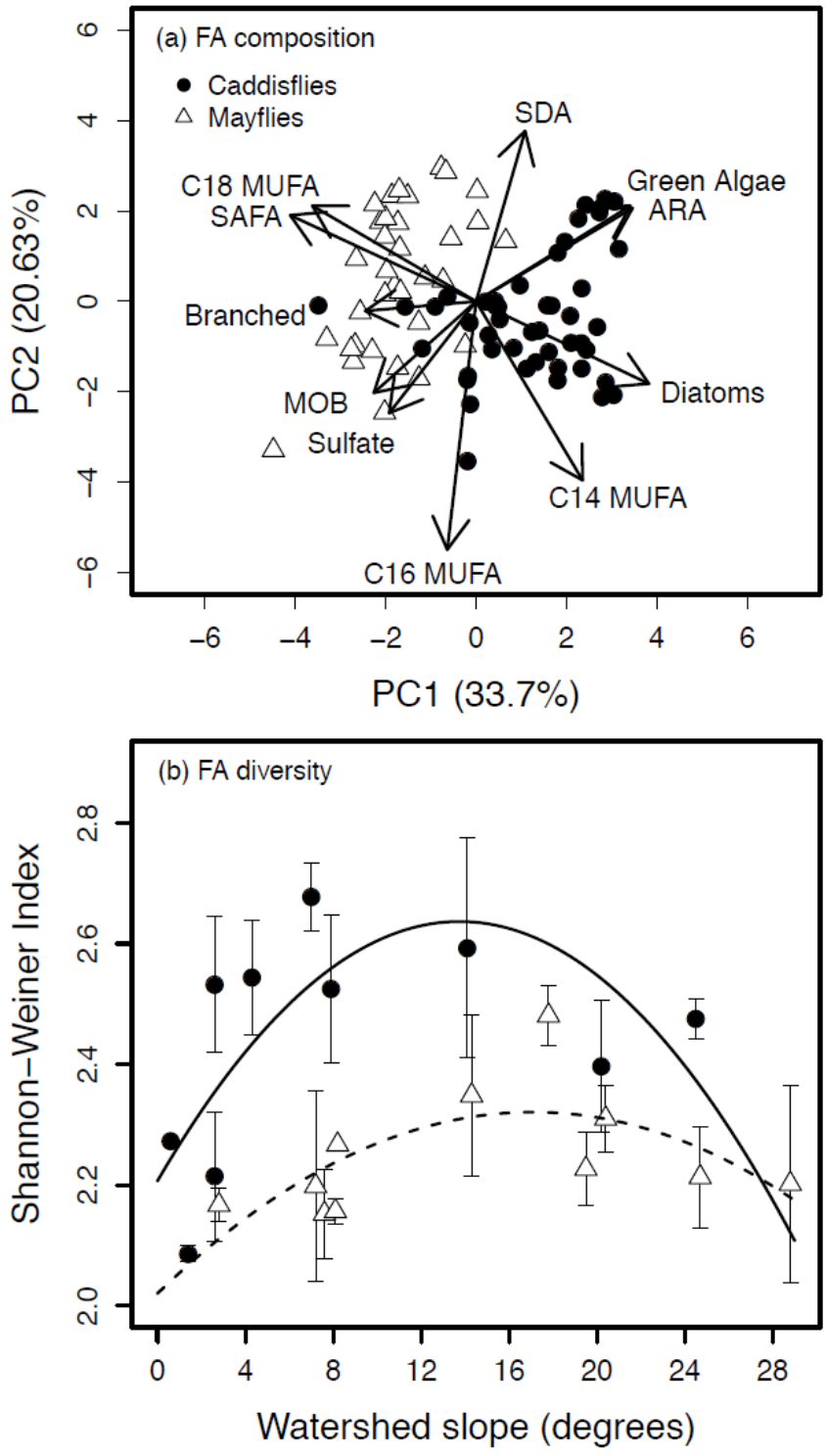

Figure 2:

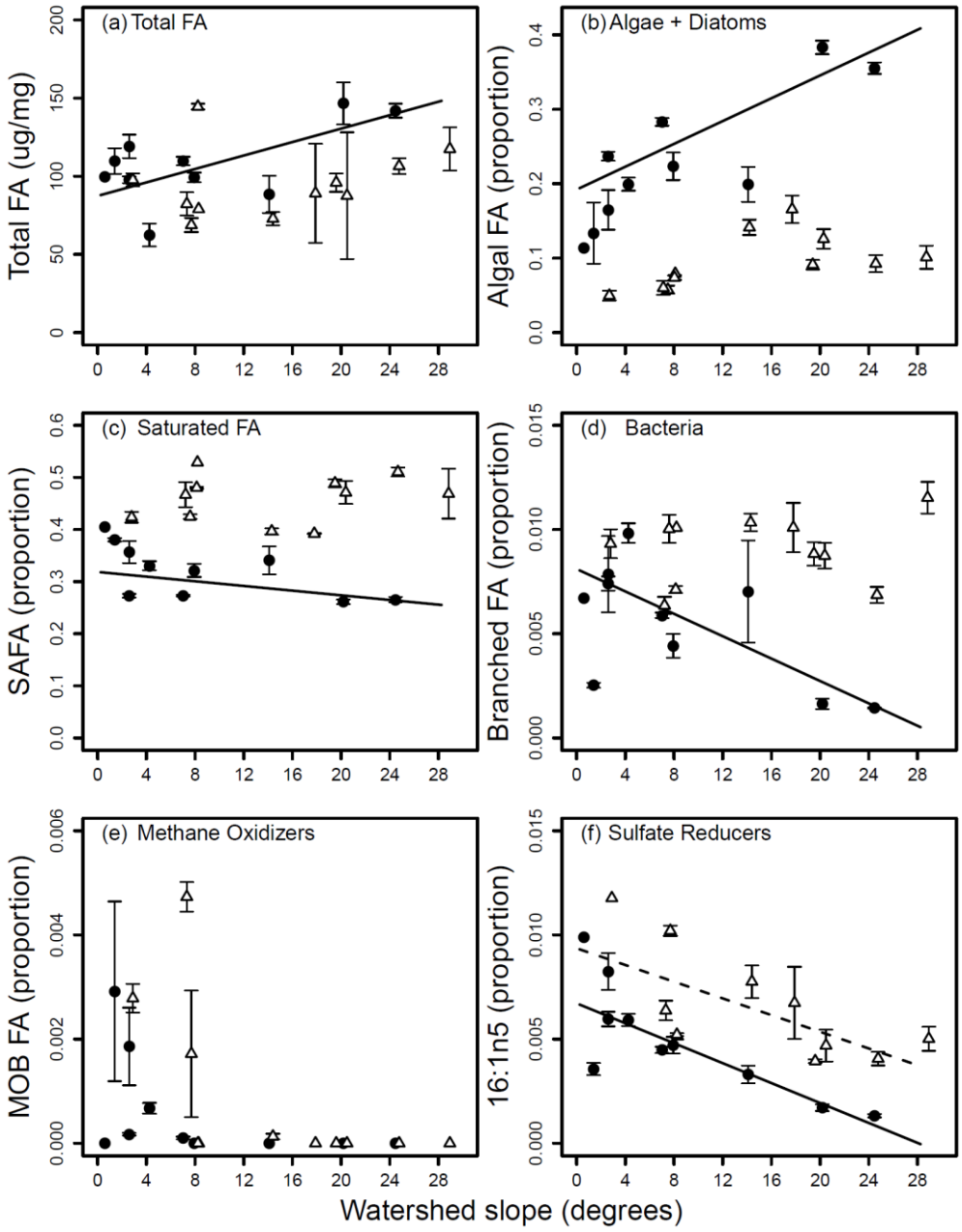
(a) Total FA
Total FA (ug/mg)
(b) Algae + Diatoms
Algal FA (proportion)
(c) Saturated FA
SAFA (proportion)
(d) Bacteria
Branched FA (proportion)
(e) Methane Oxidizers
MOB FA (proportion)
(f) Sulfate Reducers
16:1n5 (proportion)
Watershed slope (degrees)

Supplementary Information

Relationships between watershed slope and other geomorphic characteristics in the Wood River System

Results from two previous studies conducted within the Wood River basin in SW Alaska provide evidence that watershed slope is a dominant underlying control on physical and biological processes in streams. Lisi *et al.* (2013) found strong correlations between five watershed geomorphic characteristics (mean slope, watershed area, mean elevation, mean stream substrate size (D84), and total lake area), stream temperatures, and salmon spawn timing. A principal component analysis of the geomorphic attributes of 36 watersheds showed mean slope to be one of the strongest drivers of variation among sites, and that slope was highly correlated with mean elevation and stream substrate size. Jankowksi *et al.* (2014) found additional correlation between watershed geomorphology and the carbon quantity and quality in streams: watershed slope alone explained 68% of the variation in DOC concentration among streams.

Given that 11 out of 16 of our own study streams were included in the Lisi et al. (2013) analysis, and 4 out of 16 included in the Jankowski et al. (2014), we hypothesized that watershed slope, by determining stream conditions such as temperature, carbon quantity, and carbon quality, would also ultimately influence the trophic base of food webs within this system. We performed a PCA of the same geomorphic variables used in the Lisi et al. (2013) analysis on 11 of our study streams for which all such data currently exists (some streams lack substrate size measurements), and also added average summer stream temperature as a variable. We then used the resulting PC scores in regressions against our invertebrate FA data in order to test whether

using watershed slope alone as a predictor was sufficient, or whether additional variables added significant explanatory power.

Results: The first two principal component axes explained 65% and 22% of the variation among streams respectively, though only the first axis was significant ($p < 0.0001$, Figure B1). Watershed slope was strongly negatively correlated with PC1 (Table B1). Because PC2 did not explain significant variation among sites, we did not use it as a predictor in regressions.

While for some FA, using PC1 score as a predictor resulted in significantly better model fits than using only watershed slope (branched, MOB, and total FA in caddisflies, sulfate-reducing FA in mayflies), for most others it did not (Table B2).Given our original hypothesis, as well as the high correlation among geomorphic variables in the PCA, we retained watershed slope as the sole predictor variable in further analyses, rather than introduce additional explanatory variables.

Figure S1: Ordination biplot showing first two PC axes (only PC1 is significant). Open circles represent the 11 study streams included in the analysis, and vectors represent the loading of each geomorphic variable onto the pc axes. Data points close together share more similar geomorphic attributes than those that are far apart.

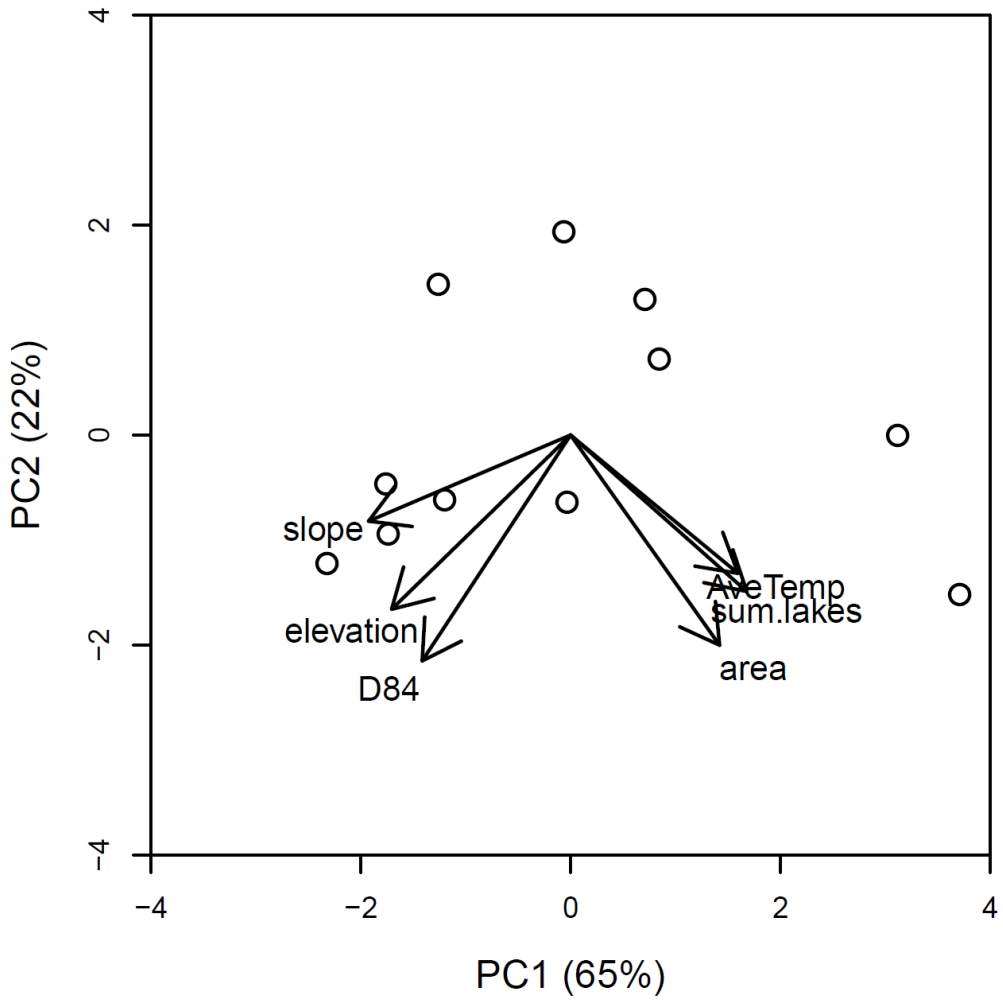

Table S1. Correlations between PC scores of each watershed and the original geomorphic variables.

Geomorphic variable	Correlation with PC1	Correlation with PC2
Mean slope (°)	-0.953	-0.24
Mean elevation (meters above sea level)	-0.844	-0.485
Watershed area (km^2)	0.703	-0.585
D84 (substrate size)	-0.7	-0.629
Sum.lakes (total lake area in the watershed, km^2)	0.832	-0.436
AveTemp (mean summer stream temperature, ° C)	0.791	-0.385

Table S2. Comparisons of regressions between geomorphic variables (either mean watershed slope or PC1 score, a linear combination of six variables) and FA proportions in invertebrates. Analyses were performed on a subset of the full data (11 out of 16 streams) for which all geomorphic attributes (slope, area, elevation, substrate size, lake area, temperature) were known.

		Predictor	
Invertebrate Group	Response variable	Slope	PC1
Caddisfly	Total FA	R^2= 0.25; p < 0.01	R^2= 0.33; p < 0.001
Caddisfly	Algal FA	R^2= 0.32; p < 0.001	R^2= 0.33; p < 0.001
Caddisfly	SAFA	p=0.4	p=0.23
Caddisfly	Branched FA	R^2= 0.36; p < 0.001	R^2= 0.45; p < 0.0001
Caddisfly	MOB FA	R^2= 0.07; p < 0.1	R^2= 0.20; p < 0.01
Caddisfly	Sulfate-reducing FA	R^2= 0.35; p < 0.0001	R^2= 0.33; p < 0.001
Mayfly	Total FA	p=0.67	p=0.76
Mayfly	Algal FA	p=0.18	p=0.16
Mayfly	SAFA	p=0.24	p=0.13
Mayfly	Branched FA	p=0.52	p=0.68
Mayfly	MOB FA	R^2= 0.33; p < 0.01	R^2= 0.36; p < 0.001
Mayfly	Sulfate-reducing FA	R^2= 0.16; p < 0.05	R^2= 0.32; p < 0.01

Table S3. List of the fatty acids that were summed into composite variables in the principal components analysis. References are included where fatty acids have been attributed to specific groups of organisms (ex. Diatoms):

Composite variable	**Fatty acids**	**References**
SAFA	C14:0, C15:0, C16:0, C17:0, C18:0, C20:0, C22:0	
Green Algae	18:2n6, 18:3n3	Torres-Ruiz *et al.* 2007
Diatoms	20:5n3, 16:4n3	Torres-Ruiz *et al.* 2007
SDA	18:4n3	
Branched (i.e. bacterial)	iso-17:0, iso-16:0, ante-iso-15:0, iso-15:0	Kharlamenko *et al.* 1995
MOB	16:1n8	Sundh *et al.* 2005; Taipale *et al.* 2012
Sulfate-reducing bacteria	16:1n5	Elvert *et al.* 2003
C16 MUFA	16:1n7, 16:1n9	
C14 MUFA	14:1n7, 14:1n5	
C18 MUFA	18:1n7, 18:1n9	
ARA	20:4n6	

References

Bartz, K. K., and R. J. Naiman. 2005. Effects of salmon-borne nutrients on riparian soils and vegetation in southwest Alaska. Ecosystems 8:529–545.

Benke, A. C., and J. B. Wallace. 1997. Trophic basis of production among riverine caddisflies: implications for food web analysis. Ecology 78:1132–1145.

Brett, M. T., M. J. Kainz, S. J. Taipale, and H. Seshan. 2009. Phytoplankton, not allochthonous carbon, sustains herbivorous zooplankton production. Proceedings of the National Academy of Sciences of the United States of America 106:21197–201.

Cole, J. J., S. R. Carpenter, M. L. Pace, M. C. Van de Bogert, J. L. Kitchell, and J. R. Hodgson. 2006. Differential support of lake food webs by three types of terrestrial organic carbon. Ecology letters 9:558–68.

Cummins, K. W. 1974. Structure and function of stream ecosystems. BioScience 24:631–641.

Dalsgaard, J., M. S. John, G. Kattner, D. Muller-Navarra, and W. Hagen. 2003. Fatty acid trophic markers in the pelagic marine environment. Pages 225–340Advances in Marine Biology.

Elvert, M., A. Boetius, K. Knittel, and B. B. Jørgensen. 2003. Characterization of specific membrane fatty acids as chemotaxonomic markers for sulfate-reducing bacteria involved in anaerobic oxidation of methane. Geomicrobiology Journal 20:403–419.

Finlay, J., S. Khandwala, and M. Power. 2002. Spatial scales of carbon flow in a river food web. Ecology 83:1845–1859.

France, R. L. 2011. Leaves as “crackers”, biofilm as “peanut butter”: Exploratory use of stable

isotopes as evidence for microbial pathways in detrital food webs. Oceanological and Hydrobiological Studies 40:110–115.

Hall, R. O., and J. L. Meyer. 1998. The trophic significance of bacteria in a detritus-based stream food web. Ecology 79:1995–2012.

Jankowski, K., D. E. Schindler, and P. J. Lisi. 2014. Temperature sensitivity of community respiration rates in streams is associated with watershed geomorphic features. Ecology 95:2707–2714.

Jones, R. I., and J. Grey. 2011. Biogenic methane in freshwater food webs. Freshwater Biology 56:213–229.

Kharlamenko, V. I., N. V Zhukova, S. V Khotimchenko, V. I. Svetashev, and G. M. Kamenev. 1995. Fatty acids as markers of food sources in a shallow- water hydrothermal ecosystem (Kraternaya Bight , Yankich Island , Kurile Islands). Marine Ecology Progress Series 120:231–241.

King, R. S., C. M. Walker, D. F. Whigham, S. J. Baird, and J. a. Back. 2012. Catchment topography and wetland geomorphology drive macroinvertebrate community structure and juvenile salmonid distributions in south-central Alaska headwater streams. Freshwater Science 31:341–364.

Krebs, C. 1999. Ecological methodology. Page tocs.ulb.tu-darmstadt.de. Second ed. Benjamin/Cummings, Menlo Park, CA.

Lau, D. C. P., T. Vrede, J. Pickova, and W. Goedkoop. 2012. Fatty acid composition of consumers in boreal lakes - variation across species, space and time. Freshwater Biology

57:24–38.

Lisi, P. J., D. E. Schindler, K. T. Bentley, and G. R. Pess. 2013. Association between geomorphic attributes of watersheds, water temperature, and salmon spawn timing in Alaskan streams. Geomorphology 185:78–86.

Marcarelli, A. M., C. V Baxter, M. M. Mineau, and R. O. Hall. 2011. Quantity and quality: unifying food web and ecosystem perspectives on the role of resource subsidies in freshwaters. Ecology 92:1215–1225.

McNeely, C., S. M. Clinton, and J. M. Erbe. 2006. Landscape variation in C sources of scraping primary consumers in streams. Journal of the North American Benthological Society 25:787–799.

McNeely, C., J. C. Finlay, and M. E. Power. 2007. Grazer traits, competition, and carbon sources to a headwater-stream food web. Ecology 88:391–401.

Moore, J. C., E. L. Berlow, D. C. Coleman, P. C. Ruiter, Q. Dong, A. Hastings, N. C. Johnson, K. S. McCann, K. Melville, P. J. Morin, K. Nadelhoffer, A. D. Rosemond, D. M. Post, J. L. Sabo, K. M. Scow, M. J. Vanni, and D. H. Wall. 2004. Detritus, trophic dynamics and biodiversity. Ecology Letters 7:584–600.

Moore, J., and D. Schindler. 2008. Biotic disturbance and benthic community dynamics in salmon-bearing streams. Journal of Animal Ecology 77:275–284.

Nichols, P. D., Guckert, J. B., & White, D. C. 1986. Determination of monosaturated fatty acid double-bond position and geometry for microbial monocultures and complex consortia by capillary GC-MS of their dimethyl disulphide adducts. Journal of Microbiological Methods

5:49–55.

Oksanen, J. F., et al. 2012. vegan: community ecology package. R package version 2.0-4. http://CRAN.R-project.org/packag=vegan

Pess, G. R. 2009. Patterns and processes of salmon colonization. University of Washington.

R Core Team. 2012. R: A language and environment for statistical computing. R Foundation for Statistical Computing. Vienna, Austria, ISBN 3-900051-07-0, URL http://www.R-project.org/.

Schlechtriem, C., M. T. Arts, and I. D. Zellmer. 2006. Effect of temperature on the fatty acid composition and temporal trajectories of fatty acids in fasting Daphnia pulex (Crustacea, cladocera). Lipids 41:397–400.

Spencer, R. G. M., G. R. Aiken, K. P. Wickland, R. G. Striegl, and P. J. Hernes. 2008. Seasonal and spatial variability in dissolved organic matter quantity and composition from the Yukon River basin, Alaska. Global Biogeochemical Cycles 22.

Strandberg, U., S. J. Taipale, M. J. Kainz, and M. T. Brett. 2014. Retroconversion of docosapentaenoic acid (n-6): an alternative pathway for biosynthesis of arachidonic acid in Daphnia magna. Lipids 49:591–5.

Sundh, I., D. Bastviken, and L. J. Tranvik. 2005. Abundance, activity, and community structure of pelagic methane-oxidizing bacteria in temperate lakes. Applied and environmental microbiology 71:6746–52.

Taipale, S., M. Brett, and M. Hahn. 2014. Differing Daphnia magna assimilation efficiencies for terrestrial, bacterial, and algal carbon and fatty acids. Ecology 95:563–576.

Taipale, S. J., M. T. Brett, K. Pulkkinen, and M. J. Kainz. 2012. The influence of bacteria-dominated diets on Daphnia magna somatic growth, reproduction, and lipid composition. FEMS Microbiology Ecology 82:50–62.

Taipale, S., U. Strandberg, E. Peltomaa, A. Galloway, a Ojala, and M. Brett. 2013. Fatty acid composition as biomarkers of freshwater microalgae: analysis of 37 strains of microalgae in 22 genera and in seven classes. Aquatic Microbial Ecology 71:165–178.

Thorp, J., and M. Delong. 2002. Dominance of autochthonous autotrophic carbon in food webs of heterotrophic rivers. Oikos 3:543–550.

Torres-Ruiz, M., J. D. Wehr, and A. A. Perrone. 2007. Trophic relations in a stream food web: importance of fatty acids for macroinvertebrate consumers. Journal of the North American Benthological Society 26:509–522.

Trimmer, M., A. G. Hildrew, M. C. Jackson, J. L. Pretty, and J. Grey. 2009. Evidence for the role of methane-derived carbon in a free-flowing, lowland river food web. Limnology and Oceanography 54:1541–1547.

Vannote, R. L., G. W. Minshall, K. W. Cummins, J. R. Sedell, and C. E. Cushing. 1980. The river continuum concept. Canadian Journal of Fisheries and Aquatic Sciences. 37*:* 130–137.

Walker, C. M., R. S. King, D. F. Whigham, and S. J. Baird. 2012. Landscape and wetland influences on headwater stream chemistry in the Kenai Lowlands, Alaska. Wetlands 32:301–310.

Wetzel, R. G. 1990. Land-water interfaces: metabolic and limnological regulators. Internationale Vereinigung fuer Theoretische und Angewandte Limnologie . 24: 6–24.

Xu, W., L. Shi, O. Chan, J. Li, P. Casper, and X. Zou. 2013. Assessing the effect of litter species on the dynamic of bacterial and fungal communities during leaf decomposition in microcosm by molecular techniques. PloS one 8:e84613.

CHAPTER 3: THERMAL CONSTRAINTS ON STREAM CONSUMER RESPONSES TO A MARINE RESOURCE SUBSIDY*

Abstract

Spawning migrations of Pacific salmon (*Oncorhynchus spp.*) to coastal watersheds provide a rich resource subsidy to freshwater consumers. However, variation in thermal regimes and spawning activity across the landscape constrain the ability of poikilothermic consumers to assimilate eggs and carcasses. We investigated how sockeye salmon (*O. nerka*) spawning density and stream temperature affect the growth, body condition, and fatty acid composition of juvenile coho salmon (*O. kisutsh*), a known egg predator, in 7 tributaries of the Wood River in southwest Alaska. We compared mean body size of juvenile coho salmon in late summer among 3-7 years per stream and found that the largest mean size occurred in warm streams where sockeye salmon spawned, though overall subsidy magnitude (spawner density) had no effect on consumer body size. Individuals that consumed more salmon eggs (estimated from $\delta^{15}N$) were larger, and had altered fatty acid composition, but did not have higher relative body condition. These results indicate that effects of marine subsidies on freshwater consumers depend both on local habitat conditions and on individual variation in energy allocation.

***Full Citation:** *Adrianne P. Smits, Daniel E. Schindler, Jonathan B. Armstrong, Michael T. Brett, Jackie L. Carter, and Bianca S. Santos. 2016. Canadian Journal of Fisheries and Aquatic Sciences, 10.1139/cjfas-2015-0420*

Introduction

Resource subsidies between ecosystems, for example from ocean to land, or from forests to freshwaters, are ubiquitous and increasingly well-described, with much focus applied to quantifying subsidy magnitudes (Marczak et al. 2007). These efforts have resulted in the realization that the effects of subsidies on recipient ecosystems vary according to food web structure, consumer life histories, and local environmental conditions (Marczak et al. 2007, Yang et al. 2010). Interactions between local conditions and ecosystem responses to subsidies occur across diverse geographic regions and taxonomic groups. For example, nutrient additions from seabird guano to South Pacific island soils enhance tree growth only after strong El Niño rains, which cause seabirds to abandon nesting colonies, thereby relieving trees from the damage they cause (Molina-Montenegro et al. 2013). Abundance of alternative food sources can also mediate consumer responses to subsidies—migratory geese subsidize Arctic fox reproduction in tundra environments, but only make up a significant portion of fox cub diets when local rodent populations are low (Giroux et al. 2012). Despite emerging evidence for strong interactions between local ecological conditions and consumer responses to subsidies, many studies are conducted at coarse scales that integrate across local variation, and are designed primarily to quantify effects of different subsidy magnitudes (Marczak et al. 2007).

Returns of Pacific salmon (*Oncorhynchus spp.*) to spawning grounds along the west coast of North America provide a substantial marine-derived resource subsidy to aquatic and terrestrial consumers such as bears, birds, insects, and resident fishes (Gende et al. 2002, Schindler et al. 2003). Consumption of salmon eggs and carcasses enhance growth and productivity of many stream organisms (Chaloner et al. 2002, Scheuerell et al. 2007, Bentley et al. 2012, Swain et al. 2014). However, even in regions with high overall salmon returns, spawning occurs patchily across space and time, constraining the ability of consumers to access marine-derived resources.

In SW Alaska, landscape features such as the presence of nursery lakes determine suitable spawning habitat for sockeye salmon (*O. nerka*), and therefore create spatial variation in access to eggs and carcasses. Sockeye returns to individual spawning sites can also vary by orders of magnitude among years (Rogers and Schindler 2008). Large, mobile consumers such as bears and birds track variation in salmon resources across space and time (Schindler et al. 2013), but less mobile consumers such as insects and small fishes likely cannot, potentially creating differences in growth and condition among populations and individuals.

Salmon eggs and carcasses are more nutrient and energy rich than other food sources available to stream predators in high latitude streams (Gende et al. 2004). As a result, consumption of salmon resources should increase growth and fat accumulation in stream organisms, and ultimately improve their survival at subsequent life stages. Experimental addition of salmon eggs and carcasses to stream reaches or enclosures often induce rapid, positive changes in growth and lipid composition of consumers (Wipfli et al. 2003, Heintz et al. 2004). Poly-unsaturated fatty acids (PUFA) such as docosahexaenoic acid (DHA), eicosapentaenoic acid (EPA), and arachidonic acid (ARA) are chemical precursors for a range of important cellular components and hormones and cannot be synthesized de novo by most vertebrates, therefore adequate dietary inputs of these lipids are crucial for fish development and growth (Ahlgren, Vrede, and Goedkoop 2009). Adult salmon tissues, like many other marine fishes, are much higher in DHA, EPA, and ARA than freshwater organisms, making them an important potential source of these lipids for stream consumers (Heintz et al. 2010).

The strong positive effects of egg and carcass consumption on growth and body condition observed in small-scale experiments demonstrate the potential benefits of salmon resources to stream consumers, but complexity in natural environments may mediate these effects in wild

populations (Armstrong et al. 2010). At high latitudes, temperature acts as an additional constraint on the capacity for ectotherms to exploit resource subsidies. By strongly mediating metabolic rate, temperature affects the serial processes in the food-to-fuel pathway, spanning from foraging to fat deposition and somatic growth (Weiner 1992). For example, cold temperatures can generate digestive constraints on foraging when food is abundant (Elliott and Persson 1978). Armstrong et al. (2013) showed that juvenile coho salmon are digestively constrained when foraging on salmon eggs, and that these constraints were especially severe when temperatures were reduced from 10 °C to 6°C. Therefore even if high quality resources such as salmon eggs are present, low water temperatures may limit the benefits that cold-blooded consumers derive from them.

In this study we investigated how local environmental conditions (i.e., water temperature) regulate the ability of juvenile coho salmon (*O. kisutsh*), a known egg predator, to capitalize on resource subsidies provided by spawning sockeye salmon. Streams within our study watershed (Wood River system, southwest Alaska) differ significantly in their thermal regimes due to variation in geomorphic conditions (Lisi et al. 2013), and receive highly variable numbers of adult sockeye salmon each year. We asked 1) how juvenile coho salmon in different thermal environments and receiving different subsidy magnitudes varied in body size at the end of the summer growth season, and 2) how individual consumers within these populations differed in their physiological responses to resource subsidies, as measured by their body condition and fatty acid composition.

To address the first question, we compared mean end-of-summer size of age-0 and age-1 coho salmon in 7 study streams across multiple years to test the effects of variation in the density of spawning sockeye salmon and water temperature on growth. We expected that coho salmon

would be larger in streams and years with higher sockeye spawner densities, in response to higher egg abundance. We also predicted that higher stream temperatures would result in larger coho salmon body size, as mean temperatures at our study sites are low relative to their thermal optima (Stewart and Ibarra 1991). We expected that the effects of sockeye salmon spawner abundance (i.e. egg abundance) on growth would be temperature-dependent, with coho salmon achieving larger body size in warm streams where energy-rich eggs were present. In cold streams, on the other hand, we expected coho salmon would be limited in their ability to assimilate eggs, and thus would not grow as large despite the presence of energy-rich food resources.

To address our second question, we tested whether individual variation in egg consumption was associated with differences in body size, condition, and fatty acid composition. We compared body size, relative body condition, and fatty acid composition of age-1 coho salmon collected in late summer in 2010 and 2011 from the same 7 study streams and used muscle tissue $\delta^{15}N$ to estimate their assimilation of salmon resources. We predicted that juvenile coho salmon showing high egg predation would grow larger and have better relative body condition than individuals who assimilated fewer marine resources. We also expected that egg-consumption would shift the fatty acid composition of lipid stores within coho salmon muscle tissue by elevating concentrations of omega-3 fatty acids such as DHA (22:6n3) and EPA (20:5n3), which are crucial to salmonid development (Heintz et al. 2010).

Methods

Field sampling

Juvenile coho salmon were sampled from seven streams in the Wood River watershed in the Bristol Bay region of southwest Alaska (59°20′ N, 158°40′W). Annual sockeye salmon (*O.*

nerka) escapement to this system has averaged 1.1 million over the last 50 years (Baker et al. 2006). Three of the streams (Bear, Yako, Whitefish) are tributaries of Lake Aleknagik, two (Fifer, Silver Salmon) are tributaries of the lower Wood River, one (Squaw) flows into Nushagak Bay, and one (Lynx Creek) is a tributary of Lake Nerka. Sampling sites within all streams are low gradient (0.5-1%), low elevation (<100 m above sea level), and range in bank-full width from 4 to 15 m (Marriott 1964). Four of these streams (Bear, Yako, Whitefish, Lynx) are habitat for spawning sockeye salmon, while three are not (Squaw, Fifer, Silver Salmon). The streams without sockeye salmon spawning lack suitable nursery lake habitat for juvenile sockeye salmon, and receive an occasional small number of spawning pink salmon, but are otherwise similar to sockeye spawning streams.

Between ten and thirty juvenile coho salmon were collected for stable isotope and fatty acid analyses with a stick seine on one sampling date per stream (late August through early September in 2010 or 2011). Sockeye streams were sampled concurrently or after the active sockeye salmon spawning period. Fork length and wet mass were measured on site (Table S1), with fork length ranging from 70 to 140 mm, large enough to prey on sockeye eggs (Armstrong et al. 2010). Fish were frozen at -20 °C until further analysis. Aquatic insect taxa previously detected in juvenile coho salmon diets (Trichoptera, Ephemeroptera, Plecoptera, Diptera; Armstrong et al. 2010, Armstrong and Schindler 2013) were collected by Surber sampling from at least three reaches in each stream except for Fifer Creek. Insect samples were sorted by order and frozen at -20 °C until analysis for carbon and nitrogen stable isotope ratios.

The effects of stream temperature and sockeye salmon spawner abundance on late summer size distributions of juvenile coho populations were assessed using multi-year data collected in Bear (2007-2012), Whitefish (2007-2012), Yako (2007-2012), Lynx (2008-2013),

Silver Salmon (2007-2012) , Fifer (2009-2011), and Squaw (2012-2013) creeks. Juvenile coho salmon were collected in each stream by stick seining in the last week of August or first week of September. Fish were then anaesthetized with MS-222 and measured for fork length. A subset of the fish were weighed on an electronic scale.

In streams that support sockeye salmon spawning (Bear, Whitefish, Yako, Lynx), live and dead spawners were counted at least three times per season, by walking upstream and recording numbers in 200 m stream reaches until at least three consecutive reaches without salmon were observed. Peak spawner density (spawners*m^{-2}) was calculated by dividing peak spawner count by the distance surveyed and mean stream width.

In each of the sampling years, I-button temperature recorders (Maxim Integrated Products, Sunnyvale, CA) were placed in stream mouths, suspended 3-5 cm above the streambed, to record temperatures at 90-min intervals with 0.125 to 0.5 °C resolution from June 30 to September 1. Mean summer temperature for each stream was calculated from these data (Lisi et al. 2013).

Stable isotope analysis

Because sockeye salmon put on the majority of their mass in the ocean where they occupy a relatively high trophic position, and rarely feed upon re-entry to freshwater, their tissues, including eggs, are enriched in heavier isotopes of carbon and nitrogen (Kline et al. 1990), allowing the tracing of these resources through aquatic food webs. We used carbon ($\delta^{13}C$) and nitrogen ($\delta^{15}N$) stable isotope ratios of coho dorsal muscle tissue as measures of diet composition and trophic level. Reichert et al. (2008) measured seasonal change in muscle tissue stable isotope signatures of juvenile coho salmon in the Skagit River, WA, and found elevated $\delta^{15}N$ in coho salmon in spring after over-winter feeding on salmon carcasses. Our samples were

collected in late August or early September, allowing juvenile coho salmon at least four weeks of access to sockeye salmon resources, and thus muscle $\delta^{15}N$ and $\delta^{13}C$ should reflect this diet source if it was assimilated. Samples were analyzed at the Isolab at University of Washington on a Thermally-Coupled Elemental Analyzer (TC-EA) coupled to a Thermo-Finnigan MAT253 Mass Spectromoter to determine $\delta^{13}C$ and $\delta^{15}N$. Results are reported as deviations from international standards (‰; Vienna Pee Dee Belemnite for $\delta^{13}C$, atmospheric N for $\delta^{15}N$). Because the coho muscle samples had high C:N ratios (mean = 3.53), $\delta^{13}C$ values were adjusted for lipid content based on empirical corrections provided in Post et al. (2007).

Fatty acid analysis

Fatty acid extraction and analysis of coho salmon muscle tissue was performed as described in Strandberg et al. (2014). Samples were weighed (1-2 mg dry weight), then extracted with chloroform/methanol/water (2:1:0.8, by volume). Lipids were dissolved in toluene and trans-methylated at 50 C for 16 h, using an acidic catalyst (1 % H2SO4 in methanol). The resulting fatty acid methyl esters (FAME) were analyzed at the University of Washington, with a HP6890 gas chromatograph (GC), equipped with flame ionization detection (FID), using a DB-23 capillary column (length 30 m, ID 0.25 mm, film thickness 0.25 mm, Agilent) with helium as carrier gas (1 mL min-1). FAME were tentatively identified by comparison of retention times with known standards (37-component FAME mix, Supelco).

For final determination of peak identities, a subset of samples was analyzed by gas chromatography/mass spectrometry (Shimadzu GCMS QP2010 plus; Agilent DB-23 column) with splitless injection. Double-bond configuration of C16 and C18 mono-unsaturated fatty acids (MUFA) was determined by analysis of their dimethyl disulphide adducts (Nichols et al. 1986).

In all, 40 fatty acids were identified, and all data were mass corrected as well as converted to proportion of total fatty acids ([g FA methyl ester/g total FA methyl ester]).

We used the following shorthand notation for referring to fatty acids: A:BnX, where 'A' is the number of carbon atoms, 'B' is the number of double bonds, and 'X' is the position of the first double bond relative to the methyl end. Saturated fatty acids (SAFA) have no double bonds, mono-unsaturated fatty acids (MUFA) have one double bond, and poly-unsaturated fatty acids (PUFA) have 2 or more double bonds.

The fatty acid composition of an animal's storage lipids should reflect a mixture of the FA compositions of its prey, and ultimately the FA produced at the base of the food web by plants, algae, and bacteria (Dalsgaard et al. 2003). Certain fatty acids are produced in higher concentrations by marine organisms—for example 20:1n9 and 20:1n11 are most likely derived from marine calanoid copepods and are found in elevated concentrations in adult salmon tissue (Heintz et al. 2010). Adult salmon returning from the ocean also have substantially higher proportions of omega-3 fatty acids such as EPA and DHA than do freshwater organisms such as aquatic insects or juvenile coho salmon. As a result, freshwater consumers that assimilate salmon carcasses or eggs can accumulate marine-derived lipids in their own fat stores (Heintz et al. 2010). Therefore, elevated concentrations of these biomarkers in freshwater organisms can indicate consumption of marine-derived resources such as salmon tissue.

Effect of temperature and subsidy magnitude on body size in juvenile coho salmon

Because juvenile coho salmon in Alaskan streams typically rear in freshwater for two years (Quinn 2005), stream populations are mixtures of two age classes with potentially different responses to temperature and sockeye egg abundance. For example, previous work shows that coho salmon are gape-limited in their ability to consume water-hardened salmon eggs until they

grow to approximately 70 mm in length, thus limiting the benefit of this resource subsidy for all but the largest age-0 fish (Armstrong et al. 2010). Late summer size distributions of juvenile coho salmon in all 7 study streams were roughly bimodal (Figures S1-S7): size thresholds for the two age classes present (age 0 and age 1) were determined from these distributions. Coho salmon in a given stream and year were assigned an age class based on the size threshold for that stream-year combination.

We tested the effects of temperature, sockeye spawning presence/absence, sockeye spawner density, and any interactions on mean late summer body size of age-0 and age-1 coho salmon using multiple linear regression in R (R Core Development Team 2013). To account for non-independence of data collected from the same stream, we followed the model selection protocol outlined in Zuur et al. (2009). We first compared random model structures using Akaike's information criterion, corrected for small sample sizes (AICc; Burnham and Anderson 2002). We compared the following model structures: no random effects, a random intercept, and random intercept and slope, and found that the model without random effects fit the data best (ΔAICc >2 for models that included random effects of stream). Fixed effects only models were then fit using maximum likelihood and compared using AICc. AICc model weights were calculated as described in Burnham and Anderson (2002).

Individual variation in physiological responses to salmon resource subsidies

We examined differences in late summer energetic status and fatty acid composition of age-1 juvenile coho salmon collected in 2010 and 2011. Variation in fatty acid composition among coho salmon from different streams (and therefore different access to marine-derived resources) was first assessed with principal component analysis (PCA), using the vegan package in R (Oksanen et al. 2012). For ease of interpretation, proportions of structurally similar FA's

were summed, resulting in 22 FA variables used in subsequent analyses (results were similar using all 40 variables). Prior to statistical analyses, FA data were log-transformed to adjust for right-skew. Significance of the resulting eigenvalues was tested using Monte Carlo randomization (1000 permutations). To test whether coho salmon differed significantly in overall FA composition among streams, we used analysis of similarity (ANOSIM; Clarke 1993), a non-parametric multivariate procedure analogous to an ANOVA. The test statistic, R, if greater than zero, denotes that between-group dissimilarities are significantly larger than within-group dissimilarity. In addition, we tested for differences in proportions of specific FAs (22:6n3, DHA; C_{20}+C_{22} MUFA; 20:5n3, EPA; 18:2n6, LIN; 18:3n3, ALA) between 'sockeye' versus 'non-sockeye' groups, using mixed effects regression with the lme4 package in R (Bates et al. 2015).

We tested whether the contribution of sockeye salmon resources to age-1 coho diets (n=90) affected measures of body size, condition, and FA composition using mixed effects linear regression models in the lme4 package in R (Bates et al. 2015), following the model selection protocol described in Zuur et al. (2009).

Coho diet proportions were estimated by treating an individual's $\delta^{15}N$ as a mixture of two sources (sockeye eggs and aquatic invertebrates; Figure 1). Aquatic invertebrates from each stream except Fifer creek were analyzed for $\delta^{15}N$, thus we were able to use stream-specific $\delta^{15}N$ values in diet mixture calculations. For Fifer creek we used Squaw creek insect $\delta^{15}N$ values, because Squaw is the closest study stream and is similar in habitat characteristics. We used an average $\delta^{15}N$ value for sockeye eggs (11.97 ‰ ± 0.20, mean, standard deviation, n = 13) in calculations, from samples collected in the Wood River watershed in 2013. Invertebrate and sockeye egg $\delta^{15}N$ values were corrected for trophic discrimination before calculating diet

contributions (+ 3.4 ‰; Post 2002). We used the following equations to calculate the fraction of coho salmon diet made up by eggs (f_{egg}):

$$\delta^{15}N_{coho} = f_{insect}\delta^{15}N_{insect} + f_{egg}\delta^{15}N_{egg}$$

$$f_{insect} + f_{egg} = 1$$

F_{egg}, hereafter referred to as 'egg consumption', was subsequently used as predictor variable in regression models.

We calculated the relative body condition (e.g. wet mass residual) of each coho salmon and used this as a response variable in our regression models. Individuals with a positive relative body condition are heavier given their length than the population average. We defined relative body condition as an individual's residual from the linear relationship between log-mass and log-length of the entire population. Data from juvenile coho salmon measured between 2007 and 2012 in all seven study streams were included in the length-weight regression (n=7927). Relative body condition of individual coho salmon was calculated using the regression coefficients output from this model. Yako creek fish used in FA analyses lacked wet weight measurements and were thus excluded from this analysis.

Results

Effect of temperature and subsidy magnitude on body size in juvenile coho salmon

Juvenile coho salmon in both age classes grew largest in warm streams (average >10 °C) where sockeye salmon spawned (Whitefish, Lynx; Figure 2a and 2c). Increased subsidy magnitude (spawner density) did not result in larger average body size for either age class at the end of the growing season (Figure 2b and 2d).

The best model for late summer body size attained by age 0 coho salmon included a significant positive interaction between sockeye spawning presence and stream temperature (AIC_c weight = 0.95; see Table 1 for model comparisons). Models including sockeye spawning density as a predictor variable fit the data significantly worse than alternative models (ΔAICc > 17).

Similar to age 0 coho salmon, the best model for age 1 body size included a significant positive interaction between temperature and sockeye spawning presence (AIC_c weight = 0.70; Table 1), whereas a model including sockeye spawner density had significantly less support (ΔAIC_c >20).

Effects of sockeye egg consumption on individual size, condition and FA composition

The first two axes of the PCA comparing fatty acid compositions of age 1 coho salmon were significant and explained 28% and 21% respectively of the variation among individuals (n=90; $p < 0.001$, Figure S8). All 22 FA variables loaded onto both axes, though PC axis 2 roughly characterized a gradient in marine-derived/associated fatty acids (C20 + 22 MUFA, EPA, and DHA versus LIN, ALA; Table S2). While there was substantial overlap in FA composition between coho salmon from sockeye and non-sockeye streams, the two groups separated weakly along PC axis 2, and the ANOSIM indicated that they differed significantly in overall FA composition ($R = 0.24$, $p < 0.001$). Stream populations also had significantly different FA compositions ($R= 0.36$, $p < 0.001$).

Coho salmon in sockeye spawning streams had higher proportions of marine derived or associated FA such as DHA (n= 55, mean = 0.27 ± 0.049, p=0.24) and C_{20} + C_{22} MUFA (0.01 ± 0.0061, p=0.10) than those in non-sockeye streams (n= 35, DHA 0.23 ± 0.07, C_{20}+C_{22} MUFA 0.0057±0.0049), but differences were not statistically significant when random effects (stream)

were included in models. Coho salmon in non-sockeye streams had higher proportions of LIN (0.051±0.017, p=0.10) and ALA (0.043±0.014, p=0.51) than coho salmon in sockeye streams (LIN: 0.037±0.009 , ALA: 0.028±0.008) but differences were not statistically significant; these FA are abundant in freshwater invertebrates (Torres-Ruiz et al. 2007, Smits et al. 2015). Coho salmon did not differ significantly in their proportion of EPA (overall mean 0.09 ± 0.017). Coho salmon in sockeye spawning streams had higher total FA concentration in their muscle tissue (38.14 ± 20.65 µg/mg dry weight, p=0.34) than those in non-sockeye streams (30.97 ± 17.27 µg/mg).

Body size of age 1 coho salmon was positively related both to stream temperature and to egg consumption (Figure 3). The best model fit the data significantly better than alternative models and included both egg consumption as well as its positive interaction with stream temperature as significant predictors of individual body size (AIC_c weight = 0.96; Table 2).

Relative body condition, which has been correlated with the recent growth rate in other fish species within our study watershed (Bentley and Schindler 2013), was positively but weakly related to egg consumption and to stream temperature. The best model was an intercept only model, including random effect of stream (Table 2), but there was little statistical support for any one model (AIC_c weight < 0.5 for all models). Within individual stream sites, higher egg fraction in coho salmon diets did not result in higher relative body condition (Figure 4), but stream populations differed from one another, with the highest condition fish occurring in warm, sockeye spawning streams (Whitefish and Lynx creeks).

Consumption of sockeye salmon eggs was associated with altered FA composition of age 1 coho salmon (Figure 5), though it did not affect the total FA concentration within their muscle tissue (p = 0.25; Figure 5a). As expected, individuals who consumed more sockeye eggs had

elevated proportions of $C_{20} + C_{22}$ MUFA, reflecting a marine-derived food source (Figure 5b). The best model included a random effect of stream on the intercept, as well as egg consumption as a direct effect: models including stream temperature as a predictor fit the data significantly worse ($\Delta AIC_c > 2$, Table 2). Coho salmon that ate more eggs had higher omega 3: omega 6 FA ratios (Figure 5c): the best model included a random effect of stream on the intercept, as well as egg consumption as a predictor variable (AIC_c weight = 0.60; Table 2). Models that included stream temperature as a predictor fit the data significantly worse than alternative models ($\Delta AIC_c > 2$).

Discussion

Multiple years of juvenile coho salmon size data showed that temperature strongly controls consumer growth responses to a marine resource subsidy. The presence of sockeye salmon eggs as a food resource substantially increased the mean body size of juvenile coho salmon in warm streams (> 10° C): coho salmon in Whitefish and Lynx creeks were on average 20 mm larger in late August than those in Silver Salmon Creek, a stream with comparable summer temperatures (Figure 2). On the other hand, the presence of sockeye eggs did not enhance growth in cold streams: coho salmon were no larger on average in Bear or Yako creeks than in Fifer or Squaw creeks. These divergent size distributions in cold and warm sockeye spawning streams are consistent with previous findings that warm temperatures allow age 0 coho salmon to outgrow gape limitation and consume sockeye eggs, which then further accelerates their growth (Armstrong et al. 2010). While juveniles in warm streams such as Silver Salmon Creek have higher growth potential than those in cold streams (Armstrong et al. 2010), this potential remains unrealized in non-sockeye streams, presumably because these sites lack the energy-dense resources fish need to overcome increased metabolic costs.

Contrary to our initial hypotheses, juvenile coho salmon did not grow larger in streams or years with higher subsidy magnitudes (sockeye spawner density). While the presence of sockeye salmon spawning, and thus eggs, significantly increased coho salmon growth in warm streams, and egg consumption by individuals was associated with larger body size, growth was not affected by sockeye salmon abundance in these streams. This was somewhat surprising because small resident fishes must prey on eggs ejected from the gravel during spawning or nest-digging: in high return years, redd superimposition greatly increases egg availability to consumers in the stream channel (Moore et al. 2008). Our findings contrast with studies conducted in south central Alaska and the Pacific Northwest; $\delta^{15}N$ enrichment and condition in sculpins was positively correlated with salmon spawning density in British Columbia streams (Swain et al. 2014), and juvenile coho salmon were more $\delta^{15}N$-enriched and had higher growth rates in south central Alaska streams with higher salmon spawner biomass (Rinella et al. 2011). Growth responses by other resident fish species (grayling, rainbow trout) to egg subsidies within the Wood River system corresponded with sockeye salmon run size as well as underlying stream productivity, though the growth responses saturated at relatively low spawner densities (Bentley et al. 2012). However, similar studies in the Copper River Delta, Alaska, did not detect strong growth responses by juvenile coho salmon with access to spawning salmon resources (Lang et al. 2006), despite $\delta^{15}N$ enrichment at multiple trophic levels (Hicks et al. 2005).

There are several potential reasons why sockeye density (i.e. egg abundance) is uncorrelated with juvenile coho salmon growth in Wood River watersheds. First, competition among juvenile coho salmon for eggs is likely weak due to a food-saturated environment in sockeye spawning streams. Juvenile coho salmon density is low, whereas sockeye salmon density varies between years but can be relatively high for 1^{st} – 3^{rd} order streams (>1 spawner*m^{-2}). In lower latitude

streams with reduced salmon spawning populations, on the other hand, egg abundance may be low enough to constrain consumer growth. Second, stream temperature controls assimilative capacity in juvenile coho salmon: a tagging study in Bear Creek showed that individuals who migrated to warm microhabitats after consuming eggs grew substantially larger than individuals that did not (Armstrong et al. 2013). Further, even in warm habitats closer to the physiological optimum for coho salmon (~ 15°C; Stewart and Ibarra 1990), individuals were strongly digestively constrained (i.e. digestion rates were 200 - 400 % slower than maximum foraging rates) due to their large meal size and the long gut retention time for eggs (Armstrong et al. 2013). Most streams within the Wood River watershed are colder than thermally optimal for coho salmon, therefore the distribution of favorable thermal habitat may present a greater constraint on digestive capacity and growth than egg abundance.

Consistent with previous experimental and observational studies (Heintz et al. 2004, 2010), egg consumption shifted the FA composition of juvenile coho salmon towards higher proportions of marine-associated biomarkers (20:1n9, 20:1n11, DHA). However, contrary to the rapid fat accumulation observed in other studies, wild individuals in Wood River streams that consumed more salmon resources did not accumulate higher total concentrations of FA in their muscle tissue (Figure 5A). Further, while we observed differences in relative body condition among six stream populations, with the heaviest fish occurring in warm sockeye spawning streams (Whitefish, Lynx), within individual sockeye spawning streams, relative body condition was unrelated to egg consumption. Long winters at northern latitudes present a substantial period of resource scarcity for consumers, and fishes with higher lipid levels in autumn survive winter at higher rates (Post and Parkinson 2001b, Biro et al. 2004). Therefore, we expected juvenile coho salmon with access to abundant, high quality resources to allocate excess energy towards fat

stores. Instead, there was a high degree of variation in the allocation of energy to FA storage and growth among individuals living in the same environment, and consuming similar diets (as inferred from $\delta^{13}C$ and $\delta^{15}N$). The lack of clear responses (FA accumulation, body condition) to egg consumption by fish in this study, which contrasts with previous findings (Heintz et al. 2004; Rinella et al. 2011), may stem from ontogenetic shifts in lipid storage and metabolism. We analyzed only age 1 coho salmon for FA composition and body condition, whereas other studies showing responses in lipid accumulation analyzed mainly age 0 coho salmon (Heintz et al. 2004; Rinella et al. 2011). Because we did not analyze any age 0 fish, we cannot test for different responses among age classes, but this presents an important gap in our understanding of the effects of salmon egg subsidies on juvenile salmonids.

Tradeoffs between fat storage and somatic growth in temperate and high latitude fishes may occur for several reasons: large fish are less vulnerable to predation, while mass-specific metabolic rate decreases with larger body size (lower starvation risk; Post and Parkinson 2001, but see Connolly and Petersen 2003). Egg consumption was most directly related to increased body size rather than FA content or body condition—it may be more advantageous for consumers in these streams to grow larger during the summer than to allocate energy to lipid reserves. Armstrong et al. (2013) observed highly variable foraging strategies among juvenile coho salmon within a single sockeye-spawning stream (Bear Creek); our results show similar diversity in energy allocation among individuals. Extreme inter-annual variation in sockeye salmon abundance (Rogers and Schindler 2008), coupled with spatial heterogeneity in flow and temperature (Armstrong and Schindler 2013), likely support multiple evolutionarily stable strategies for resource use and energy allocation by juvenile coho salmon.

The individual variation in FA composition we observed in juvenile coho salmon, while largely related to differences in diet, may also reflect differential retention of essential FAs versus non-essential FAs. There is some evidence that fish can preferentially retain or metabolize FAs depending on environmental and physiological conditions: Bendiksen and Jobling (2003) found that Atlantic salmon parr strongly retained omega-3 essential FA, but not omega-6 FA, relative to the proportions in diets, and that retention increased at lower temperatures and with low-lipid diets. While most studies of FA metabolism involve laboratory feeding experiments rather than natural populations, it is likely that FA composition in wild individuals varies for reasons besides diet. For example, age 1 coho salmon in Squaw creek, a non-sockeye stream, had DHA proportions (mean= 0.29 ± 0.07) as high as juvenile coho salmon in Whitefish creek, a sockeye stream (mean = 0.26 ± 0.03), despite lacking DHA-rich food resources such as salmon eggs (stream insects contain only trace levels of DHA; Smits et al. 2015). Squaw creek coho salmon had the lowest relative body condition of all individuals sampled (Figure 4), thus high DHA retention (and preferential metabolism of non-essential FA) may reflect physiological responses to caloric deficits. High proportions of DHA, or conversely, low proportions of other marine biomarkers such as $C_{20} + C_{22}$ MUFA in consumer tissue, should not necessarily be interpreted as an individual's degree of reliance on marine resources.

Geomorphology, hydrology, and climate interact to generate complexity in habitats and resources for freshwater consumers. Consumer responses to resource subsidies should reflect this complexity. Much of the literature on marine subsidies provided by spawning Pacific salmon ignore the mediating effects of local environment on consumer responses. While it is now recognized that incorporation of salmon-derived nitrogen by freshwater and riparian primary producers depends on the presence of alternative nitrogen sources within watersheds (i.e. N-

fixing plants such as alder; Helfield and Naiman 2002, Hocking and Reynolds 2011), similar interactions at higher trophic levels remain less well characterized. Our results show that the benefits of salmon subsidies to consumers often depend as strongly on environmental conditions as on the magnitude of resource pulses.

As boreal and arctic regions warm due to climate change, production and growth of freshwater organisms may improve as temperatures approach thermal optima for certain species. However, resultant increases in metabolic costs for consumers must be offset by adequate food resources to sustain higher production. A forty year time series of juvenile sockeye salmon size data in SW Alaska lakes showed that while earlier spring ice breakup and higher zooplankton abundance led to higher summer growth, the negative effects of con-specific density were on average twice as large, demonstrating the complexity of ecological responses to climate change (Schindler et al. 2005). Our results show that warm temperatures must be coupled with an abundant food resource subsidy to enhance body size in juvenile coho salmon. As temperatures continue to warm, releasing freshwater consumers from thermal constraints, resource abundance may become an increasingly important control on production in high latitude systems. Managing populations in the future may be improved by understanding the interactions between the physical and chemical attributes of landscapes and resource availability for consumers. Maintaining habitat heterogeneity may be an effective management approach where future climate impacts on species and landscapes remain uncertain.

Tables

Table 1. Linear models considered for mean late summer body size of age 0 and age 1 coho salmon (2007-2014) in Bear, Yako, Whitefish, Lynx, Silver Salmon, Fifer, and Squaw Creek. K is the number of parameters estimated in each model. The optimal models for age 0 and age 1 coho mean body size are highlighted in bold font. No random effects were included in models.

	Predictors	Sample Size	K	AICc	ΔAICc	AICc Weight	Adjusted R^2
Age 0	**Temperature; Spawner presence; Interaction**	**39**	**5**	**215.0**	**0.0**	**0.95**	**0.74**
	Temperature; Spawner presence	39	4	221.0	5.7	0.05	0.6785
	Temperature; Spawner density; Interaction	39	5	233.0	17.9	0	0.558
	Temperature; Spawner density	39	4	234.0	18.5	0	0.527
	Temperature	39	3	234.0	18.7	0	0.501
	Spawner presence	39	3	253.0	37.5	0	0.1192
	Spawner density	39	3	257.0	42.4	0	-0.021
Age 1	**Temperature; Spawner presence; Interaction**	**33**	**5**	**218.7**	**0.0**	**0.70**	**0.672**
	Temperature; Spawner presence	33	4	220.4	1.6	0.30	0.637
	Spawner presence	33	3	240.5	21.7	0	0.3
	Temperature; Spawner density	33	4	240.8	22.0	0	0.326
	Temperature	33	3	241.7	22.9	0	0.274
	Temperature; Spawner density; Interaction	33	5	242.7	24.0	0	0.32
	Spawner density	33	3	253.3	34.6	0	-0.03

Table 2. Mixed effects linear regression models considered for body size (fork length; mm), relative body condition, and fatty acid composition (proportion of total) of individual age 1 coho collected in 2010 and 2011 from Bear, Yako, Whitefish, Lynx, Silver Salmon, Fifer, and Squaw Creek. F_egg refers to the proportion of coho salmon diet made up by sockeye eggs (i.e. egg consumption). The optimal models are highlighted in bold font.

Response	Random effects	Predictors	Sample Size	K	AICc	ΔAICc	AICc weight
Fork Length (mm)	None	**f_egg; Temperature; Interaction**	**76**	**5**	**578.0**	**0.0**	**0.96**
		f_egg; Temperature	76	4	584.4	6.4	0.04
		f_egg	76	3	593.5	15.5	0
		Temperature	76	3	594.3	16.3	0
		Intercept only	76	1	602.6	24.6	0
Relative Body Condition	Random effect of stream on intercept	**Intercept only**	**65**	**3**	**-134.7**	**0.0**	**0.46**
		f_egg	65	4	-133.2	1.1	0.26
		Temperature	65	4	-132.3	2.0	0.17
		f_egg; Temperature	65	5	-130.9	3.3	0.09
		f_egg; Temperature; Interaction	65	6	-128.6	5.6	0.03
C20 + 22 MUFA	Random effect of stream on intercept	**f_egg**	**76**	**4**	**-598.5**	**0.0**	**0.64**
		f_egg; Temperature	76	5	-596.2	2.3	0.20
		f_egg; Temperature; Interaction	76	6	-595.5	2.9	0.15
		Intercept only	76	3	-588.7	9.7	0
		Temperature	76	4	-586.6	11.8	0
Omega 3: Omega 6 FA ratio	Random effect of stream on intercept	**f_egg**	**76**	**4**	**300.6**	**0.0**	**0.61**
		f_egg; Temperature	76	5	302.6	2.0	0.22
		f_egg; Temperature; Interaction	76	6	304.7	4.0	0.08
		Intercept only	76	3	305.1	4.5	0.06
		Temperature	76	4	307.2	6.6	0.02

Figures Legends

Figure 1. The left panel shows isotopic signatures of all age 1 coho salmon collected from 7 study streams in 2010 and 2011, as well as their potential food sources (sockeye eggs, stream invertebrates). Black dots represent individual coho salmon from non-sockeye streams, while pink dots are individuals collected in sockeye spawning streams. Isotopic values for sockeye eggs and stream invertebrates were corrected for trophic discrimination (Post 2002). Small right-hand panels show examples of data from two of the study streams: proportional egg consumption by individual coho salmon was calculated using stream-specific invertebrate $\delta^{15}N$. All axes share the same units and scale.

Figure 2. Effects of stream temperature and sockeye spawner density on mean late summer body size of age 0 (panels a and b) and age 1 (panels c and d) juvenile coho salmon in seven streams between 2007 and 2014. Unique symbols correspond to data from the same stream in different years. Data from sockeye spawning streams are denoted by pink colored symbols. Dashed lines show linear relationships between mean coho body size and stream temperature in sockeye spawning streams (pink) and non-spawning streams (black).

Figure 3. Fork length (mm; y-axis) and egg consumption (proportion; x-axis) of individual age 1 coho salmon collected in 2010 and 2011. Colored dots are coho salmon collected from sockeye spawning streams (Whitefish, Lynx, Bear, Yako), and black dots are coho salmon from non-sockeye streams (Silver Salmon, Fifer, Squaw). Average summer stream temperature (June-August; ° C) during the year sampled is included below stream name in each panel.

Figure 4. Marine resource (i.e. egg) consumption (proportion; x-axis) versus relative body condition (y-axis) of age 1 coho salmon (n = 76). Each panel shows individuals collected in one

stream in 2010 or 2011. Colored dots represent coho salmon collected in sockeye salmon spawning streams. We did not calculate the relative body condition of Yako Creek coho salmon because they lacked wet weight measurements. Average summer stream temperature (June-August; ° C) during the year sampled is included below stream name in each panel.

Figure 5: Marine resource consumption (proportion; x-axis) of age 1 coho salmon versus a) total FA concentration (µg/mg dry mass), b) proportion of marine-origin FA (C_{20}+ C_{22} MUFA) and c) omega-3 to omega-6 FA ratio of muscle tissue. Black dots represent individuals collected from non-sockeye spawning streams, while colored dots represent individuals collected from streams where sockeye salmon spawn.

Figures

Figure 1

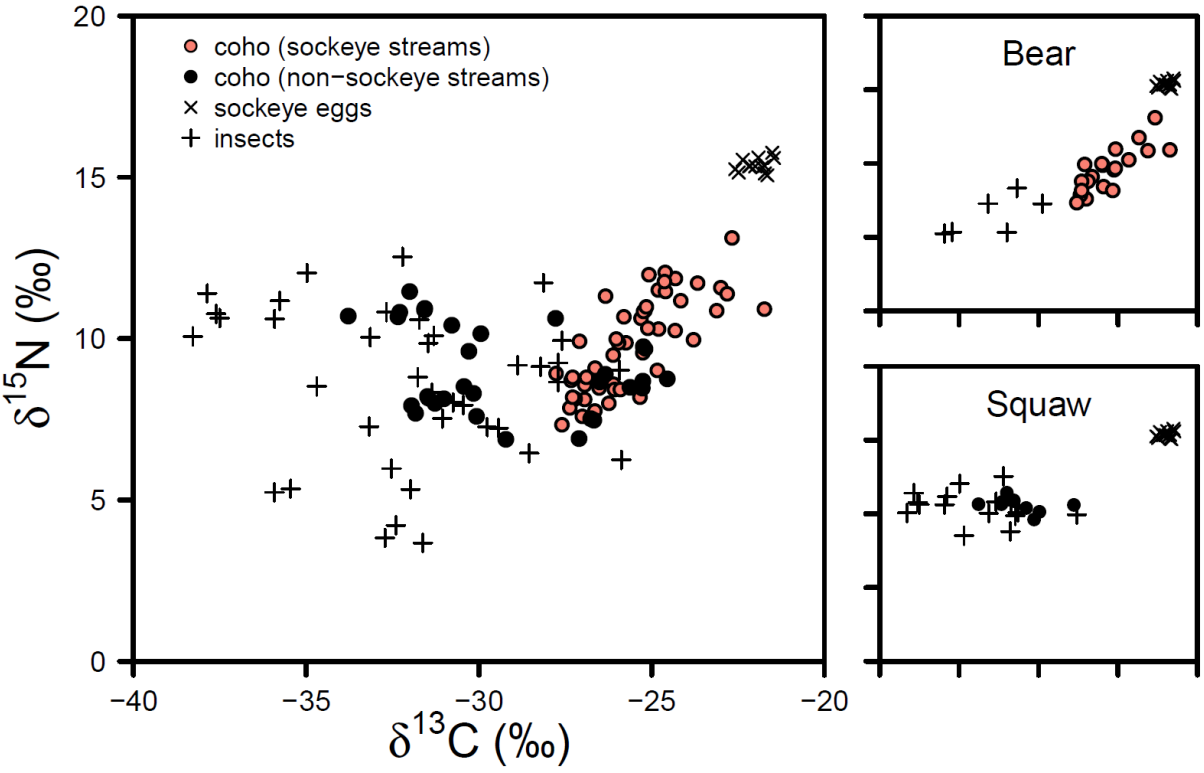

Figure 2

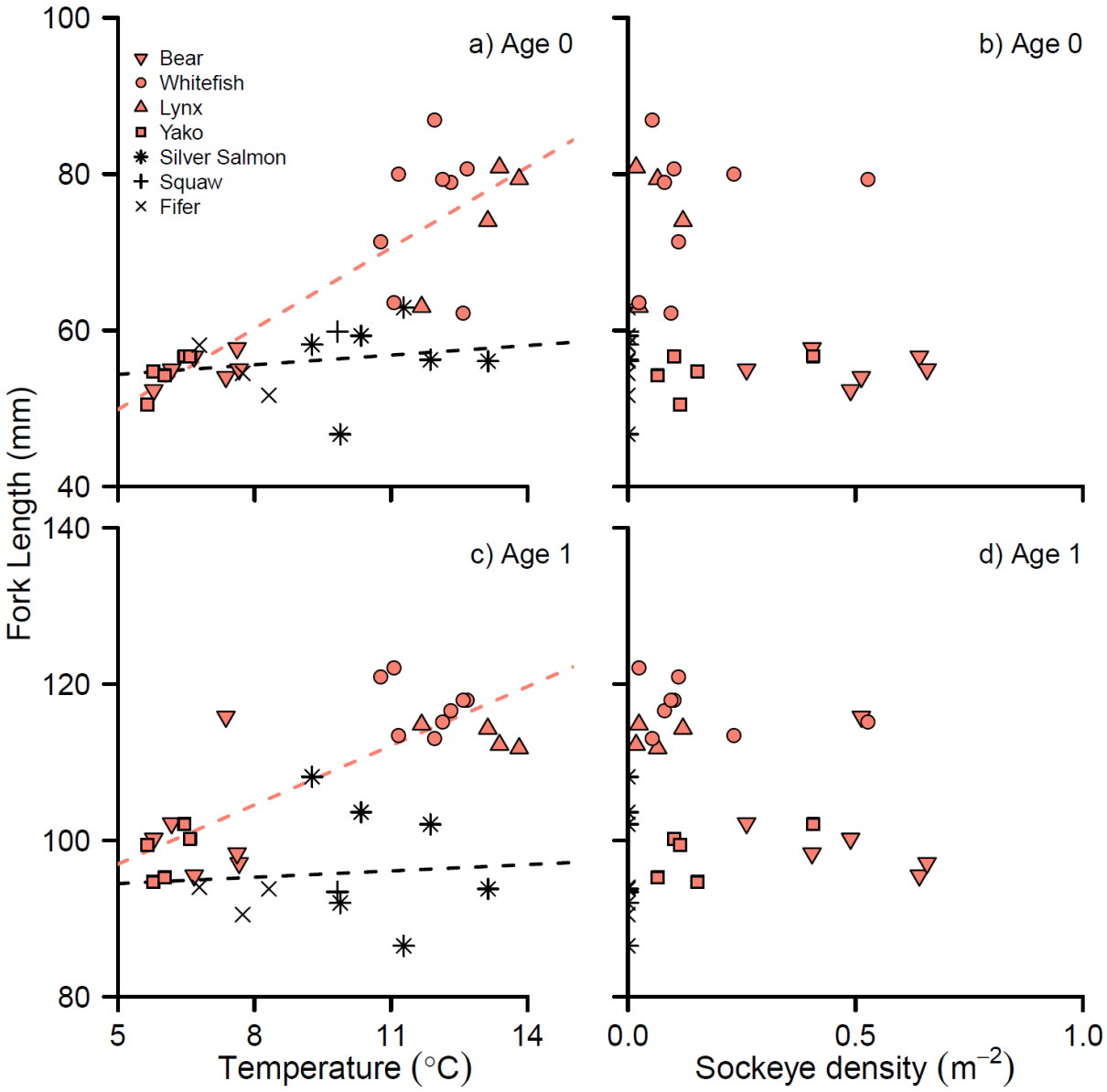
a) Age 0
b) Age 0
c) Age 1
d) Age 1
Bear
Whitefish
Lynx
Yako
Silver Salmon
Squaw
Fifer
Fork Length (mm)
Temperature (°C)
Sockeye density (m^{-2})
100
80
60
40
140
120
100
80
5
8
11
14
0.0
0.5
1.0

Figure 3

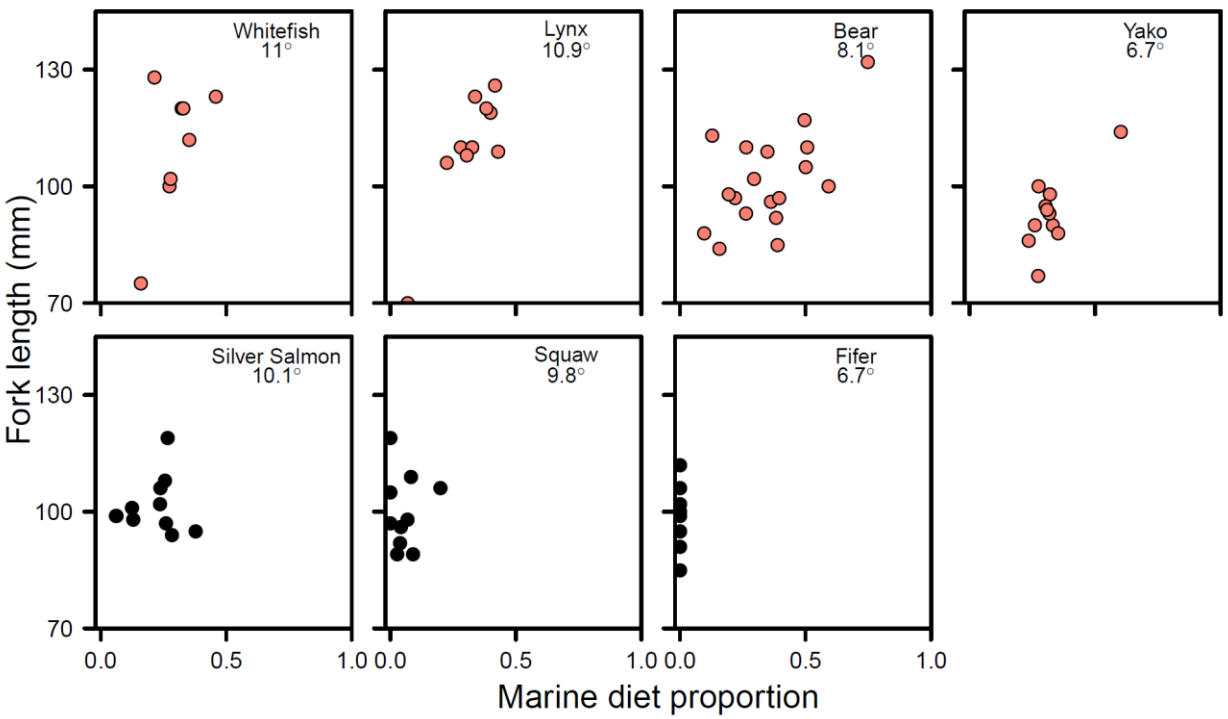
Whitefish
11°
Lynx
10.9°
Bear
8.1°
Yako
6.7°
Silver Salmon
10.1°
Squaw
9.8°
Fifer
6.7°
Fork length (mm)
130
100
70
0.0
0.5
1.0
Marine diet proportion

Figure 4

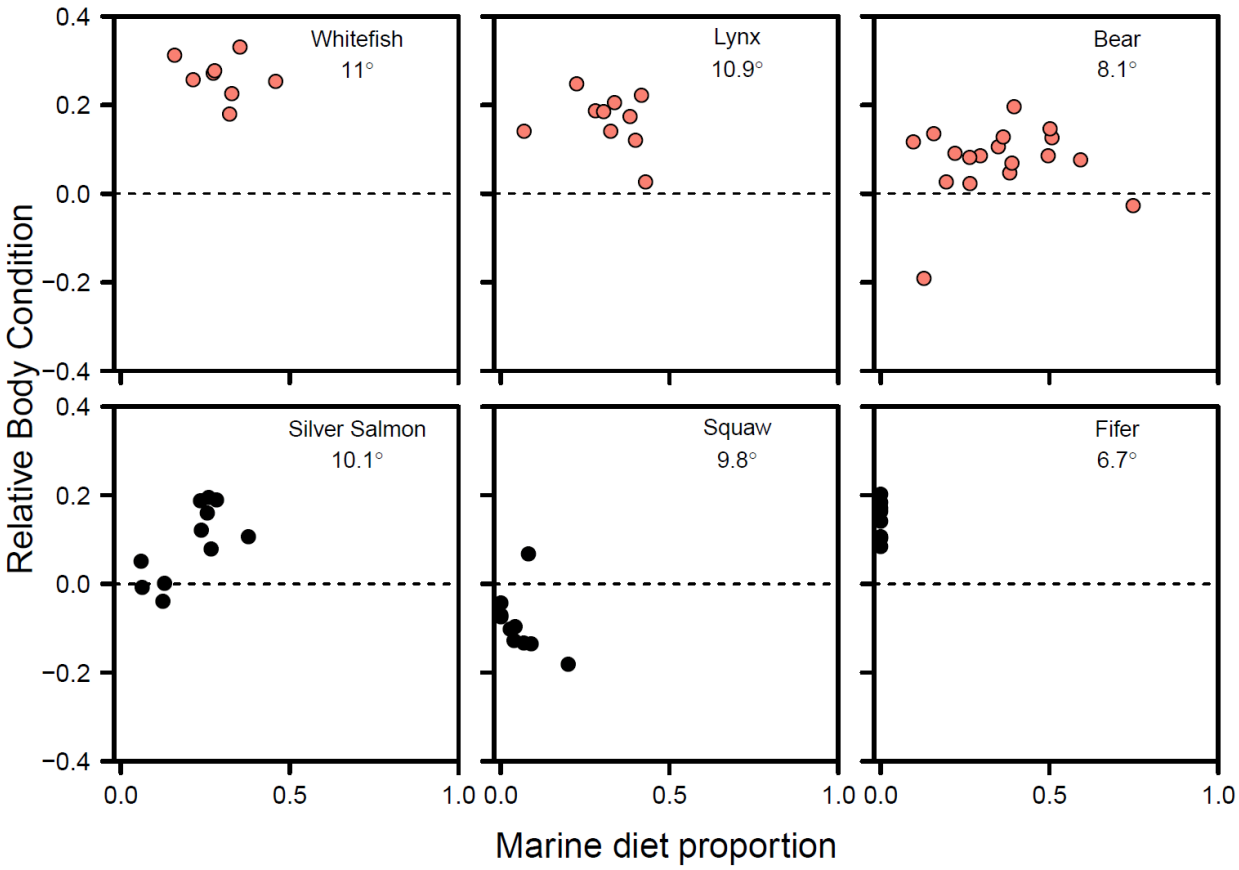
Whitefish
11°
Lynx
10.9°
Bear
8.1°
Silver Salmon
10.1°
Squaw
9.8°
Fifer
6.7°
Relative Body Condition
Marine diet proportion
0.4
0.2
0.0
−0.2
−0.4
0.0
0.5
1.0

Figure 5

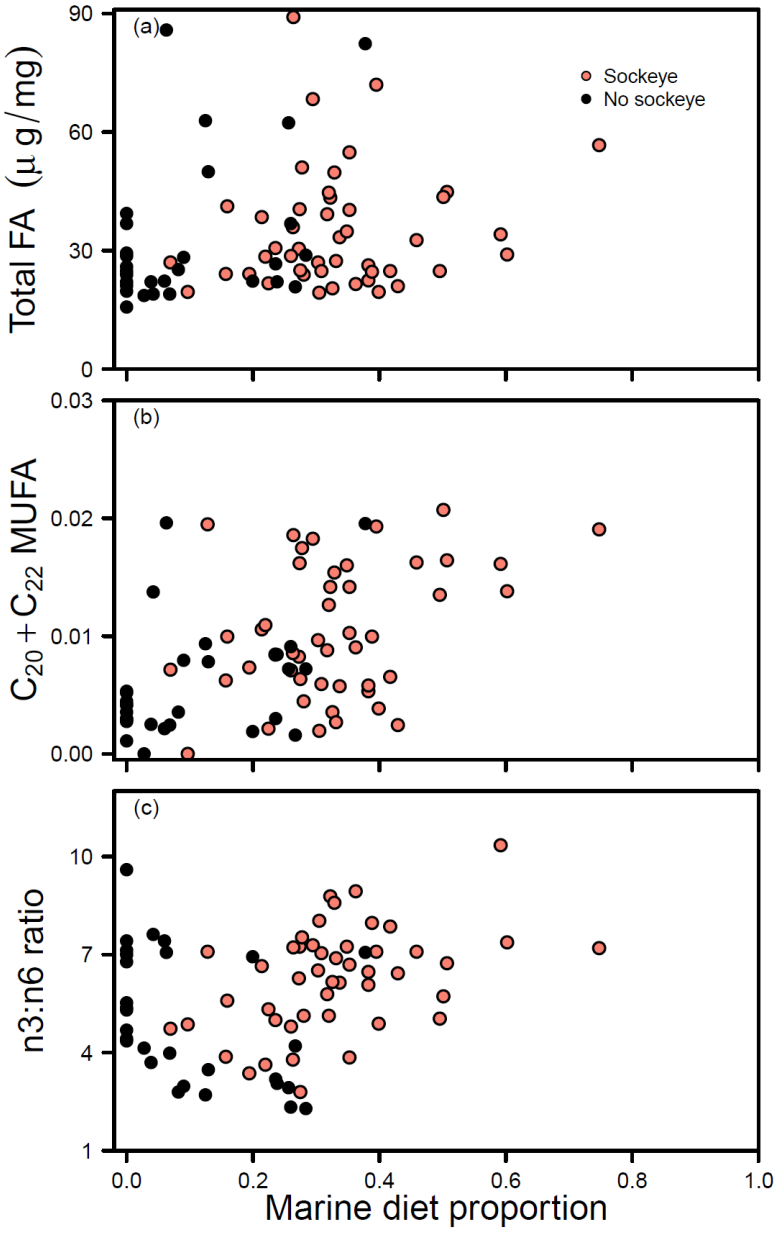
(a)
Sockeye
No sockeye
Total FA (µg/mg)
90
60
30
0
(b)
$C_{20}+C_{22}$ MUFA
0.03
0.02
0.01
0.00
(c)
n3:n6 ratio
10
7
4
1
0.0
0.2
0.4
0.6
0.8
1.0
Marine diet proportion

Supplementary Information

Figure S1. Size distributions of juvenile coho salmon seined in late summer in Bear Creek (2007-2012)

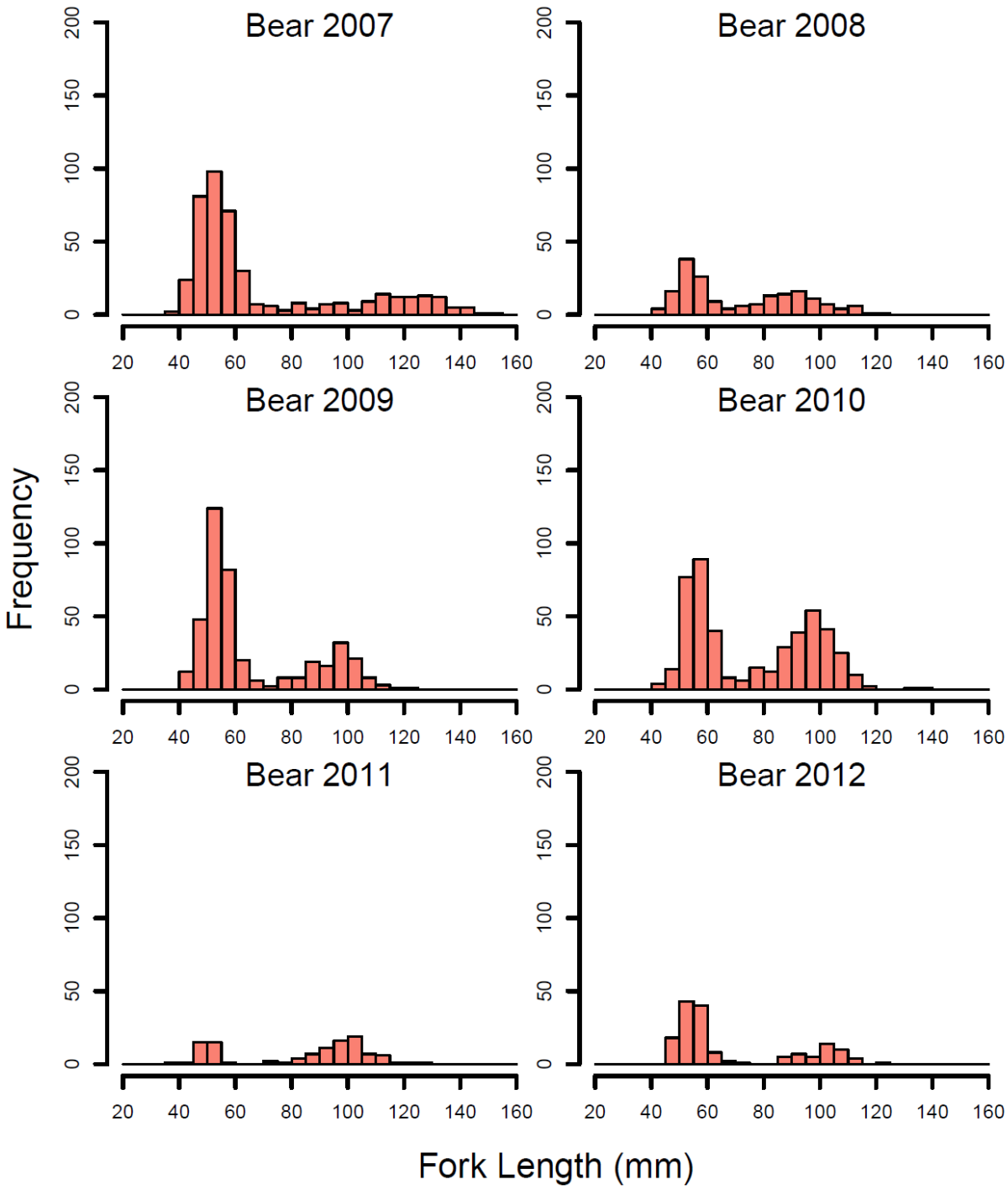

Figure S2. Size distributions of juvenile coho salmon seined in late summer in Lynx Creek (2008-2013)

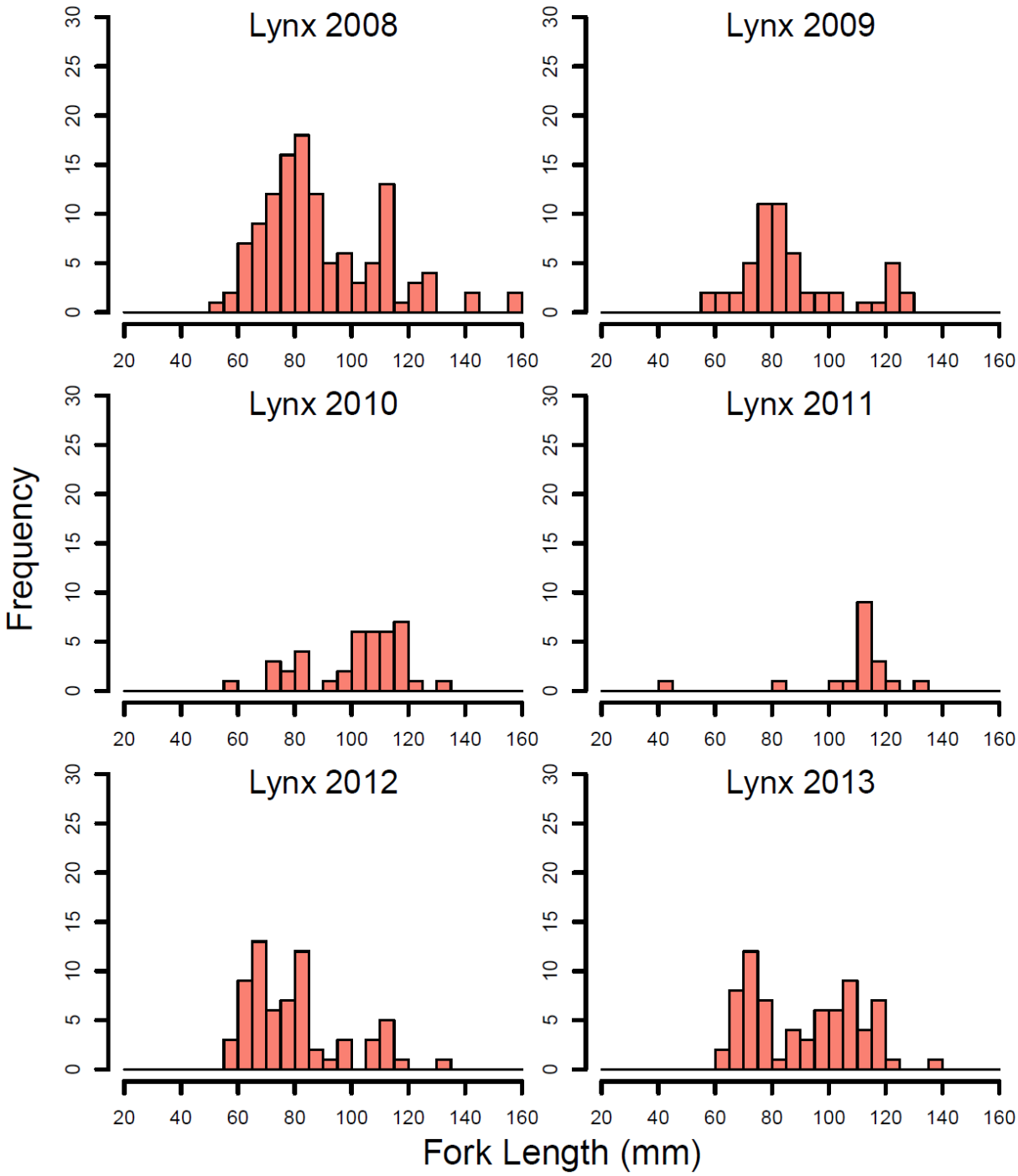

Figure S3. Size distributions of juvenile coho salmon seined in late summer in Yako Creek (2007-2012)

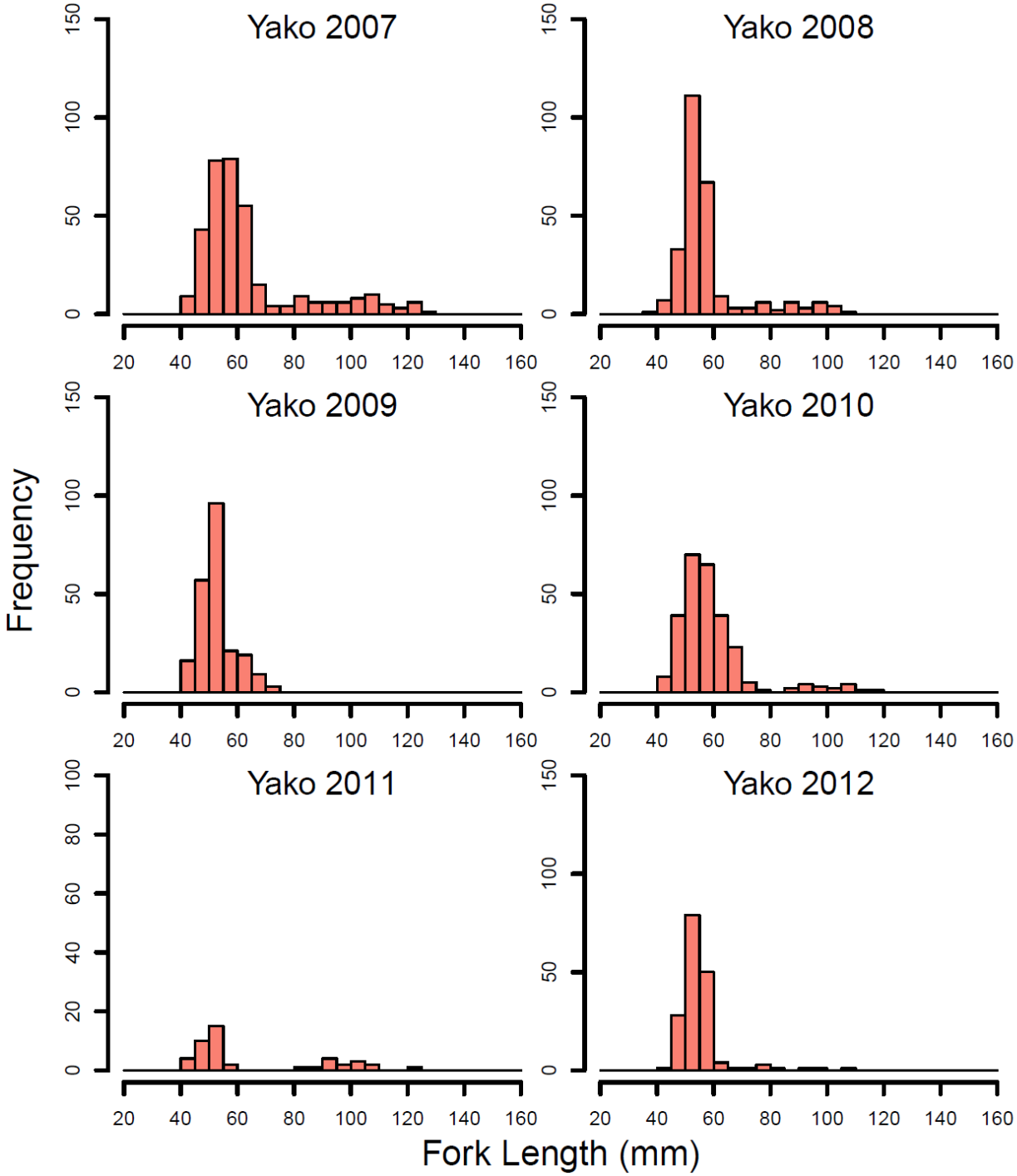

Figure S4. Size distributions of juvenile coho salmon seined in late summer in Whitefish Creek (2007-2012). Note that scale of y-axis is different for 2008 than for other years.

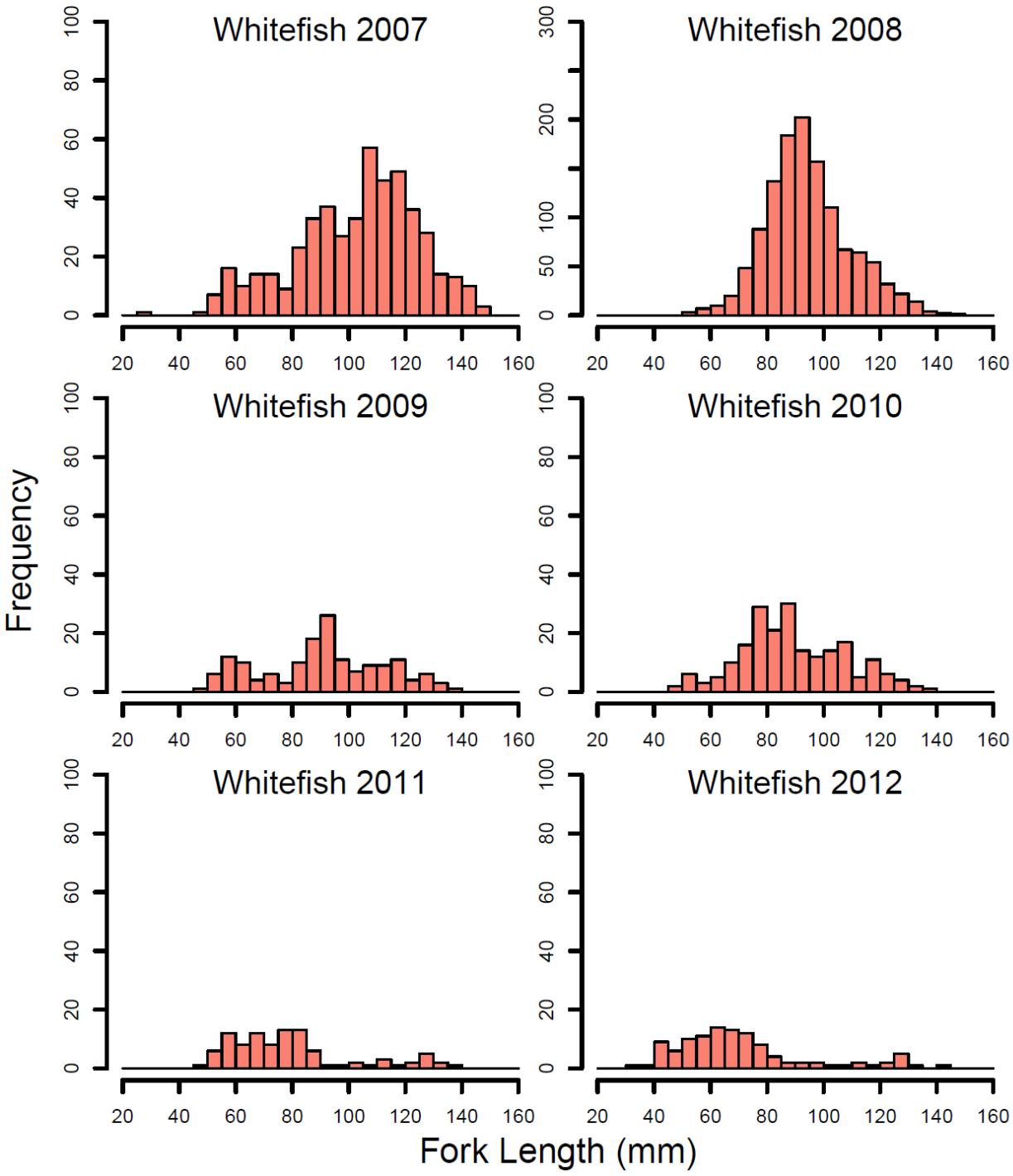

Figure S5. Size distributions of juvenile coho salmon seined in late summer in Silver Salmon Creek (2007-2012)

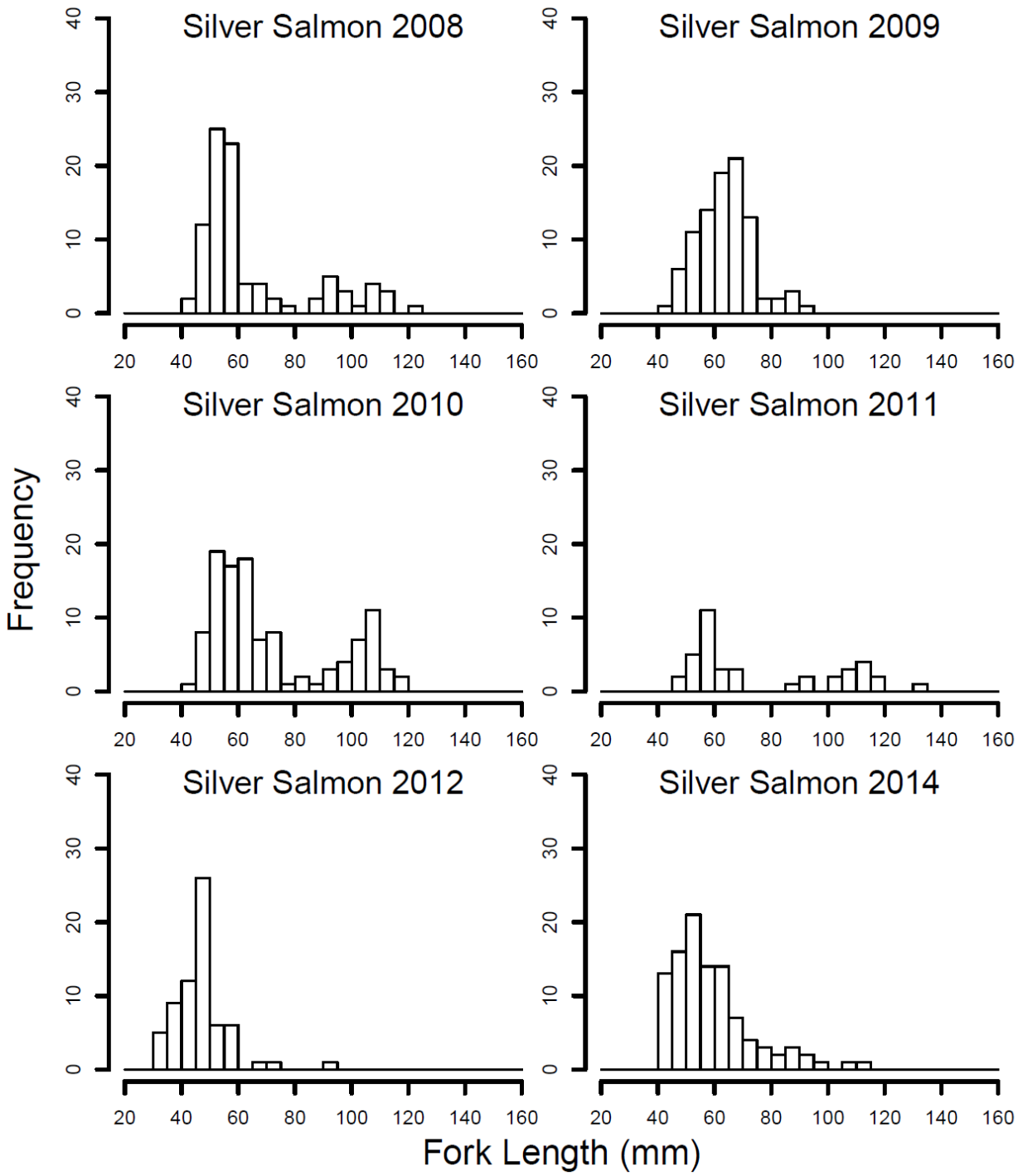

Figure S6. Size distributions of juvenile coho salmon seined in late summer in Squaw Creek (2012-2013)

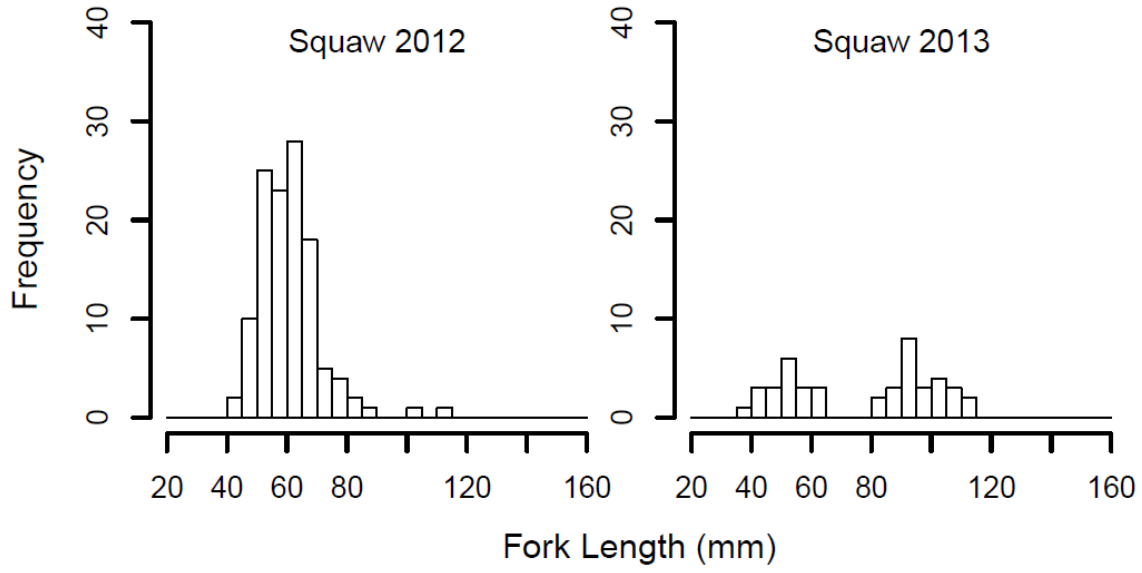

Figure S7. Size distributions of juvenile coho salmon seined in late summer in Fifer Creek (2009-2011)

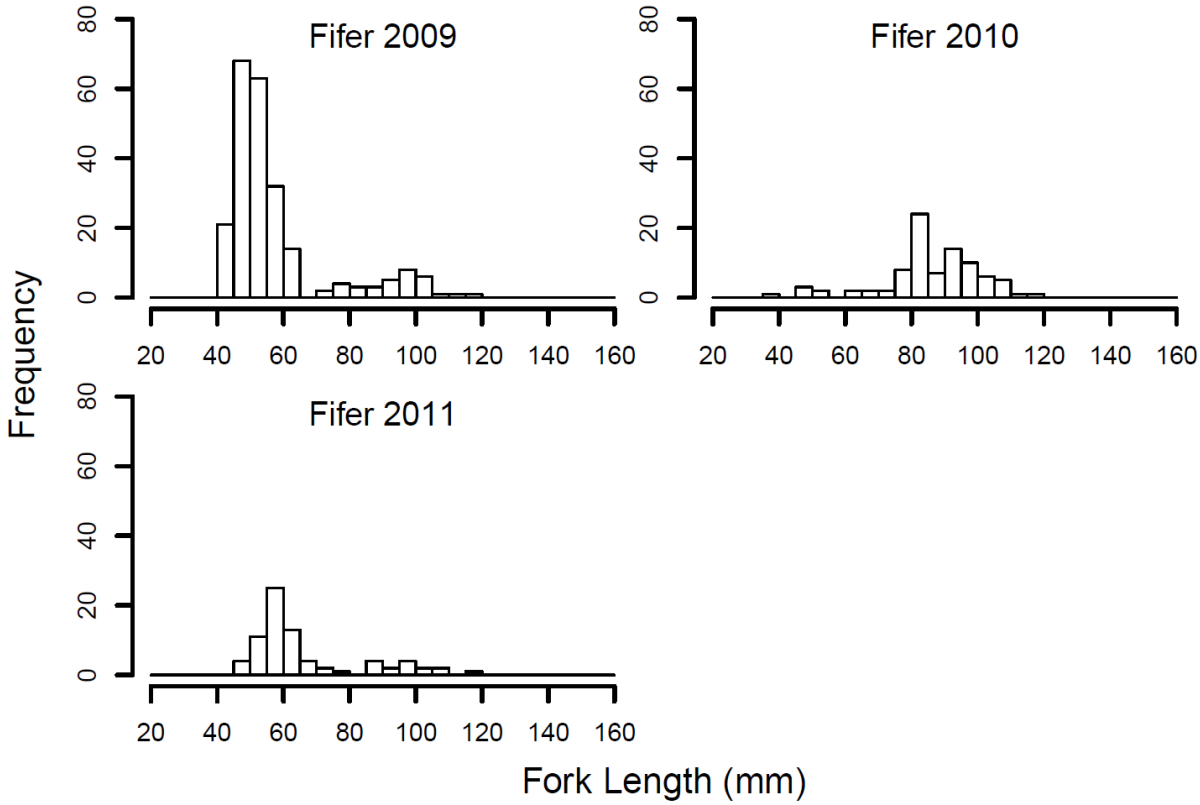

Figure S8. Biplot showing the first two axes of a principal components analysis using 22 FA variables. Principal components 1 and 2 explain 28% and 21.4% of the variation in FA composition among juvenile coho salmon, respectively. Dots represent the mean score for juvenile coho salmon from each study stream (WF = Whitefish, B = Bear, Y = Yako, L = Lynx, F = Fifer, Sq = Squaw, SS = Silver Salmon). Error bars represent one standard deviation.

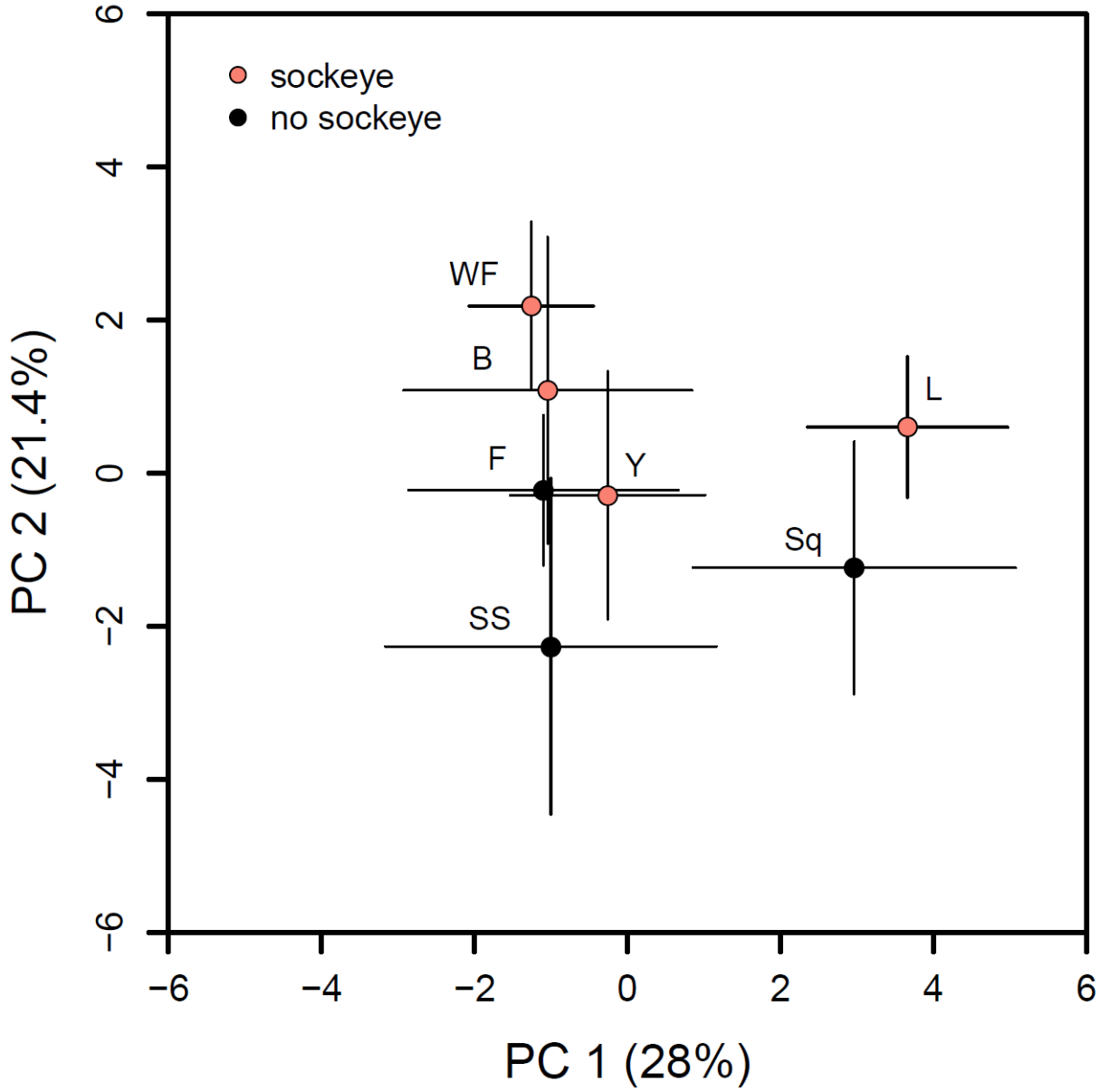

Table S1. Fork length and wet mass of age 1 juvenile coho salmon analyzed for fatty acid composition and stable isotope ratios. Means plus or minus one standard deviation are reported. Wet mass was not measured for Yako Creek fish.

Stream	Sample size	Fork length (mm)	Wet mass (g)
Bear	18	101.55 ± 12.18	13.22 ± 4.76
Whitefish	8	110.00 ± 17.26	20.97 ± 8.16
Yako	11	93.18 ± 9.31	NA
Lynx	10	110.1 ± 15.73	19.14 ± 6.91
Silver Salmon	11	101.64 ± 7.16	13.31 ± 3.32
Squaw	10	100.00 ± 9.65	10.73 ± 3.74
Fifer	8	98.75 ± 8.48	12.76 ± 3.07

Table S2. Correlations between FA variables and the first two principal components axes (PC1 and PC2), which together explain half the variation in FA composition among coho salmon muscle samples (n = 90). FA variables are sums of structurally similar FA's, which are listed below.

Variable name	FA	PC1	PC2
C_{14} MUFA	14:1n?	0.044	-0.465
C_{16} MUFA	16:1n5; 16:1n7; 16:1n9	-0.76	-0.316
MOB	16:1n6; 16:1n8	0.335	-0.223
C_{16} PUFA	16:2n?	-0.514	-0.25
C_{17} MUFA	17:1n8	-0.786	-0.085
C_{18} MUFA	18:1n5; 18:1n7; 18:1n9	-0.829	0.135
gLA	18:3n6	-0.328	-0.441
LIN	18:2n6	-0.149	-0.883
C_{19} MUFA	19:1n9	0.568	0.111
C_{20} + C_{22} MUFA	20:1n7; 20:1n9; 20:1n11; 22:1n11	-0.594	0.582
C_{20} n6 PUFA	20:2n6; 20:3n6	0.162	-0.624
C_{20} n3 PUFA	20:3n3; 20:4n3	-0.345	0.501
ALA	18:3n3	-0.217	-0.663
DHA	22:6n3	0.722	0.602
C_{24} MUFA	24:1n9	0.149	0.538
SDA	18:4n3	-0.56	0.061

C_{14}_C_{17} SAFA	C14:0; C15:0; C16:0; C17:0	0.414	-0.632
C18:0	C18:0	0.605	-0.519
C_{20}_C_{22} SAFA	C20:0; C22:0	-0.509	-0.391
Branched	i15:0; i16:0; i17:0; a17:0	-0.815	-0.18
ARA	20:4n6	0.738	-0.402
EPA	20:5n3	-0.105	0.427

References

Ahlgren, G., T. Vrede, and W. Goedkoop. 2009. Fatty Acid Ratios in Freshwater Fish, Zooplankton and Zoobenthos–Are There Specific Optima? In *Lipids in aquatic ecosystems* (pp. 147-178). Springer New York.

Armstrong, J. B., and D. E. Schindler. 2013. Going with the Flow: Spatial Distributions of Juvenile Coho Salmon Track an Annually Shifting Mosaic of Water Temperature. Ecosystems 16:1429–1441.

Armstrong, J. B., D. E. Schindler, K. L. Omori, C. P. Ruff, and T. P. Quinn. 2010. Thermal heterogeneity mediates the effects of pulsed subsidies across a landscape. Ecology 91:1445–54.

Armstrong, J. B., D. E. Schindler, C. P. Ruff, G. T. Brooks, K. E. Bentley, and C. E. Torgersen. 2013. Diel horizontal migration in streams: Juvenile fish exploit spatial heterogeneity in thermal and trophic resources. Ecology 94:2066–2075.

Bates D, Maechler M, Bolker B and Walker S. 2015. lme4: Linear mixed-effects models using Eigen and S4. R package version 1.1-8, http://CRAN.R-project.org/package=lme4.

Bendiksen, E. A., and M. Jobling. 2003. Effects of temperature and feed composition on essential fatty acid (n-3 and n-6) retention in Atlantic salmon (Salmo salar L.) parr. Fish Physiology and Biochemistry 29:133–140.

Bentley, K. T., D. E. Schindler, J. B. Armstrong, R. Zhang, C. P. Ruff, and P. J. Lisi. 2012. Foraging and growth responses of stream-dwelling fishes to inter-annual variation in a pulsed resource subsidy. Ecosphere 3:113.

Biro, P. A., A. E. Morton, J. R. Post, and E. A. Parkinson. 2004. Over-winter lipid depletion and mortality of age-0 rainbow trout (*Oncorhynchus mykiss*). Canadian Journal of Fisheries and Aquatic Sciences 61:1513–1519.

Burnham, K. P., and D. R. Anderson. 2002. Avoiding pitfalls when using information- theoretic methods. The Journal of Wildlife Management 66:912–918.

Chaloner, D. T., K. M. Martin, M. S. Wipfli, P. H. Ostrom, and G. a Lamberti. 2002. Marine carbon and nitrogen in southeastern Alaska stream food webs: evidence from artificial and natural streams. Canadian Journal of Fisheries and Aquatic Sciences 59:1257–1265.

Connolly, P., and J. Petersen. 2003. Bigger is not always better for overwintering young-of- year steelhead. Transactions of the American Fisheries Society. 8487:37–41.

Elliott, J. M., and L. Persson. 1978. The Estimation of Daily Rates of Food Consumption for Fish. J. anim. ecol. 47:977–991.

Gende, S. M., R. T. Edwards, M. F. Willson, and M. S. Wipfli. 2002. Pacific salmon in aquatic and terrestrial ecosystems. BioScience 52:917–928.

Giroux, M. A., D. Berteaux, N. Lecomte, G. Gauthier, G. Szor, and J. Bêty. 2012. Benefiting from a migratory prey: Spatio-temporal patterns in allochthonous subsidization of an arctic predator. Journal of Animal Ecology 81:533–542.

Heintz, R. A., B. D. Nelson, J. Hudson, M. Larsen, L. Holland, and M. Wipfli. 2004. Marine Subsidies in Freshwater : Effects of Salmon Carcasses on Lipid Class and Fatty Acid

Composition of Juvenile Coho Salmon. Transactions of the American Fisheries Society 133:559–567.

Heintz, R. a., M. S. Wipfli, and J. P. Hudson. 2010. Identification of Marine-Derived Lipids in Juvenile Coho Salmon and Aquatic Insects through Fatty Acid Analysis. Transactions of the American Fisheries Society 139:840–854.

Helfield, J. M., and R. J. Naiman. 2002. Salmon and alder as nitrogen sources to riparian forests in a boreal Alaskan watershed. Oecologia 133:573–582.

Hicks, B. J., M. S. Wipfli, D. W. Lang, and M. E. Lang. 2005. Marine-derived nitrogen and carbon in freshwater-riparian food webs of the Copper River Delta, southcentral Alaska. Oecologia 144:558–569.

Hocking, M. D., and J. D. Reynolds. 2011. Impacts of salmon on riparian plant diversity. Science 331:1609–1612.

Kline Jr., T. C., J. J. Goering, O. A. Mathisen, P. H. Poe, and P. L. Parker. 1990. Recycling of elements transported upstream by runs of Pacific Salmon: I. d15N and d13C evidence in Sashin Creek, Southeastern Alaska.

Lang, D. W., G. H. Reeves, J. D. Hall, and M. S. Wipfli. 2006. The influence of fall-spawning coho salmon (*Oncorhynchus kisutch*) on growth and production of juvenile coho salmon rearing in beaver ponds on the Copper River Delta, Alaska. Canadian Journal of Fisheries and Aquatic Sciences 63:917–930.

Lisi, P. J., D. E. Schindler, K. T. Bentley, and G. R. Pess. 2013. Association between geomorphic attributes of watersheds, water temperature, and salmon spawn timing in Alaskan streams. Geomorphology 185:78–86.

Marczak, L. B., R. M. Thompson, and J. S. Richardson. 2007. Meta-analysis: Trophic level, habitat, and productivity shape the food web effects of resource subsidies. Ecology 88:140–148.

Marriott, R. 1964. Stream catalog of the Wood River lake system, Bristol Bay, Alaska.

Molina-Montenegro, M. A., C. Torres-Diaz, J. Gallardo-Cerda, M. Leppe, and E. Gianoli. 2013. Seabirds modify El Nino effects on tree growth in a southern Pacific island. Ecology 94:2415–2425.

Moore, J., and D. Schindler. 2008. Biotic disturbance and benthic community dynamics in salmon-bearing streams. Journal of Animal Ecology 77:275–284.

Moore, J. W., D. E. Schindler, and C. P. Ruff. 2008. Habitat saturation drives thresholds in stream subsidies. Ecology 89:306–312.

Nichols, P. D., Guckert, J. B., & White, D. C. 1986. Determination of monosaturated fatty acid double-bond position and geometry for microbial monocultures and complex consortia by capillary GC-MS of their dimethyl disulphide adducts. Journal of Microbiological Methods 5:49–55.

Oksanen, J. F. ,Guillaume Blanchet, Roeland Kindt, Pierre Legendre, Peter R. Minchin, R. B. O' Hara, Gavin L. Simpson, Peter Solymos, M. Henry H. Stevens and Helene Wagner 2013. vegan: Community Ecology Package. R package version 2.0-10. http://CRAN.R-project.org/package=vegan

Post, D. 2002. Using stable isotopes to estimate trophic position: models, methods, and assumptions. Ecology 83:703–718.

Post, D. M., C. a. Layman, D. A. Arrington, G. Takimoto, J. Quattrochi, and C. G. Montana.

2007. Getting to the fat of the matter: Models, methods and assumptions for dealing with lipids in stable isotope analyses. Oecologia 152:179–189.

Post, J. R., and E. a Parkinson. 2001. Energy allocation strategy in young fish : allometry and survival. Ecology 82:1040–1051.

Quinn, T. P. 2011. The behavior and ecology of Pacific salmon and trout. UBC Press.

R Development Core Team (2013). R: A language and environment for statistical computing. R Foundation for Statistical Computing,Vienna, Austria. ISBN 3-900051-07-0, URL http://www.R-project.org.

Rinella, D. J., M. S. Wipfli, C. A. Stricker, R. A. Heintz, and M. J. Rinella. 2012. Pacific salmon (*Oncorhynchus spp*.) runs and consumer fitness : growth and energy storage in stream-dwelling salmonids increase with salmon spawner density. Canadian Journal of Fisheries and Aquatic Sciences 69:73–84.

Rogers, L. A., and D. E. Schindler. 2008. Asynchrony in population dynamics of sockeye salmon in southwest Alaska. Oikos 117:1578–1586.

Scheuerell, M. D., J. W. Moore, D. E. Schindler, and C. J. Harvey. 2007. Varying effects of anadromous sockeye salmon on the trophic ecology of two species of resident salmonids in southwest Alaska. Freshwater Biology 52:1944–1956.

Schindler, D. E., J. B. Armstrong, K. T. Bentley, K. Jankowski, P. J. Lisi, and L. X. Payne. 2013. Riding the crimson tide: mobile terrestrial consumers track phenological variation in spawning of an anadromous fish. Biology letters 9:20130048.

Schindler, D. E., D. E. Rogers, M. D. Scheuerell, and C. A. Abrey. 2005. Effects of changing climate on zooplankton and juvenile sockeye salmon growth in Southwestern Alaska.

Ecology 86:198–209.

Schindler, D. E., M. D. Scheuerell, J. W. Moore, S. M. Gende, T. B. Francis, and W. J. Palen. 2003. Pacific salmon and the ecology of coastal ecosystems. Frontiers in Ecology and the Environment 1:31–37.

Smits, A. P., D. E. Schindler, and M. T. Brett. 2015. Geomorphology controls the trophic base of stream food webs in a boreal watershed. Ecology 96:1775–1782.

Stewart, D. J., and M. Ibarra. 1991. Predation and production by salmonine fishes in Lake Michigan, 1978–88. Canadian Journal of Fisheries and Aquatic Sciences 48:909–922.

Strandberg, U., S. J. Taipale, M. J. Kainz, and M. T. Brett. 2014. Retroconversion of docosapentaenoic acid (n-6): an alternative pathway for biosynthesis of arachidonic acid in *Daphnia magna*. Lipids 49:591–5.

Swain, N. R., M. D. Hocking, J. N. Harding, and J. D. Reynold. 2014. Effects of salmon on the diet and condition of stream-resident sculpins. Canadian Journal of Fisheries and Aquatic Sciences 71:521–532.

Torres-Ruiz, M., J. D. Wehr, and A. a. Perrone. 2007. Trophic relations in a stream food web: importance of fatty acids for macroinvertebrate consumers. Journal of the North American Benthological Society 26:509–522.

Weiner, J. 1992. Physiologoical limits to sustainable energy expenditure in birds and mammals - ecological implications. Trends in Ecology & Evolution 7:384–388.

Wipfli, M. S., J. P. Hudson, J. P. Caouette, and D. T. Chaloner. 2003. Marine Subsidies in Freshwater Ecosystems : Salmon Carcasses Increase the Growth Rates of Stream- Resident Salmonids Marine Subsidies in Freshwater Ecosystems : Salmon Carcasses. Transactions of

the American Fisheries Society:37–41.

Yang, L. H., K. F. Edwards, J. E. Byrnes, J. L. Bastow, A. N. Wright, and K. O. Spence. 2010. A meta-analysis of resource pulse – consumer interactions. Ecological Monographs 80:125–151.

Zuur, A., Ieno, E. N., Walker, N., Saveliev, A. A., & Smith, G. M. 2009. Mixed effects models and extensions in ecology with R. Springer Science & Business Media.

CHAPTER 4: WATERSHED GEOMORPHOLOGY INTERACTS WITH PRECIPITATION TO INFLUENCE THE MAGNITUDE AND SOURCE OF CO_2 EMISSIONS FROM ALASKAN STREAMS

Abstract

Boreal ecosystems sequester a large fraction of the world's soil carbon and are warming rapidly, prompting efforts to understand the role of freshwaters in carbon export from these regions. We examined geomorphic controls on the magnitude of stream CO_2 emissions and sources of stream dissolved inorganic carbon (DIC) across a heterogeneous river basin in SW Alaska. We found that watershed slope and precipitation interact to control terrestrial carbon fluxes into and out of streams. Watershed slope influences C loading and stream CO_2 fluxes by determining the amount of carbon accumulation in watersheds, and to a lesser extent by determining gas transfer velocity across the air-water interface. Low gas transfer velocity in low gradient streams offsets some of the effects of higher terrestrial C loading at those sites, resulting in lower than expected vertical CO_2 fluxes. While the isotopic composition of stream DIC ($\Delta^{14}C$ and $\delta^{13}C$) was highly variable across space and time, shifts towards younger, more terrestrial sources after rain events were most pronounced in low gradient watersheds. At base flow DIC was a mixture of modern and aged sources of biogenic and geologic origin ($\Delta^{14}C$, -198.3 ‰ to 27.9 ‰, n=23). Aged C sources contributed to food webs via an indirect pathway from DIC to algae to invertebrate grazers. We observed coherent changes in stream carbon chemistry after rainstorms despite considerable physical heterogeneity among watersheds. These patterns provide a way to extrapolate across boreal landscapes by constraining CO_2 concentration and flux estimates by local geomorphic features.

Introduction

Since the initial realization that freshwaters transform and emit substantial amounts of

terrestrial carbon to the atmosphere and oceans [*Coyne and Kelley*, 1974, *Schindler et al.*, 1975, *Kling et al.*, 1991, *Cole et al*., 1994], there has been increasing effort to understand the role of freshwaters in global and regional carbon cycling [e.g., *Cole and Caraco,* 2001; *Richey et al*., 2002]. More recent efforts have largely focused on aquatic export of terrestrial carbon from boreal and arctic ecosystems, which contain almost a third of the world's organic soil carbon and are also subject to rapid climate warming [*McGuire et al.*, 2009]. The fate of these aged soil carbon deposits, accumulated over millennia in cold, moist conditions, remains uncertain, but most scenarios predict higher mobilization rates into streams and rivers as temperatures increase [*Frey and Smith*, 2005; *Schuur et al.*, 2015]. Arctic rivers transport large quantities of dissolved organic carbon (DOC) to the ocean, most of which is fairly young in origin [<10 years old; *Raymond et al.*, 2007]. In addition, gaseous emissions (CO_2, CH_4) from large Arctic rivers roughly equal lateral carbon transport (DOC, POC, dissolved inorganic carbon (DIC)) to the ocean [*Striegl et al.*, 2012]. Studies of smaller streams in tundra or peatland catchments tend to confirm this 1:1 ratio of vertical gas emissions to downstream lateral flux [*Teodoru et al.*, 2009; *Wallin et al.*, 2013].

While predicting regional-scale ecosystem responses to climate change does not inherently require detailed accounting of carbon emissions at local scales, understanding local drivers of carbon cycling is necessary to understand watershed or basin-scale responses to changes in temperature and precipitation, which will in turn affect food web processes and ecosystem function. Classic ecological frameworks such as the River Continuum Concept [RCC; *Vannote et al.,* 1980] and the Flood Pulse Concept [FPC; *Junk et al.,* 1989] describe basic physical controls on the strength of aquatic-terrestrial coupling; the RCC predicts decreased coupling strength from small headwaters to large, higher order rivers[*Vannote et al.*, 1980], and

the FPC hypothesizes that the majority of riverine carbon derives from floodplain production, which is mobilized into the main channel by seasonal inundation [*Junk et al.*, 1989]. However, landscape variables beyond network position or flood stage should also influence carbon inputs and export from high latitude rivers.

Controls on dissolved carbon export from boreal watersheds are becoming better understood: wetlands often provide the dominant source of DOC to stream networks [*Olefeldt et al.*, 2013], while precipitation acts to mobilize accumulated DOC from wetland and upland soils into streams [*Laudon et al.*, 2011; *Raymond et al.*, 2016]. In fact the majority of annual DOC export may occur after only a few large storms in forested watersheds [*Raymond and Saiers*, 2010].

Efforts to quantify the magnitude, sources, and controls of carbon gas emissions (CO_2 and CH_4) from boreal rivers and streams have revealed considerable spatial and temporal variability rather than clear patterns across landscapes. Dissolved CO_2 concentrations tend to be both higher and more variable in small streams than in larger rivers [*Teodoru et al.*, 2009; *Crawford et al.*, 2013], presumably due to greater connectivity with organic soils [*Hope et al.*, 2004], but often landscape-scale variables such as vegetation cover and lithology correlate poorly with CO_2 flux [*Giesler et al.*, 2013]. Carbon export (DOC and DIC) from an intensively monitored watershed in northern Sweden varied three-fold among years over a 12 year period [6-18 g C m^2 $year^{-1}$; *Leach et al.*, 2016], reflecting both variation in precipitation and discharge among years, but also inter-annual and seasonal differences in ecosystem productivity and respiration rates. Dissolved CO_2 concentration and flux generally vary considerably both within and among streams in boreal drainage networks [*Crawford et al.*, 2013].

CO_2 flux from streams is a function both of CO_2 concentration in water, which reflects C loading and remineralization rates, and of gas transfer velocity across the air-water interface. Landscape heterogeneity in CO_2 fluxes may therefore arise from features that affect either of these processes. Slope (i.e. steepness) is a basic geomorphic characteristic of watersheds that should strongly influence CO_2 fluxes from streams through controls on both C loading and gas transfer velocity. Watershed slope determines long-term carbon accumulation in riparian soils (i.e. wetlands form in low-gradient watersheds), thus setting the potential magnitude of terrestrial C loads (DIC, DOC, POC) to streams. Watershed slope also influences stream-riparian connectivity; streams in low gradient watersheds are more closely linked to terrestrial C pools due to longer water residence times in soil and in the stream channel. Finally, watershed slope influences stream channel gradient, flow velocity, and surface turbulence, all of which affect gas transfer velocity [*Wallin et al.*, 2011; *Raymond et al.*, 2012]. While many studies have investigated patterns in C loading to streams, work in a Swedish watershed showed not only that gas transfer velocity (K_{CO2}) was highly heterogeneous across space, but that K_{CO2}, rather than CO_2 concentration, explained the most variation in CO_2 fluxes among sites [*Wallin et al.*, 2011]; sites with high K_{CO2} tended to have the highest CO_2 fluxes despite having lower CO_2 concentrations.

Anthropogenic disturbances such as urban development, forestry, and agriculture may mask natural variation in impacted landscapes, however pristine systems offer an opportunity to understand underlying natural drivers of variation in C cycling at watershed and basin scales. In this study, we examine geomorphic controls on the magnitude of stream CO_2 emissions and sources of stream DIC across a heterogeneous boreal Alaskan landscape that varies markedly in the geomorphic features of individual tributaries [*Lisi et al.*, 2013]. We ask two main questions:

1) is the influence of watershed morphology (slope) on stream CO_2 emissions mainly via effects on terrestrial C loading (i.e. strength of aquatic-terrestrial linkages), or due to effects on gas transfer velocity, and how do these relationships change after large rainstorms? 2) How does watershed geomorphology affect sources of stream DIC at base flow and after rain events?

We expected that streams draining low gradient watersheds would have greater accumulated soil C, leading to higher DOC and DIC concentrations in stream waters. We also expected streams draining high gradient watersheds to have more turbulent flow due to higher water velocity and larger substrate size [*Lisi et al.*, 2013]. Therefore, streams in high gradient watersheds should have higher gas transfer velocity than streams in low gradient watersheds. As a consequence of these two opposing landscape patterns, CO_2 fluxes out of streams should not scale linearly with CO_2 concentration. We expected more homogeneous CO_2 fluxes than CO_2 concentrations among streams, because low gradient streams with the highest C loading would also have the lowest gas transfer velocity.

We expected that watershed slope would also significantly influence the sources (as reflected in the isotopic composition) of stream DIC. Specifically we hypothesized that older, terrestrially-derived C (soil DIC or terrestrial DOC respired in situ) would contribute more to stream DIC in low gradient watersheds than in steep, soil-poor watersheds, resulting in more depleted Δ^{14}C-DIC and δ^{13}C-DIC in low gradient streams. In turn we expected the isotopic signatures of invertebrate (larval caddisflies and mayflies) to reflect stream DIC, and therefore assimilation of pre-modern carbon sources. Following major precipitation events, we expected Δ^{14}C-DIC enrichment and δ^{13}C-DIC depletion relative to base flow conditions, reflecting inputs of recently fixed terrestrial C transported via shallow or surface flow paths.

Methods and Analyses

Watershed Description

We collected water samples and stream measurements across the Wood River basin in the Bristol Bay region of southwest Alaska (59°20′ N, 158°40′W, Figure 1). The high degree of landscape heterogeneity in this undeveloped, pristine basin allowed us to quantify geomorphic controls on carbon cycling and emissions in boreal streams. Over 50 watersheds for 2^{nd}-4^{th} order streams comprise the Wood River system, which has a total drainage area of 3,950 km^2. We sampled streams that flow directly into three large lakes (Aleknagik, Nerka, Beverley), which are connected to one another by short rivers. Underlying geology in this region includes mainly volcanic and sedimentary deposits. This region was last glaciated during the late Wisconsin period [~ 10,000 years BP; *Briner and Kaufman*, 2008], and glacial till and gravels underlie soils throughout the basin. There is a general longitudinal gradient of peat accumulation across the basin, associated with a shift from high gradient, mountainous terrain on the western side to low gradient, wetland dominated terrain in the east. Temperature and flow regimes also generally reflect this slope gradient, wherein steep, high elevation streams are colder and snow-melt dominated, and low gradient, low elevation streams are warmer and primarily rain-fed [*Lisi et al.*, 2013]. The mean watershed slope of sampled streams, calculated in ArcGIS from a digital elevation map, ranges from 0.5 to 29 degrees [*Lisi et al.*, 2013]. Mean watershed elevation ranges from 32 to 502 m above mean sea level. Geomorphic characteristics of study catchments within the basin are reported in the supporting information (Table S1).

Vegetation at lower elevations (<150 m) is dominated by a white spruce (*Picea glauca*) and paper birch (*Betula papyrifera*) mixed forest, interspersed with areas of moist tundra and sphagnum bog. Stands of green alder (*Alnus crispa*) cover steep, high elevation hill slopes.

Riparian areas are dominated by feltleaf willow (*Salix alexensis*), as well as alder and cottonwood in steeper watersheds [*Bartz and Naiman*, 2005]. Higher gradient streams tend to have higher canopy cover presumably due to water-saturated soils hindering riparian tree growth at low gradient sites.

Stream chemistry has previously been shown to vary systematically across the Wood River basin. The concentration of DOC and dissolved nutrients, as well the temperature dependence of stream metabolism, reflect local conditions dictated by geomorphic characteristics such as watershed slope [*Jankowski et al.*, 2014]. Streams draining flat watersheds tend to be characterized by relatively high DOC and low NO_3 concentrations, whereas streams draining steep watersheds tend to the opposite [*Jankowski et al.*, 2014].

Sample Collection and Analysis

We measured pCO_2, total DIC, and DOC, and collected DIC samples for isotope analyses, from streams and rivers within the Wood River basin during two summers (23 streams in 2014; 26 streams in 2015). Some measurements (total DIC, isotopic signatures) were not collected in both years or at all sites. All streams were sampled at least once in June or July at base flow conditions; we collected few samples in August due to significant disturbance caused by abundant sockeye salmon spawning later in summer, which has been shown to affect C dynamics within these streams [*Holtgrieve and Schindler*, 2011]. In addition, we opportunistically sampled a subset of sites in August 2014 (n = 12) and July 2015 (n = 20) immediately after significant rain storms to assess stream responses to large precipitation events (Figure S1). All measurements and samples were collected within 500 m of stream outlets to lakes in order to take an integrative measure of processes occurring upstream. At a representative

subset of streams in 2015 (n=9) we also measured pCO_2 and total DIC at an upstream site (0.5 - 2 km) to investigate coarse spatial variation in C fluxes along the stream channel.

Dissolved CO_2 concentration (pCO_2) and total DIC concentration in stream water were measured using headspace equilibration techniques as described in Alin et al.[2011; modified from *Cole et al.*, 1994]. Triplicate headspace samples from stream water and ambient air above the stream surface were analyzed for partial pressure of CO_2 using a Li-Cor LI-6262 benchtop infra-red gas analyzer (IRGA). Total DIC was measured by acidifying triplicate 30-mL stream water samples with 5% phosphoric acid, thereby converting carbonate and bicarbonate to CO_2, and equilibrating the acidified water sample with a headspace. Concentrations of all carbon species (dissolved CO_2 gas, bicarbonate, carbonate, pH) were calculated from pCO_2, total DIC concentration, air pressure, and stream temperature using the program CO2SYS [*Lewis and Wallace*, 1998].

In both years we collected duplicate water samples for DOC concentration at all sites where we measured pCO_2, and duplicate samples for total DIC were collected at a subset of these sites (19 streams; the duplicate was not analyzed unless the first sample was damaged). DOC samples were collected and analyzed as described in Jankowski et al. [2014]. Water samples collected for isotopic analysis of DIC were poisoned with saturated mercuric chloride in the field and stored in glass bottles at room temperature until analysis within six months according to the methods of Quay et al. [1992]. Sample aliquots of 100-mL were acidified and bubbled with helium to strip inorganic carbon from the solution, and concentrations were measured manometrically. CO_2 remaining in ampoules from DIC analyses was analyzed for $\delta^{13}C$ and radiocarbon content at an accelerator mass spectrometry (AMS) facility. $\delta^{13}C$ DIC is a useful natural tracer because potential DIC sources (atmospheric, biological, geologic) differ in their

isotopic signatures [*Finlay*, 2003]. Likewise, $\Delta^{14}C$ can further distinguish DIC sources based on relative age: older C sources (ex. deep organic soil layers, carbonate minerals) are more depleted than younger C sources (atmospheric CO_2, modern terrestrial plants).

To examine how variation in C sources to streams affected the age and origin of carbon incorporated into stream food webs, we collected invertebrate consumers from 12 streams and analyzed their tissues for $\delta^{13}C$ and $\Delta^{14}C$. Caddisfly larvae (Trichoptera) and mayfly nymphs (Ephemeroptera) were collected in conjunction with a separate field study [*Smits et al*., 2015] during the summers of 2012, 2013, and 2014. We collected insects with a Surber sampler in riffle and pool habitat in three different stream reaches at each site. Insects from each stream were sorted to order, and if possible, family, and then combined to provide adequate biomass for isotopic analysis. Combined samples were freeze-dried and homogenized, and then stored frozen until analysis.

Isotopic analyses ($\delta^{13}C$ and $\Delta^{14}C$) of DIC and stream invertebrates were performed at an AMS facility (Accium Biosciences, Seattle, WA). ^{13}C data are reported in $\delta^{13}C$ notation against the Vienna PDB standard. All radiocarbon results are reported as $\Delta^{14}C$, adjusted for sample $\delta^{13}C$ to account for mass-dependent fractionation (Δ in Stuiver and Polach 1977). $\Delta^{14}C$ is in per mil units (‰), where $\Delta^{14}C = \delta^{14}C - 2(\delta^{13}C+25)*(1+ \delta^{14}C/1000)$, $\delta^{14}C = (F_{mod}-1)\times1000$, and F_{mod} = fraction modern [*Stuiver and Polach*, 1977]. The average analytical error for F_{mod} ($\pm$ 1 σ) was 0.0031. $\Delta^{14}C$ greater than 0 ‰ reflects the presence of radiocarbon released by nuclear weapons testing in the 1950s and 1960s, though it does not preclude the presence of aged carbon fractions in a sample. Negative $\Delta^{14}C$ values imply the presence of pre-modern C (by definition before 1890) in a sample: if highly aged (i.e. ^{14}C-dead; $\Delta^{14}C$ = -1000 ‰) carbonate minerals or fossil carbon are present, sample $\Delta^{14}C$ may become depleted with even small contributions of these

sources. $\delta^{13}C$ of C_3 terrestrial vegetation ranges from -30 to -25 ‰ [*Deines*, 1980], and organic soil carbon should reflect this source. $\Delta^{14}C$ and $\delta^{13}C$ of atmospheric CO_2 vary seasonally, regionally, and locally, but average values for the Northern Hemisphere in summer are ~-8 ‰ for $\delta^{13}C$ and ~30 ‰ for $\Delta^{14}C$ [*Hua et al*., 2013]. Isotopic values for carbonates (either marine deposits or deposits within older rock formations) are not well described but should be 'radiocarbon-dead' ($\Delta^{14}C$ = -1000 ‰) and enriched in $\delta^{13}C$ [≥ 0 ‰; *Clark and Fritz,* 1997]. Bicarbonate formed via chemical weathering of carbonate minerals by plant-produced acids should have intermediate isotopic composition between carbonates and C_3 vegetation [*Clark and Fritz*, 1997].

Estimating gas transfer velocity and CO_2 fluxes

We calculated instantaneous vertical CO_2 fluxes out of streams as the temperature-corrected CO_2 concentration difference between stream water and the atmosphere, multiplied by a gas transfer velocity (K_{CO2}) according to:

Equation 1: $\text{Flux} = \left(\text{pCO}_2(\text{water}) - \text{pCO}_2(\text{air})\right) * K_{CO_2} * \text{K}_\text{H}$;

where pCO_2 is the partial pressure of carbon dioxide in stream water or air above the stream surface, measured directly in units of µatm. K_{CO2} is the CO_2 exchange velocity coefficient, in $m*day^{-1}$. K_H is Henry's constant corrected for water temperature [*Weiss*, 1974].Fluxes are in units of g C m^2 day^{-1}.

One of the most uncertain aspects of quantifying gas fluxes from water bodies involves estimating the air-water gas exchange velocity. Gas transfer velocity across the air-water interface is controlled by surface turbulence, the kinematic viscosity of water, and the diffusivity of the measured gas [a temperature-dependent property; *Wanninkhof*, 1992; *Zappa et al.,* 2007].

We used two different modelling approaches to estimate K_{CO2} values for our study streams. To allow comparisons of gas transfer velocity between streams with different water temperatures, we modelled K_{600}, the normalized air-water gas exchange velocity, rather than K_{CO2}. K_{600} estimates from models were then converted back to K_{CO2} in flux calculations using site-specific water temperature and Schmidt number scaling as described below [*Raymond et al.*, 2012]. Briefly, K_{600} can be related to K_{CO2} by the following equations:

Equation 2: $K_{600} = (600/Sc_{CO2})^{-0.5} * K_{CO2}$

Equation 3: $Sc_{CO2} = A - B * T + C * T^2 - D * T^3; \quad A = 1911.10 ; B = 118.11 ; C = 3.45; D = 0.04$

Sc_{CO2} is the Schmidt number for CO_2 (ratio of the kinematic viscosity of water to the diffusivity of CO_2), T is water temperature in degrees Celsius, and coefficients A-D are taken from Wanninkhof [1992].

Our first approach for calculating K_{600} for our study streams was to develop linear models between watershed geomorphic variables and estimates of K_{600} derived from an oxygen-based stream metabolism model within the Wood River system [*Holtgrieve et al*., 2010] as modified by Schindler et al. [in review]. We used model-estimated values of K_{600} from 24 streams throughout the basin [51 total estimates; oxygen measurements collected 2010 – 2014; see *Holtgrieve et al.,* 2010 for description of sampling] and regressed these against watershed geomorphic characteristics. We considered only geomorphic variables that should influence stream surface turbulence, and thus gas transfer velocity, via effects on stream bed roughness, flow velocity, and stream hydraulic geometry. We used stream gradient (averaged for the lower 1200 meters of the stream), substrate size (D84), the average depth and width of study reaches at which oxygen data

were collected, and 1/depth (reflects ratio of reach surface area to reach volume) as predictors in regression models. Mean reach depth of sites from the metabolism studies ranged from 0.03 to 0.57 m (mean = 0.25 m), and mean reach width ranged from 1.28 to 17.06 m (mean = 5.73 m). We did not include watershed slope as a predictor variable because it is highly correlated with stream substrate size in the Wood River system [*Lisi et al.*, 2013]. We never included more than one reach geometry variable (width, depth, depth^{-1}) in any model. Additive effects of multiple predictors, as well as interactive effects, were tested using regular multiple linear regression rather than mixed effects regression for repeat-measures, as there was no statistical support for including random effects of sampling stream in the models [following protocol in *Zuur et al.,* 2009]. Following model selection, we used the best regression model (hereon after the 'oxygen-based regression model') to generate K_{600} for all of our sampling streams in the Wood River system. We used 1000 Monte Carlo simulations to generate a normal distribution of K_{600} for each stream, with mean and variance based on the 95% confidence intervals from the oxygen-based regression model, using the *predict* function in R.

To assess if the K_{600} estimates derived from our basin-specific regression model were similar to K_{600} in other small streams and rivers, we compared them with K_{600} estimated using a second approach. In this second approach, K_{600} values for study streams were modelled using the relationship between K_{600}, stream slope (s, m*m^{-1}) and stream velocity (v; m*s^{-1}) reported in Raymond et al. [2012; Equation 3, hereon after 'Raymond K model']. K_{600} data in Raymond et al. [2012] were obtained from 563 gas tracer injection experiments conducted in U.S. rivers. We used the stream hydraulic geometry exponents and coefficients in Raymond et al. [2012] to predict average stream velocity at our study sites from discharge measured with a flowmeter. Average channel slope within 1200 meters of stream outlets was calculated from a 50 meter

resolution digital elevation map of the Wood River basin in ArcMap (version 10.3). We used 1000 Monte Carlo simulations to propagate model error and to generate a distribution of K_{600} for each stream sampling date.

We calculated evasion CO_2 fluxes from streams across the landscape geomorphic gradient using Equation 1. We ran 1000 Monte Carlo simulations to incorporate uncertainty in K_{600}, as well as measurement error in pCO_2 values. Each pCO_2 value used in flux calculations was drawn from a normal distribution centered around the mean measured value for a specific site and date (3 replicates). For the standard deviation of the distributions we used the average standard deviation for stream and air pCO_2 measurements (n= 105; average water SD = 23 μatm; air SD = 16 μatm).

After generating CO_2 flux estimates for each site and sampling event, we used mixed effects regression to test how watershed geomorphology (slope), precipitation, and their interaction influenced stream pCO_2 and CO_2 fluxes. pCO_2 and flux data were log-transformed prior to regression analyses. To account for non-independence of data collected from the same stream, we followed the model selection protocol outlined in Zuur et al. [2009]. We first compared random model structures using Akaike's information criterion, corrected for small sample sizes [AIC_c; *Burnham and Anderson,* 2002]. We compared models with no random effects to models including random effects of stream on the intercept, and found that the model with random effects fit the data best ($\Delta AIC_c > 10$ for no random effects models). Mixed effects models with different subsets of predictors (watershed slope, precipitation, interactions) were then fit using maximum likelihood and compared using AIC_c. Lower AIC_c indicates better model fit to the data; $\Delta AIC_c > 2$ between models indicates moderate statistical support for the model with lower AIC_c, whereas $\Delta AIC_c > 10$ indicates strong support. AIC_c model weights were

calculated as described in [*Burnham and Anderson*, 2002]. Regression analyses were performed in R [*R Core Team*, 2016] using the *lme4* package [Bates et al., 2015].

Results

Landscape gradient in stream carbon chemistry

CO_2 and DOC concentrations varied widely among streams within the Wood River basin (pCO_2, mean= 1131 µatm, sd= 1230 µatm, n = 111; DOC, mean= 4.17 ± 4.12 mg L^{-1}, n=111), while DIC concentrations tended to be less variable (DIC, mean = 356 ± 133 µmol kg^{-1}, n = 70). Of the 26 streams and rivers sampled for CO_2 concentrations, all but five were consistently supersaturated with CO_2 relative to the atmosphere (> 400 µatm). We observed higher but also more variable pCO_2 and DOC concentration in streams draining low gradient watersheds than in streams draining steep watersheds (Figure 2). pCO_2 and DOC concentration in streams were positively linearly correlated ($p < 0.0001$, $R^2 = 0.43$, n= 95). pCO_2 and total DIC concentration measured at upstream sites were generally slightly higher than measurements at stream outlets (mean upstream-downstream pCO_2 difference = 12 %, mean DIC difference = 3 % , n=9 sites). pH ranged from slightly acidic in streams draining peat wetlands to slightly basic (range: 6.19 – 7.88).

Gas transfer velocity and CO_2 evasion fluxes

Watershed geomorphic variables (substrate size, channel width, channel depth) explained substantial variability in the K_{600} estimates generated by the oxygen-based stream metabolism model. The overall best model included substrate size, average reach width, and their interaction term as predictors (ΔAIC_c of next best model > 5). The top nine models included substrate size as a predictor, and the top two models included positive interaction terms between substrate size and reach-scale stream geometry (width or depth). K_{600} was higher in streams with larger

substrate size (D84), but surprisingly, gradient within the stream channel was unrelated to K_{600} (Figure S2). Including stream gradient in multiple regressions did not improve model fit to the data. Including reach-specific depth and width measurements greatly improved model fits between geomorphic variables and oxygen-based estimates of K_{600} (a decrease in ΔAIC_c units >10; Table 1). However, reach geometry variables alone were not significant predictors of K_{600} (ΔAIC_c >20) without including substrate size (Figure S2).

However, because we did not perform similar reach-scale depth or width measurements as was done in the metabolism study while sampling for pCO_2, and given the high degree of spatial and temporal variation in depth and width both within and among streams, for the purposes of generating 'average' K_{600} values for the larger set of streams in our study, we considered only stream gradient and substrate size in our final model selection process. Of these explanatory variables, substrate size was the best predictor of K_{600} (model highlighted in bold font in Table 1), explaining 39% of the observed variation; gradient was not linearly related to K_{600} (a decrease in ΔAIC_c units > 10 from the best model; see Figure S2).

Our two modelling approaches yielded similar K_{600} estimates for our sampling streams (oxygen-based regression model, mean= 5.85 m day^{-1}; Raymond K model, mean = 6.04 m day^{-1}). Median estimates from 1000 Monte Carlo simulations from either method were significantly positively correlated for each sampling event (site and date combination; $R^2 = 0.42$, $p < 0.0001$, n=53). Residual differences are likely due to the fact that the Raymond model accounts for changes in discharge (yielding a higher K_{600} during high flows) whereas the oxygen-based regression model provides only a single 'average' K_{600} estimate per stream. Both models yielded a similar pattern of increasing K_{600} in streams from low to high gradient watersheds (Figure 3). Streams draining high gradient watersheds in the Wood River system tend to have larger

substrate size [*Lisi et al.*, 2013] and higher surface turbulence as well as faster flow velocities, thus this pattern fits theoretical expectations for K_{600}. Given the similarity in K_{600} values generated from both approaches, we report only CO_2 fluxes calculated using K_{600} values obtained from the oxygen-based regression model, as this model was developed using data from the Wood River basin and should better reflect local conditions.

Instantaneous CO_2 fluxes from Wood River streams ranged from -3.9 to 18.1 g C m^{-2} day^{-1} (median estimates from 1000 Monte Carlo simulations). At base flow, evasion fluxes were generally similar across sites (1.7 ± 2.1 g C m^{-2} day^{-1} (mean ± 1 standard deviation) despite heterogeneous geomorphic conditions and variable stream pCO_2 across the basin (Figure 4a and 4c). However, several streams in the flattest watersheds (mean slope < 4°) showed extremely high fluxes at base flow. Furthermore, pCO_2 and CO_2 fluxes increased significantly after rainstorms in streams draining flat watersheds, but not in streams draining steep watersheds (Figure 4b and 4d).

To assess the influence of watershed slope on stream pCO_2 and CO_2 fluxes under different hydrologic conditions (base flow versus after large rain events), we compared mixed effects multiple regression models with watershed slope, precipitation ('base flow' versus 'after rain'), and their interaction as predictors. All models included a random effect of stream on the intercept.

At base flow, stream pCO_2 declined with increasing watershed slope; this pattern strengthened after rain events (Figure 4a and 4b).The best fit model for pCO_2 (log-transformed) included watershed slope, precipitation, and a negative interaction term; a model with an interaction term fit the data significantly better than a model without an interaction term (ΔAIC_c > 5, n=106, 24 streams, Table 2). Stream CO_2 fluxes at base flow were similar across the

landscape, except for a few low gradient sites (Figure 4c). After rain events, CO_2 fluxes were substantially higher from streams draining low gradient watersheds than from steep watersheds (Figure 4d). The best fit model for stream CO_2 flux (log-transformed) included watershed slope, precipitation, and a negative interaction term; a model without an interaction term fit the data significantly worse ($\Delta AIC_c > 2$, n=106, 24 streams, Table 2).

Isotopic composition of DIC and stream consumers

The radiocarbon signatures of DIC in streams across the Wood River watershed in 2014 and 2015 were substantially depleted (older) than contemporary atmospheric CO_2 [currently $\Delta^{14}C \sim 30$ ‰, Hua et al. 2013], ranging from -198.3‰ to 47.2‰ (-28.38 ‰ ± 51.65, n = 45; Table S2). Average $\delta^{13}C$ DIC was slightly depleted relative to atmospheric CO_2 (currently ~ -8 ‰), but was also highly variable among and within streams (-11.6 ‰ ± 5.36, n=45). The data did not support the expected pattern of older and more $\delta^{13}C$-depleted DIC in low gradient streams, but rather showed high variability in DIC age among sites regardless of watershed slope.

$\Delta^{14}C$ DIC within streams changed heterogeneously following rain events, but in 9 out of 11 streams sampled immediately after a rainstorm in 2015, DIC age become younger (more enriched) relative to samples collected at base flow (Figure 5e). In 2014, 6 out of 8 streams showed $\Delta^{14}C$ DIC enrichment following a large rainstorm. Generally, low gradient streams had increased pCO_2, increased DOC concentration, and dilution of total DIC following the 2015 rain event, accompanied by enriched $\Delta^{14}C$ DIC and depleted $\delta^{13}C$ DIC (Figure 5b-f). High gradient streams showed smaller responses and $\Delta^{14}C$ DIC enrichment was significantly correlated with dilution of total DIC concentration following rain ($R^2 = 0.46$, $p < 0.001$, n=17).

$\Delta^{14}C$ of aquatic invertebrates ranged between -65.6 ‰ and +37.5 ‰ (Figure 6; Table S3) and was generally enriched relative to average stream $\Delta^{14}C$ DIC (Figure 6 inset). Mean $\Delta^{14}C$ of

caddisfly larvae (18.9 ‰ ± 15.9, n = 14) was enriched above 'pre-bomb' atmospheric CO_2, indicating consumption of modern C sources. Mayfly nymphs, in contrast, showed greater depletion in $\Delta^{14}C$ (mean= -4.1 ‰ ± 31.4, n = 13), and were generally close in isotopic signature to the average $\Delta^{14}C$ DIC in a stream (Figure 6 inset). Mayflies were consistently more depleted in $\delta^{13}C$ (-36.06 ‰ ± 4.9) than caddisflies (-33.1 ‰ ± 3.8).

Discussion

CO_2 fluxes and gas transfer velocity

Watershed geomorphology exerts strong controls on carbon emissions from streams in the Wood River basin, Alaska, via two opposing mechanisms. First, watershed slope appears to influence the potential magnitude of terrestrial C loading to streams. Flat watersheds with poor drainage accumulate soil carbon over millennial time scales due water-saturated, low oxygen conditions that reduce the rate of within-soil respiration of organic material [*Trumbore and Harden*, 1997]. Streams draining low gradient watersheds in the Wood River system tended to have higher pCO_2 and DOC concentration at base flow (Figure 2a and 2c). Further, differences in C loading between streams in low and high gradient watersheds widened following rain storms; streams draining low gradient watersheds show greater increases in pCO_2 following precipitation than steep streams (Figure 4a-b). However, a second mechanism attenuates differences in CO_2 fluxes across the geomorphology gradient: gas transfer velocity is higher in steep, fast-flowing, turbulent streams than in low-velocity, less turbulent streams draining flatter watersheds (Figure 3). Therefore, the effects of low gas transfer velocity on gas flux from flat streams offsets some of the effects of higher terrestrial C loading at those sites, resulting in lower than expected vertical CO_2 fluxes (Figure 7a-b). Estimates of CO_2 flux calculated using a uniform K_{600} for all streams (median estimate from oxygen-based metabolism model; K_{600} = 4.44

$m*day^{-1}$) resulted in substantially higher fluxes from low gradient streams and slightly decreased fluxes from high gradient streams, relative to estimates from a model that accounts for landscape variation in gas transfer velocity (Figure 7a-b). Previous efforts to quantify stream CO_2 emissions from boreal landscapes have often used a single K_{600} value for streams of the same order [*Teodoru et al.*, 2009; *Humborg et al.*, 2010], potentially leading to overestimation of fluxes from low gradient systems [but see *Streigl et al.*, 2012; *Crawford et al.*, 2013].

Overall, the effect of geomorphology on stream CO_2 fluxes was stronger via the first mechanism (terrestrial C loading) than via the second mechanism (K_{CO2}). Calculated fluxes were two to four times higher from the low gradient watersheds (mean slope < 5°) than from steeper watersheds, both at base flow and after rain events (Figure 4c-d). Our method of estimating K_{CO2} (oxygen-based regression model) did not account for changes in discharge, and thus may have under-estimated gas transfer velocity during high flow periods. Flow velocity and surface turbulence both change during high flow events, and may change differently in low gradient versus high gradient streams. However, using the K_{CO2} estimates from the Raymond equation, which does include discharge as an input, did not change the landscape patterns in CO_2 flux.

Stream power [proportional to discharge and channel slope; *Leopold et al*., 1995] dictates the maximum particle sizes that can be mobilized within channel beds, therefore substrate size may act both as a direct driver of turbulence and as an integrated response to other drivers such as gradient and flow velocity. As a result, distinguishing separate effects of substrate size and gradient on surface turbulence and gas transfer velocity may be difficult in natural streams. Substrate size, rather than that stream gradient, was the best predictor of oxygen-based K_{CO2} estimates in our study streams, whereas other studies have found strong correlations between gradient and gas transfer velocity [*Wallin et al.*, 2011; *Schelker et al.*, 2016]. However, this may

result from a relative lack of variation in gradients among our sites (range: 0.0001-0.05), or from using an overly coarse digital elevation model (50-m resolution) to calculate gradients. Alternatively, substrate size may simply be a more important driver of surface turbulence than gradient in our relatively small, shallow study streams. Nevertheless, estimates of K_{CO2} from the oxygen-based regression model agreed well with values from the Raymond K model (R^2= 0.42; Figure 3), giving us confidence that our model based on substrate size described significant variation in gas transfer velocity among streams. Our results also suggest that substrate size may provide a simple, integrative measure of stream power by which to estimate gas transfer velocity in streams lacking detailed measurements of channel geometry.

The strong interaction between watershed slope and precipitation may be the most significant mechanism by which geomorphology affects CO_2 flux from Wood River streams. During base flow conditions, streams can become disconnected from terrestrial C pools present within surface soils, regardless of the size of those pools. The importance of precipitation and large storms for mobilizing terrestrial DIC and DOC into boreal streams has been established previously [*Raymond and Saiers*, 2010; *Butman and Raymond*, 2011; *Laudon et al.*, 2011; *Olefeldt et al.*, 2013] , but here we show how catchment geomorphology mediates this process to produce heterogeneous CO_2 concentrations and CO_2 fluxes within a single river basin.

In addition to these different stream responses to rain events, the high variability in pCO_2 and fluxes in low gradient watersheds at base flow is likely due to biological as well as physical drivers. In the Wood River basin, low gradient streams receive more sunlight than high gradient streams due to less riparian canopy cover, presumably because tree growth is inhibited in waterlogged soils. Steep watersheds, on the other hand, frequently support dense stands of alder and cottonwood that shade the stream channel [*Bartz and Naiman*, 2005]. Thus low gradient

streams, while receiving higher terrestrial C loads, also have a tendency to support higher algal primary production [*Schindler et al*. in review]. Because we collected point measurements of pCO_2 during the day, when primary production and CO_2 draw-down occur, we are likely under-estimating terrestrial C inputs to some low-gradient streams.

Stream DIC sources and consumer isotopes

The isotopic signature of stream DIC in the Wood River basin was spatially and temporally heterogeneous and did not match our expected patterns of increasing $\Delta^{14}C$ and $\delta^{13}C$ depletion in low gradient watersheds. Rather, pre-modern carbon ($\Delta^{14}C < 0$ ‰) contributed to DIC in both steep and low gradient watersheds at base flow, and $\delta^{13}C$ -DIC was even more variable across sites, ranging from -17.2 ‰ to -2.4 ‰ at base flow. While watershed slope clearly influences C loading and fluxes in the Wood River basin, the complex mixture of potential DIC sources present (atmospheric CO_2, young terrestrial OM, aged terrestrial OM, carbonate minerals), coupled with the biological, chemical, and hydrological processes that can affect isotopic signatures, precluded simple prediction of DIC age and origin based on watershed characteristics.

Stream responses to large rainfall events provided valuable information on hydrologic controls on DIC sources. Stream DIC generally became younger after rain, and this response was accompanied by increases in pCO_2 and DOC, and dilution of DIC, implying that surface and subsurface flow paths following rainstorms transported a different mixture of DIC sources than present in streams at base flow. These changes in carbon chemistry and composition were more pronounced in low gradient watersheds than in steep watersheds (Figure 5). Similar patterns of $\Delta^{14}C$ -DIC enrichment in streams following storms have been observed in other high latitude regions [*Billett et al.*, 2012; *Garnett et al.*, 2012]. Rainwater is routed through CO_2 and DIC-rich

flow paths during storms, delivering these young terrestrial C sources to streams. We show here that the strength of this response is mediated by watershed slope.

The smaller responses we observed in high gradient watersheds may partially result from sampling limitations. While we visited all sites within a day of peak rainfall, due to the logistical difficulty of sampling multiple streams in remote areas during storm conditions, we may have missed the peak pulse of storm water out of high gradient watersheds, whereas in low gradient watersheds, storm water has a longer residence time both in soil and in the stream itself. Nevertheless, these differences in flow regime among streams likely also contribute to different amounts of terrestrial C delivery: prolonged residence time of rainwater surface or subsurface flow in flat watersheds should also increase C loading. Therefore, our conclusions would be similar regardless of whether high gradient streams were sampled later on the falling limb of the hydrograph than low gradient streams.

While DIC in Wood River streams was predominantly modern, old C sources clearly contributed to the isotopic signature at some sites. Because we did not directly measure the isotopic composition of soil DIC or soil evasion CO_2, distinguishing aged biogenic DIC sources from geologic DIC sources (carbonate weathering product) is difficult. In several streams with $\Delta^{14}C$ -DIC indicative of pre-modern C inputs, $\delta^{13}C$ -DIC was more enriched than atmospheric CO_2 (see Table S3). While in theory DIC derived from the respiration of aged terrestrial OM should have more depleted $\delta^{13}C$ than HCO_3^- derived from carbonate weathering, the phenomenon of $\delta^{13}C$ - DIC enrichment with depth in organic peat soils is well-documented [from -20 ‰ to +10 ‰; *Aravena et al.,* 1993; *Clymo and Bryant* ,2008; *Steinmann et al.* 2008]. δ^{13}-DIC in our study streams was often highly enriched relative to typical terrestrial OM (-28 ‰), potentially reflecting processes such as isotopic fractionation of soil CO_2 and DIC due to

off-gassing [i.e. lighter isotopes diffuse faster to the atmosphere; *Doctor et al.,* 2008], or methane production in anoxic soil layers via acetate fermentation or CO_2 reduction, wherein CH_4 becomes highly $\delta^{13}C$ -depleted and residual CO_2 becomes enriched [*Whiticar et al.*, 1986].

While ^{14}C -depleted carbonates are probably distributed throughout the Wood River basin within widespread glacial gravel deposits, contributing to $\Delta^{14}C$ -DIC depletion, we suspect that the depleted $\Delta^{14}C$ -DIC and enriched $\delta^{13}C$ -DIC observed in low gradient, wetland-dominated streams (e.g. Stovall, Nerka Bear, Whitefish, and Eagle creeks; Table S3) result in part from inputs of respiration products of aged biogenic soil C that has undergone fractionation. Aged soil C (> 4000 years BP) is present in Wood River watersheds containing peat (peat soil collected along Pick Creek in 2013; see Figure 6). On the other hand, chemical weathering of carbonate minerals is likely a more important source of $\Delta^{14}C$ depleted, $\delta^{13}C$ enriched DIC in steep, high-relief, soil-poor watersheds [e.g. Allah creek, Table S3]. Studies in other peatland systems have found similar patterns in DIC isotopic composition as we observed in our low gradient streams: stream DIC and evasion gases are older and $\delta^{13}C$ -enriched relative to surface peat vegetation and respiration products, which is attributed to a mixture of aged biogenic and geologic sources from deeper soil layers [*Leith et al.*, 2014; *Billett et al.*, 2015]. Regardless of the ultimate source of pre-modern DIC in Wood River streams, changes in DIC isotopic composition following large rain events likely represent shifts in water inputs from deeper soil flow paths at base flow to more shallow soil or surface flow.

Previous work using fatty acid biomarkers revealed geomorphic influence on the energy sources assimilated into stream food webs within the Wood River basin [*Smits et al.*, 2015]. Invertebrates incorporated relatively more carbon processed via microbial pathways in low gradient watersheds than in steep watersheds. In this study we measured $\Delta^{14}C$ of stream insects

to see if the influence of geomorphology on terrestrial C loading and CO_2 emissions extended to the carbon sources assimilated by consumers. On average, insect $\Delta^{14}C$ was enriched relative to stream DIC, reflecting consumption of pre-dominantly modern resources (Figure 6). However, mayflies in streams with $\Delta^{14}C$ -depleted DIC were also $\Delta^{14}C$ -depleted, whereas caddisflies in some streams were more decoupled from the DIC signature (Figure 6 inset). This suggests an indirect pathway of aged C to contemporary food webs, where DIC is taken up by primary producers during photosynthesis, which are then consumed by grazer taxa such as mayfly nymphs and some caddisfly species.

While we did not sample other potential sources of aged C to insects (POM, DOC), other studies in temperate and high latitude systems support an indirect DIC- algae- grazer pathway of aged C into food webs. Ishikawa et al. [2013] found that periphyton, insects, and fish were substantially $\Delta^{14}C$ -depleted in 15 Japanese streams with varying degrees of carbonate influence (minimum periphyton $\Delta^{14}C$ = -252 ‰), whereas stream POC was modern at all sites (> 0 ‰). Fellman et al. [2015] attributed $\Delta^{14}C$ depletion in consumers in a glacial-melt river to assimilation of heterotrophic biofilms fueled by ancient, labile glacial DOC. However $\Delta^{14}C$ DIC in the glacial river was also depleted (< -200 ‰), and biofilms likely also contained epilithic algae, thus an indirect algal pathway may also contribute to consumer $\Delta^{14}C$ depletion. Despite our modest sample sizes (two major consumer taxa in 12 streams), our findings corroborate previous observations that DIC may be a common source of aged terrestrial (or geologic) carbon to aquatic food webs.

Conclusions

Geomorphology and precipitation interact to control terrestrial carbon fluxes into and out of boreal Alaskan streams. Watershed slope strongly influences C loading and emission

dynamics from streams both by determining the strength of aquatic -riparian coupling and to a lesser extent by controlling gas transfer velocity. In low gradient watersheds, CO_2 emission fluxes are high but slightly attenuated by low gas transfer velocity, whereas in steep watersheds CO_2 emissions are low due to limited terrestrial C loading. While stream DIC sources are highly variable across space and time, DIC isotopes change more after rainfall in low gradient watersheds, suggesting an influence of watershed slope. Rainwater flushes young, terrestrial DIC into streams, whereas at base flow DIC is a mixture of modern and aged sources, mostly likely of both biogenic and geologic origin. These aged C sources partially contribute to contemporary food webs via an indirect pathway—algae take up DIC, and algae are then consumed by invertebrates.

The responses we observed in stream carbon chemistry to perturbations such as rainstorms revealed coherent landscape patterns in aquatic-terrestrial coupling despite considerable physical heterogeneity within and among watersheds. These patterns provide a way to extrapolate across boreal landscapes by constraining pCO_2 and CO_2 flux estimates by local geomorphic features. In addition, characterizing how geomorphology dictates stream responses to precipitation will aid efforts to understand climate-induced changes in carbon cycling in high latitude ecosystems.

Tables

Table 1. Multiple regression models between watershed geomorphic variables (substrate size (D84) and stream gradient), reach-scale channel geometry (width, depth, and depth^{-1}), and K_{600} (m*day^{-1}) in Wood River streams. K_{600} values are outputs from an oxygen-based stream metabolism model [*Holtgrieve et al*., 2010; *Schindler et al.* in review]. Oxygen measurements were collected over four summers (2010-2014) from 24 streams in the Wood River basin—16 of these same sites were also sampled in this study. N is the sample size, K is the number of estimated parameters. The regression model used to predict K_{600} for the streams in this study is highlighted in bold font. The ten models with the lowest AIC_c are shown (rows 1-10), as well as all the single-predictor models (rows 11-13). We show regression equations for the top five models.

Predictors	**N**	**K**	**AICc**	**ΔAICc**	**AICc weight**	**Equation**
D84; Width; Interaction	51	5	239.86	0	0.99	K_{600} = 5.086 – 0.020* D84 – 0.524*Width + 0.125*D84*Width; $p < 0.001$; $R^2 = 0.57$
D84; Depth; Interaction	51	5	248.65	8.79	0.01	K_{600} = 4.271 – 0.017* D84 – 11.390*Depth + 0.354*D84*Depth; $p < 0.001$; $R^2 = 0.49$
D84; Width	51	4	254.43	14.57	0	K_{600} = 0.266 + 0.068* D84 + 0.200*Width; $p < 0.001$; $R^2 = 0.42$
D84; Depth	51	4	255.11	15.25	0	K_{600} = -0.252 + 0.074* D84 + 5.135*Depth; $p < 0.001$; $R^2 = 0.41$
D84	**51**	**3**	**255.72**	**15.86**	**0**	**K_{600}= 1.191 + 0.072* D84; $p < 0.001$; $R^2 = 0.39$**
D84; Depth^{-1}	51	4	256.48	16.62	0	
D84; Stream Gradient	51	4	257.07	17.21	0	
D84; Depth^{-1}; Interaction	51	5	258.89	19.03	0	
D84; Stream Gradient; Interaction	51	5	259.5	19.65	0	
Width	51	3	277.5	37.64	0	
Depth	51	3	282.27	42.41	0	

$Depth^{-1}$	51	3	282.61	42.75	0
Stream Gradient	51	3	282.77	42.91	0

Table 2. Results from linear regression models between CO_2 flux (g C m^2 day^{-1}) or pCO_2 (µatm) and mean watershed slope (degrees) and precipitation (base flow versus after rain). pCO_2 and flux data were log-transformed prior to use in models. All regression models include a random effect of 'stream' on the intercept. N is the sample size, K is the number of estimated parameters.

Response	Predictors	N	K	AICc	ΔAICc	AICc weight
Log CO_2 Flux	Slope, Precipitation, Interaction	106	6	-74.83	0	0.83
	Slope, Precipitation	106	5	-71.50	3.33	0.16
	Precipitation	106	4	-65.33	9.50	0.01
	Slope	106	4	-55.42	19.42	0
	Intercept-only	106	3	-49.28	25.55	0
Log pCO_2	Slope, Precipitation, Interaction	106	6	-90.39	0	0.99
	Slope, Precipitation	106	5	-81.79	8.6	0.01
	Precipitation	106	4	-73.7	16.69	0
	Slope	106	4	-51.3	39.09	0
	Intercept-only	106	3	-43.46	46.93	0

Figure Legends

Figure 1. Stream sampling sites (black dots) within the Wood River basin, SW Alaska (59°20′ N, 158°40′W).

Figure 2. pCO_2 (a), total DIC concentration (b), DOC concentration (c), and pH (d) in streams across the Wood River basin, plotted against mean watershed slope (degrees). All measurements were collected in summer 2014 and 2015. Data include samples taken at base flow and after rain events. The dashed black line in panel A shows the current average partial pressure of CO_2 in the atmosphere (400 µatm).

Figure 3. Estimates of K_{600} for Wood River streams, plotted against mean watershed slope. The black dots show median estimates of K_{600} for each Wood River stream predicted by the oxygen-based regression model, and the grey squares show median estimates of K_{600} for each stream (sampling date) from the Raymond equation model. Black or gray bars around data points are the 95% confidence intervals calculated from 1000 Monte Carlo simulations. The black solid line and gray dashed line show linear relationships between estimated K_{600} and mean watershed slope for the oxygen-based regression model and the Raymond equation model respectively.

Figure 4. pCO_2 (panels a and b) and evasion CO_2 fluxes (panels c and d) from Wood River streams (2014 and 2015) at base flow (left column) and post-rain conditions (right column), plotted against mean watershed slope. pCO_2 data points are the mean value from triplicate samples. Flux data points represent the median of 1000 Monte Carlo simulations (used oxygen-based regression model to generate K_{600} for each stream). Grey bars represent 95% confidence intervals. The dashed line in panels a and b represents the global average atmospheric pCO_2 (~ 400 μatm). Dashed lines in panels c and d are at zero net CO_2 flux. Solid black lines represent exponential relationships between watershed slope and pCO_2 or flux. pCO_2 and CO_2 flux data were log-transformed prior to use in regression models.

Figure 5. Responses of Wood River streams to a July 2015 rainstorm for a) stream flow,b) total DIC concentration, c) pCO_2, d) DOC concentration, e) $\Delta^{14}C$ DIC, and f) $\delta^{13}C$ DIC, plotted against mean watershed slope (x-axis). All x-axes are to the same scale. Black dots represents measurements taken at base flow conditions in June or July, and arrows point to the post-rain measurement, taken with a day of the storm. The dashed black line in panel c is the current mean atmospheric pCO_2 (~400 μatm). The gray shaded region in panel e represents $\Delta^{14}C$ values that

must contain carbon fixed after the onset of nuclear weapons testing (post-bomb, defined as after 1950 AD).

Figure 6. $\Delta^{14}C$ and $\delta^{13}C$ of stream DIC (black dots; 2014-2015), stream invertebrates (triangles; 2013-2014), and peat soil (squares; samples collected from an exposed profile near Pick Creek in 2014) collected within the Wood River basin. Colored regions show 'expected' isotopic ranges for potential C sources to stream DIC. The mean mayfly (black filled triangles) and caddisfly (empty triangles) $\Delta^{14}C$ per stream are plotted against average $\Delta^{14}C$ DIC in the figure inset. The dashed line represents the 1:1 relationship.

Figure 7. A) Landscape patterns in CO_2 flux from Wood River streams, assuming a constant gas transfer velocity across sites (gray dots; overall median of all K_{600} estimates from the oxygen-based metabolism model; K_{600} = 4.44 m*day^{-1}), or variable gas transfer velocity (black dots; K_{600} values generated from oxygen-based regression model). Data points include all measurements from 2014 and 2015 during base flow and post-rain conditions. Solid curved lines represent exponential relationships between stream CO_2 flux and mean watershed slope (degree). The dashed line represents zero net CO_2 flux. B) The ratio of CO_2 fluxes calculated using constant gas transfer velocity versus CO_2 fluxes calculated using variable K_{600}, plotted against mean watershed slope. The dashed line represents a 1:1 relationship between fluxes calculated using either constant or variable K_{600}.

Figures

Figure 1

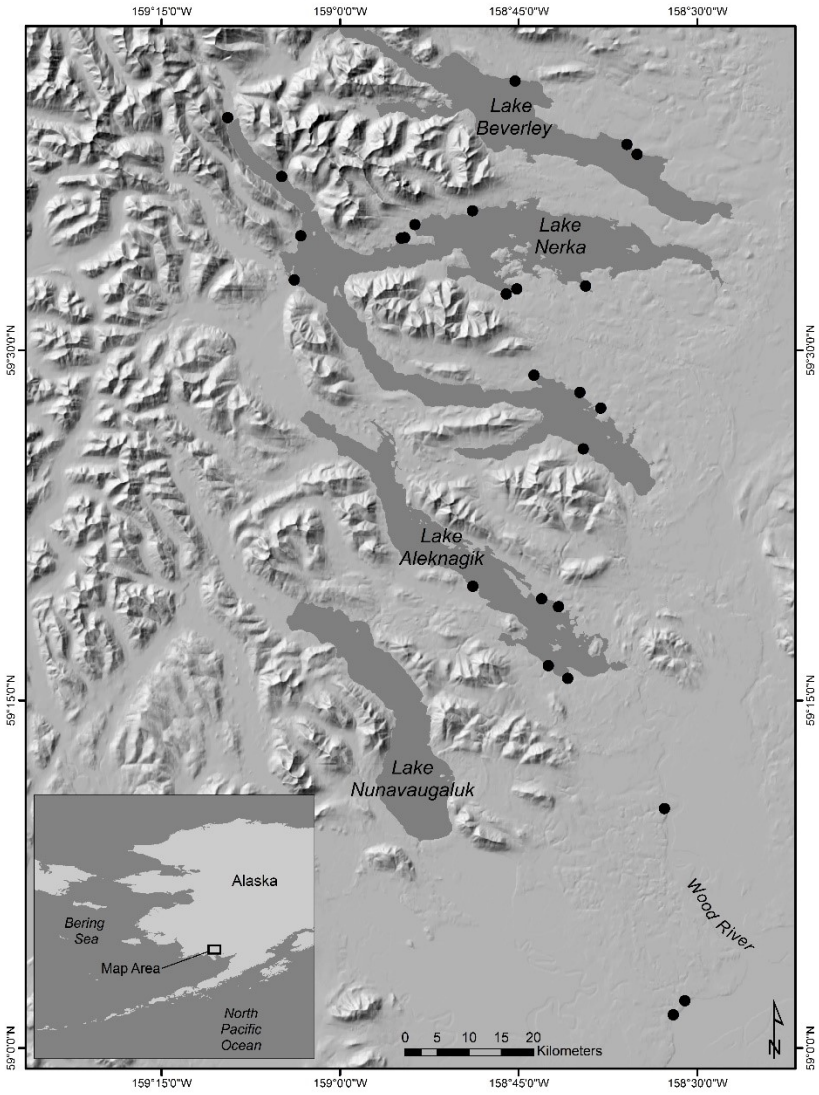

Figure 2

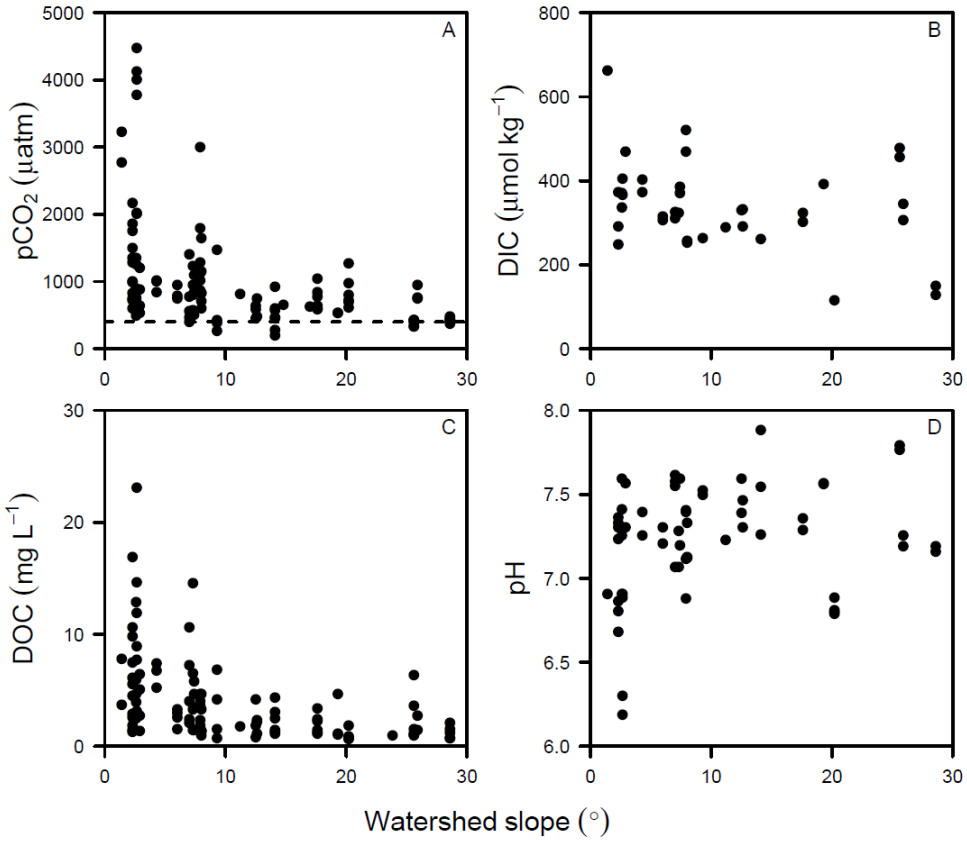

Figure 3

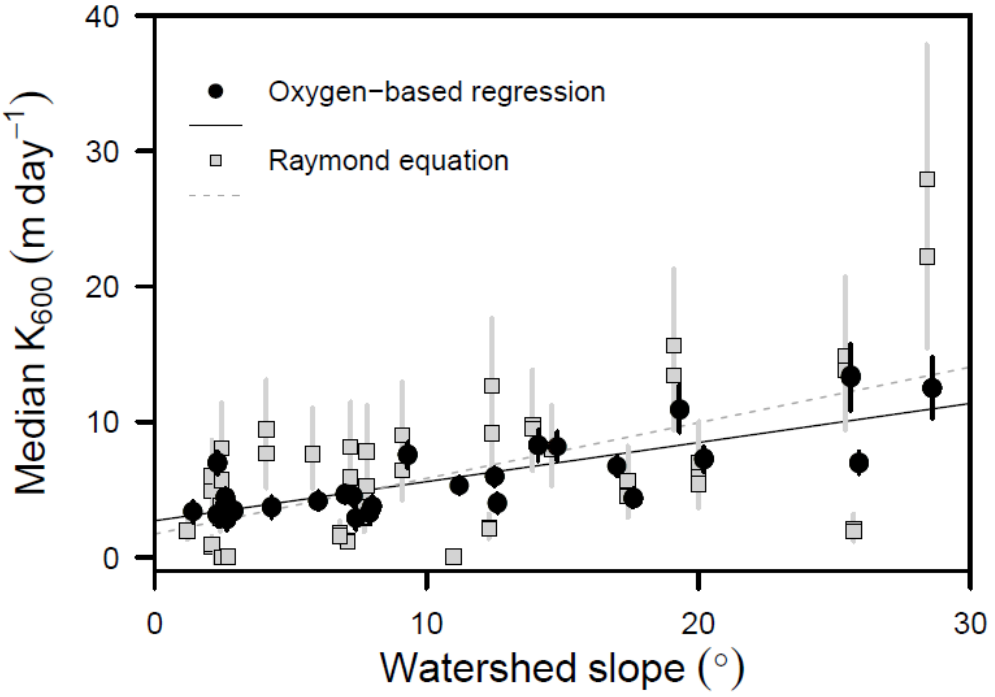
Oxygen−based regression
Raymond equation
Median K_{600} (m day^{-1})
Watershed slope (°)
0
10
20
30
40

Figure 4

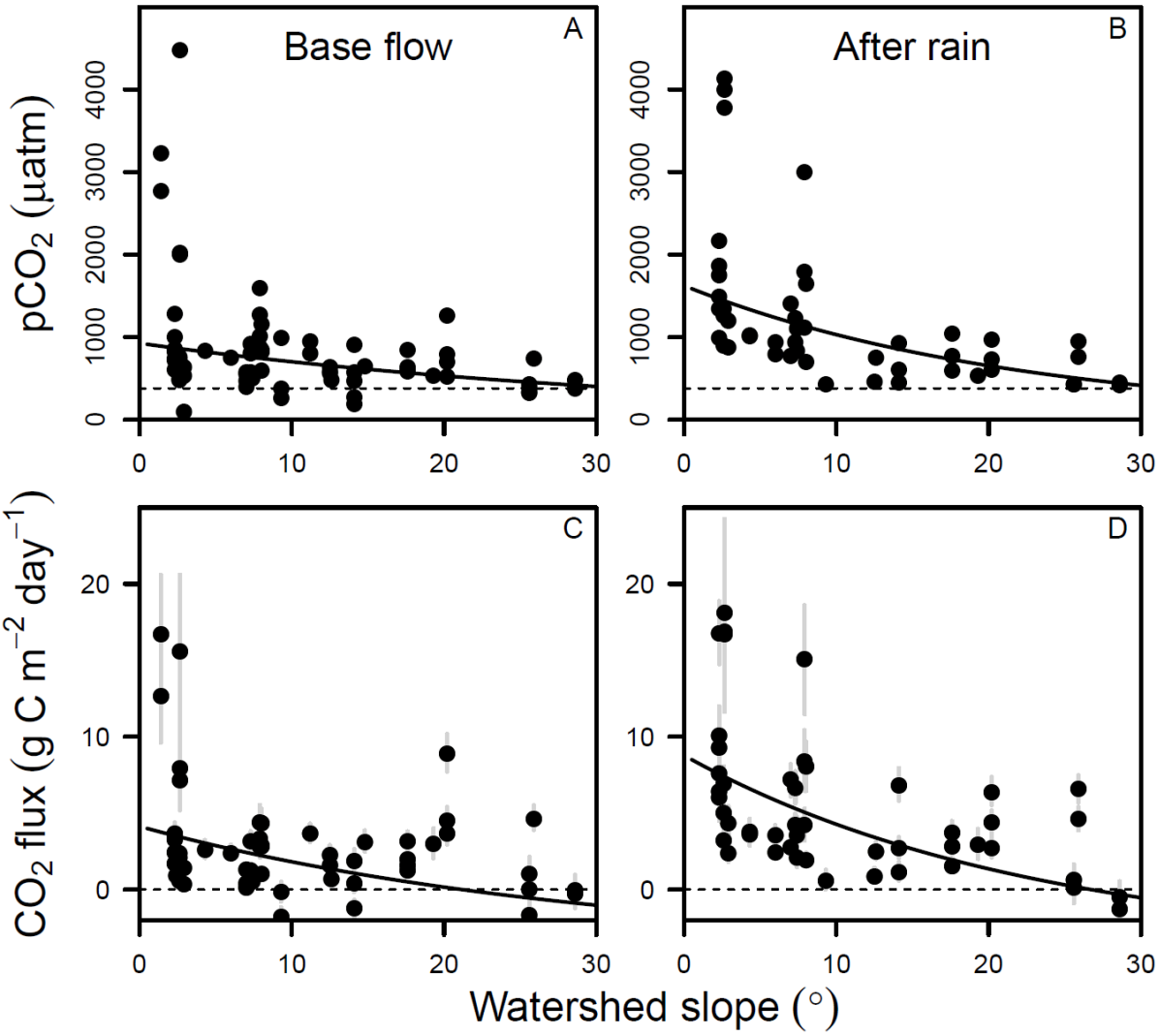
Base flow
A
After rain
B
C
D
pCO2 (µatm)
CO2 flux (g C m−2 day−1)
Watershed slope (°)
0
1000
2000
3000
4000
10
20
30

Figure 5

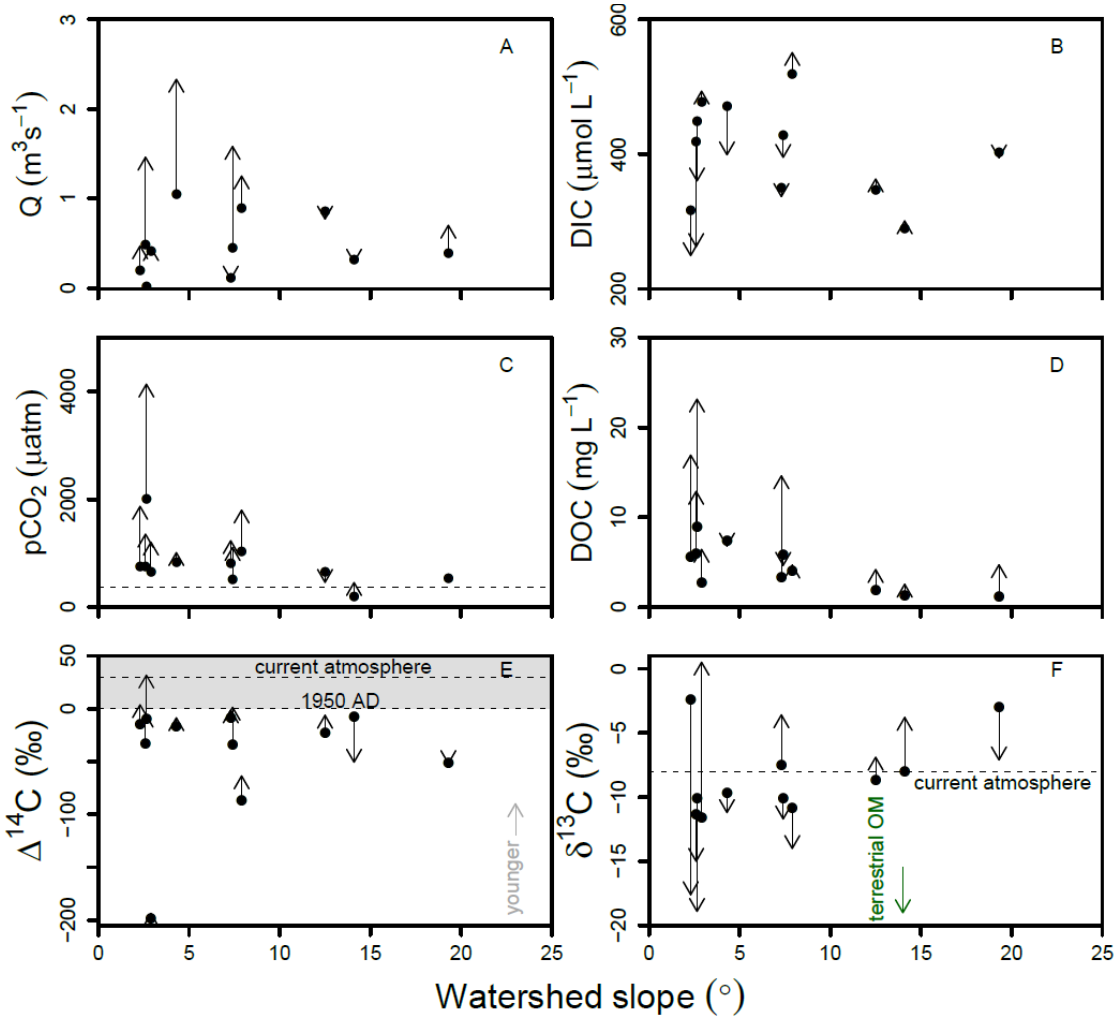
A
B
C
D
E
F
Q (m3s-1)
DIC (µmol L-1)
pCO2 (µatm)
DOC (mg L-1)
Δ14C (‰)
δ13C (‰)
current atmosphere
1950 AD
younger
terrestrial OM
current atmosphere
Watershed slope (°)

Figure 6

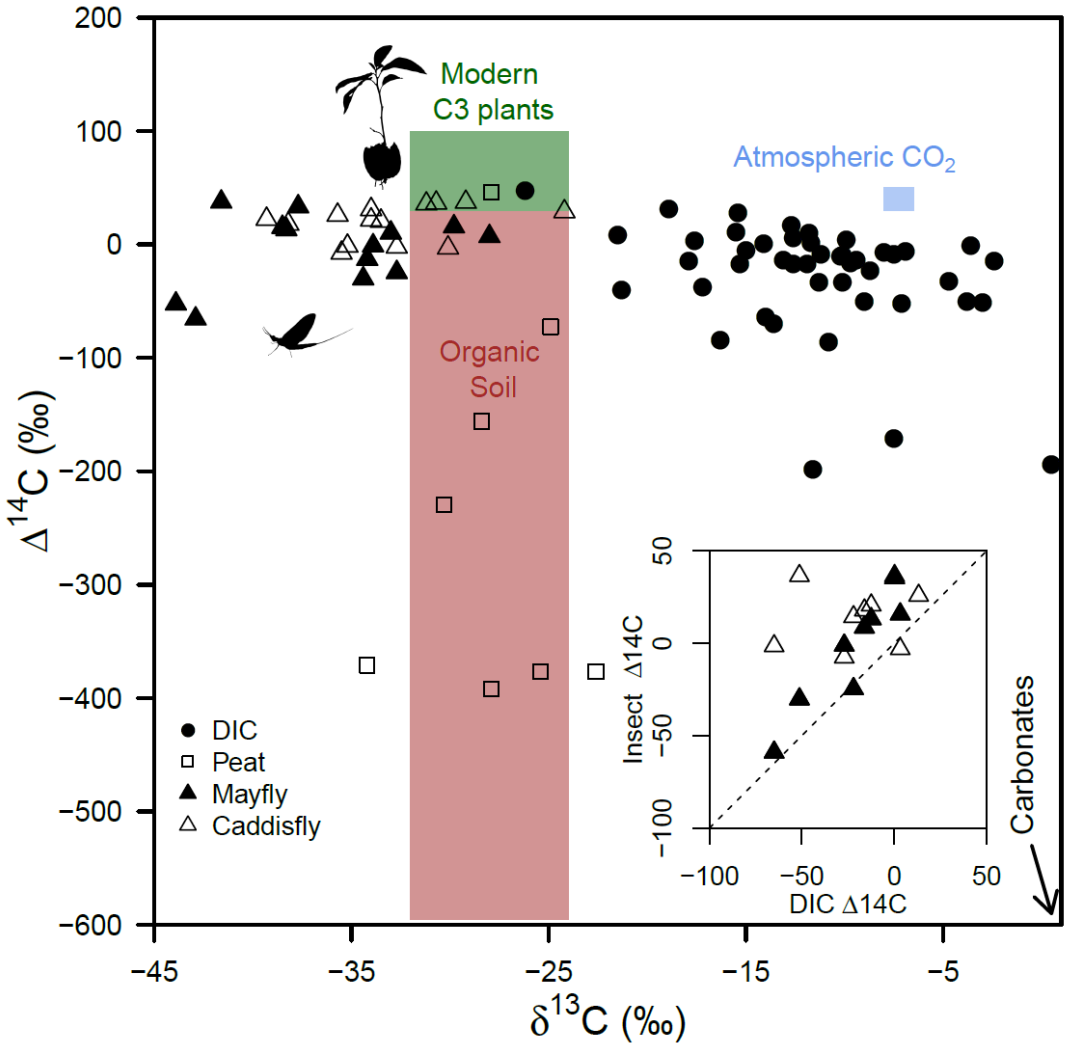
Modern
C3 plants
Atmospheric CO_2
Organic
Soil
DIC
Peat
Mayfly
Caddisfly
Carbonates
Insect Δ14C
DIC Δ14C
$\Delta^{14}C$ (‰)
$\delta^{13}C$ (‰)
200
100
0
−100
−200
−300
−400
−500
−600
−45
−35
−25
−15
−5
50
0
−50
−100

Figure 7

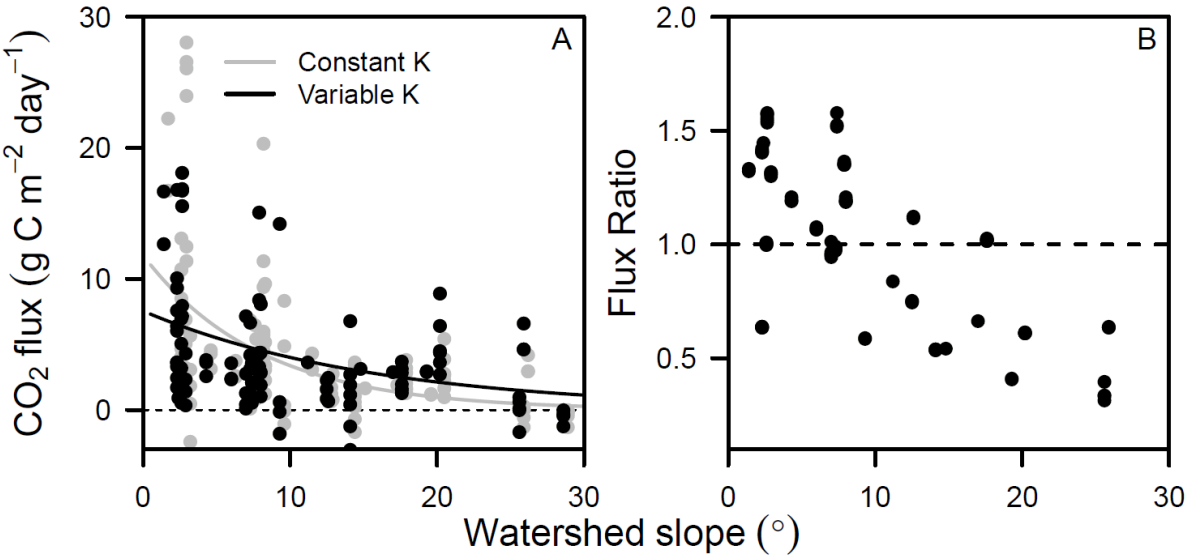
A
B
Constant K
Variable K
CO_2 flux (g C m^{-2} day^{-1})
Flux Ratio
Watershed slope (°)
30
20
10
0
2.0
1.5
1.0
0.5
0
10
20
30

Supplementary Information

Figure S1. Daily rainfall amounts (centimeters) recorded at a rain gage near Lake Nerka, Wood-Tikchik State Park, Alaska. Red stars indicate storms after which sampling occurred in 2014 and 2015.

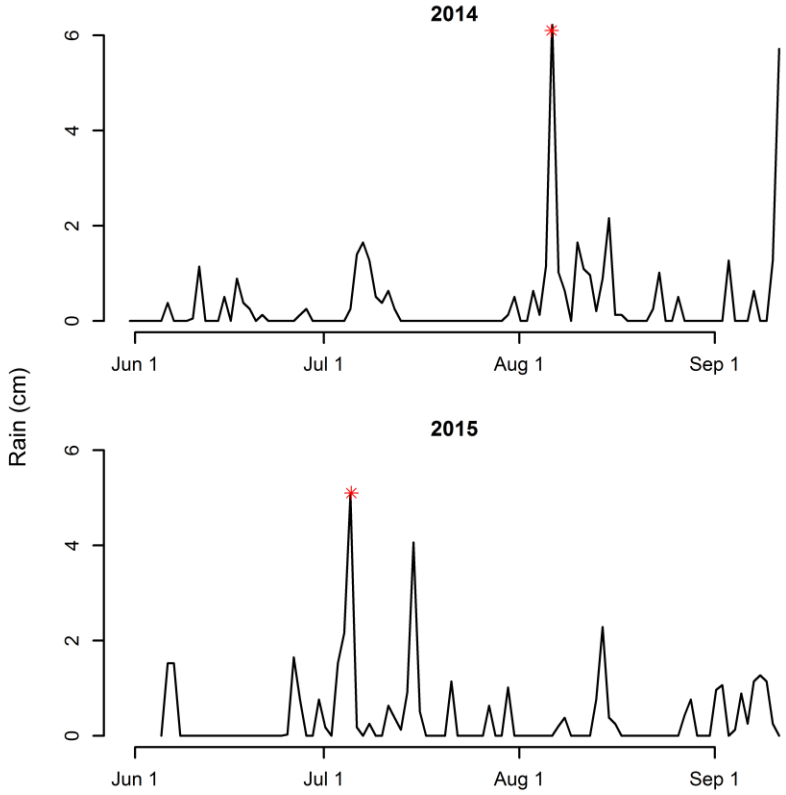

Figure S2. Relationships between estimates of K_{600} (m day^{-1}) from an oxygen-based stream metabolism model [Holtgrieve et al. 2010; Schindler et al. in review] and A) stream substrate size (D84; cm), B) stream gradient in the lower 1200 m section of each stream (meters per meter), C) average reach depth (m), and D) average reach width (m). Dashed lines represent linear relationships between K_{600} and each variable.

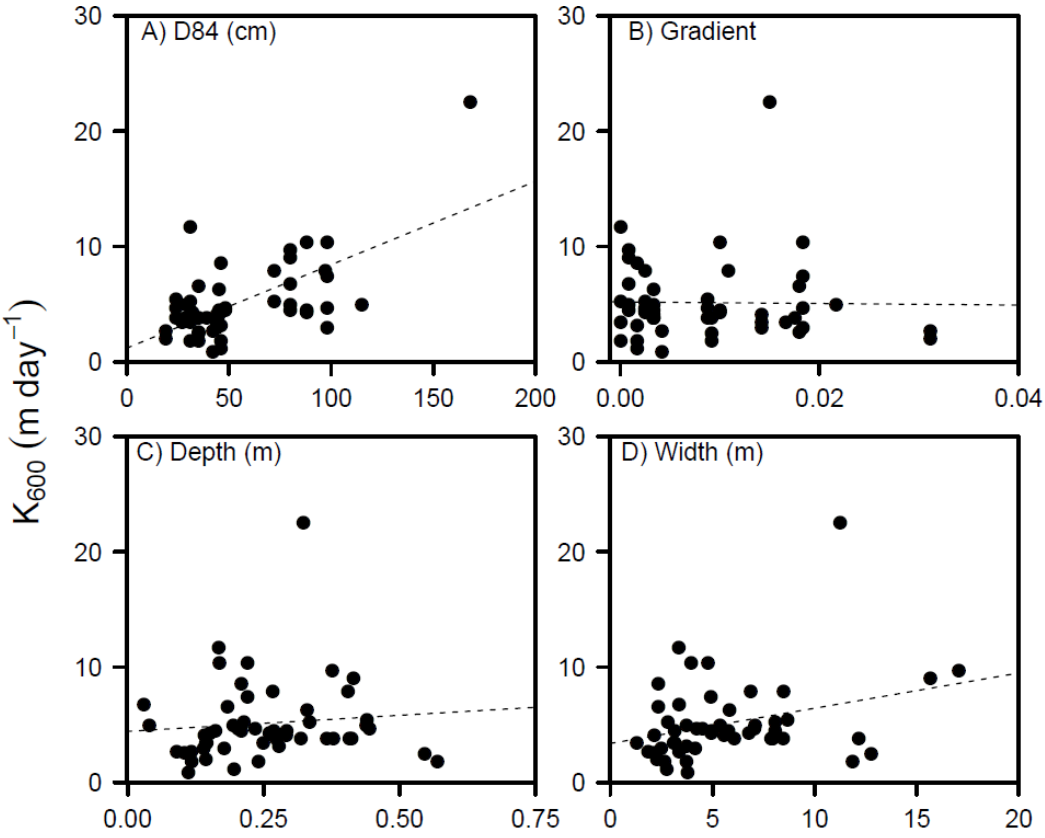

Table S1. Geomorphic characteristics measured or calculated for each sampled stream. Watershed slope, stream gradient, watershed area, and mean elevation were calculated from a 50-m resolution digital elevation map in ArcGIS. D84 (substrate size metric; 84th percentile of cumulative distribution of stream particle size) was calculated based on Wolman pebble counts within three reaches per stream as described in Lisi et al. [2013]. The latitude and longitude of each stream outlet are included in decimal degrees. Squaw creek flows into the Wood River, and Skunk Creek drains into Nushagak Bay.

Stream	Latitude	Longitude	Lake	Watershed slope (°)	Gradient (m/m)	Watershed area (km^2)	Substrate size (d84)	Elevation (m)
Allah	59.430	-158.659	Nerka	19.3	0.02583	9.5	134	278
Bear_n	59.470	-158.664	Nerka	2.3	0.00083	10.6	80	43
Belt	59.172	-158.546	NA	2.4	0.00250	23.4	27	48
Berm	59.599	-158.814	Nerka	17.6	0.01417	2.2	44	185
Chamee	59.544	-158.752	Nerka	2.3	0.01660	2.6	27	52
Cold lynx	59.500	-158.901	Nerka	17	0.01417	18.3	77	258
Cottonwood	59.623	-159.082	Nerka	28.6	0.05250	9.9	157	502
Eagle	59.317	-158.694	Aleknagik	7.3	0.00167	4.1	46	80
Elva	59.581	-159.055	Nerka	25.6	0.01500	31	168	358
Flyover	59.580	-158.910	Nerka	2.6	0.02750	NA	23	NA
Happy	59.323	-158.718	Aleknagik	12.5	0.00188	18	66	245
Hidden	59.540	-158.767	Nerka	14.1	0.01833	8.3	98	171
Hope	59.646	-158.599	Beverley	7.4	0.00875	36.7	24	159
Ice	59.332	-158.814	Aleknagik	11.2	0.00001	93.1	57	185
Kema	59.546	-158.656	Nerka	6	0.01167	20.4	41	115
Lynx	59.485	-158.920	Nerka	14.8	0.01083	25.6	97	199
Moose	59.639	-158.584	Beverley	4.3	0.00917	94.3	35	114
Pick	59.550	-159.064	Nerka	7.9	0.00333	20.1	29	101
Rainbow	59.665	-159.157	Nerka	25.9	0.00083	65.6	80	493
Sam	59.589	-158.895	Nerka	20.2	0.00750	10	84	358
Seventh	59.580	-158.914	Nerka	8	0.01794	2	35	116
Skunk	59.024	-158.534	NA	NA	0.00250	NA	NA	NA
Squaw	59.034	-158.517	NA	1.4	0.00417	8.3	30	32
Stovall	59.459	-158.635	Nerka	2.6	0.00333	30.8	45	58
Teal	59.482	-158.729	Nerka	7	0.00250	10.6	48	100
Uno	59.691	-158.755	Beverley	12.6	0.01750	17.5	39	219
Whitefish	59.266	-158.681	Aleknagik	2.9	0.00001	10.1	31	45

Yako	59.275	-158.708	Aleknagik	9.3	0.01000	13.3	88	175

Table S2. Isotopic measurements of stream DIC ($\Delta^{14}C$ and $\delta^{13}C$), collected in 2014 and 2015 before and after significant rain storms.

	2014				**2015**			
	Base Flow	**After Rain**	**Base Flow**	**After Rain**	**Base Flow**	**After Rain**	**Base Flow**	**After Rain**
Stream	**$\Delta^{14}C$ (‰)**		**$\delta^{13}C$ (‰)**		**$\Delta^{14}C$ (‰)**		**$\delta^{13}C$ (‰)**	
Allah					-50.7	-51.8	-3	-7.1
Bear_N	-13.4	-84.2	-9.4	-16.3	-14.2	3.8	-2.4	-17.6
Chamee	-37.2	8.1	-17.2	-21.5		-17.3		-12.6
Eagle					-8.1	-1.2	-7.5	-3.6
Flyover	-16.9	47.3	-15.3	-26.2	-9.0	31.8	-10.1	-18.9
Happy					-22.7	-6.2	-8.7	-6.9
Hidden	-13.5	6.2	-13.1	-12.6	-6.9	-50.5	-8	-3.8
Hope					-33.5	1.4	-10.1	-11.7
Kema					1.2		-14.1	
Moose					-16.2	-8.6	-9.7	-11.2
Pick	-69.7	-40.1	-13.6	-21.3	-86.3	-63.6	-10.8	-14
Sam	10.9	-14.8	-15.5	-17.9		4.6		-9.9
Seventh	10.3		-11.8					
Skunk	27.9		-15.4					
Stovall	-32.4	-17.2	-4.7	-11.9	-33.0	-5.2	-11.3	-15
Teal	-10.5	17.1	-10.2	-12.7				
Whitefish					-198.3	-193.7	-11.6	0.5
Yako					-49.9		-9	

Table S3. Isotopic measurements of stream invertebrates ($\Delta^{14}C$ and $\delta^{13}C$), collected between 2012 and 2014.

		Mayflies		Caddisflies	
Stream	**Collection Date**	**$\Delta^{14}C$ (‰)**	**$\delta^{13}C$ (‰)**	**$\Delta^{14}C$ (‰)**	**$\delta^{13}C$ (‰)**
Allah	6/15/2014	-30.1	-34.4	36.6	-30.7
Bear_N	6/13/2014	-1.1	-33.9	-7.5	-35.5
Cottonwood	7/11/2013	-13.0	-34.2	29.0	-24.2
Flyover	7/7/2013	NA	NA	25.9	-35.7
Hope	7/18/2013	7.2	-28.0	NA	NA
Hope	7/13/2014	10.2	-33.0	18.0	-38.2
Moose	7/13/2014	13.2	-38.3	20.7	-33.5
Pick	7/14/2013	-65.6	-42.9	NA	NA
Pick	6/16/2014	-52.4	-43.9	-1.4	-35.2
Sam	7/19/2012	37.5	-41.6	35.8	-31.2
Sam	6/20/2014	33.4	-37.7	37.3	-29.2
Seventh	7/1/2014	15.2	-38.5	21.8	-34.0
Squaw	7/16/2013	NA	NA	22.4	-39.3
Stovall	7/15/2012	NA	NA	30.9	-34.0
Stovall	6/15/2014	-24.6	-32.7	-2.2	-32.7
Teal	7/6/2014	15.8	-29.8	-2.9	-30.1

References

Alin, S. R., M. M. D. F. F. L. Rasera, C. I. Salimon, J. E. Richey, G. W. Holtgrieve, A. V. Krusche, and A. Snidvongs (2011), Physical controls on carbon dioxide transfer velocity and flux in low-gradient river systems and implications for regional carbon budgets, *J.*

Geophys. Res., *116*(G1), 17, doi:G01009 10.1029/2010jg001398.

Aravena, R., B. G. Warner, D. J. Charman, L. R. Belyea, S. P. Mathur, and H. Dinel (1993), Carbon isotopic composition of deep carbon gases in an ombrogenous peatland, northwestern Ontario, Canada, *Radiocarbon*, *35*(2), 271–276.

Bartz, K. K., and R. J. Naiman (2005), Effects of salmon-borne nutrients on riparian soils and vegetation in southwest Alaska, *Ecosystems*, *8*(5), 529–545, doi:10.1007/s10021-005-0064-z.

Bates, D., M. Maechler, B. Bolker, and S. Walker (2015), Fitting Linear Mixed-Effects Models Using lme4, *Journal of Statistical Software*, 67(1), 1-48.<doi:10.18637/jss.v067.i01>.

Billett, M. F., K. J. Dinsmore, R. P. Smart, M. H. Garnett, J. Holden, P. Chapman, A. J. Baird, R. Grayson, and A. W. Stott (2012), Variable source and age of different forms of carbon released from natural peatland pipes, *J. Geophys. Res. Biogeosciences*, *117*(2), 1–16, doi:10.1029/2011JG001807.

Billett, M. F., M. H. Garnett, and K. J. Dinsmore (2015), Should Aquatic CO2 Evasion be Included in Contemporary Carbon Budgets for Peatland Ecosystems?, *Ecosystems*, *18*(3), 471–480, doi:10.1007/s10021-014-9838-5.

Briner, J. P., and D. S. Kaufman (2008), Late pleistocene mountain glaciation in Alaska: key chronologies, *J. Quat. Sci.*, *23*(6), 659–670, doi:10.1002/jqs.

Burnham, K. P., and D. R. Anderson (2002), Avoiding pitfalls when using information- theoretic methods, *J. Wildl. Manage.*, *66*(3), 912–918.

Butman, D., and P. a. Raymond (2011), Significant efflux of carbon dioxide from streams and rivers in the United States, *Nat. Geosci.*, *4*(12), 839–842, doi:10.1038/ngeo1294.

Clark, I. and P. Fritz (1997), Environmental isotopes in hydrology, *Lewis Publishers*, Boca Raton.

Clymo, R. S., and C. L. Bryant (2008), Diffusion and mass flow of dissolved carbon dioxide, methane, and dissolved organic carbon in a 7-m deep raised peat bog, *Geochim. Cosmochim. Acta*, *72*(8), 2048–2066, doi:10.1016/j.gca.2008.01.032.

Cole, J. J., and N. F. Caraco (2001), Carbon in catchments: connecting terrestrial carbon losses with aquatic metabolism, *Mar. Freshw. Res.*, *52*, 101–110.

Cole, J. J., N. F. Caraco, G. W. Kling, and T. K. Kratz (1994), Carbon dioxide supersaturation in the surface waters of lakes, *Science (80-.).*, *265*, 1568–1570.

Coyne, P. I., and J. J. Kelley (1974), Carbon-Dioxide Partial Pressures in Arctic Surface Waters, *Limnol. Oceanogr.*, *19*(6), 928–938.

Crawford, J. T., R. G. Striegl, K. P. Wickland, M. M. Dornblaser, and E. H. Stanley (2013), Emissions of carbon dioxide and methane from a headwater stream network of interior Alaska, *J. Geophys. Res. Biogeosciences*, *118*(2), 482–494, doi:10.1002/jgrg.20034.

Deines, P (1980), The isotopic composition of reduced organic carbon, *Handbook of environmental isotope geochemistry*, 329-406.

Doctor, D. H., C. Kendall, S. D. Sebestyen, J. B. Schanley, N. Ohte, and E. W. Boyer (2008), Carbon isotope fractionation of dissolved inorganic carbon (DIC) due to outgassing of carbon dioxide from a headwater stream, *Hydrol. Process.*, *22*, 2410–2423.

Fellman, J. B., E. Hood, P. A. Raymond, J. Hudson, M. Bozeman, and M. Arimitsu (2015), Evidence for the assimilation of ancient glacier organic carbon in a proglacial stream food web, *Limnol. Oceanogr.*, *60*(4), 1118–1128, doi:10.1002/lno.10088.

Finlay, J. C. (2003), Controls of streamwater dissolved inorganic carbon dynamics in a forested

watershed, *Biogeochemistry*, *62*(3), 231–252.

Frey, K. E., and L. C. Smith (2005), Amplified carbon release from vast West Siberian peatlands by 2100, *Geophys. Res. Lett.*, *32*(9), 1–4, doi:10.1029/2004GL022025.

Garnett, M. H., K. J. Dinsmore, and M. F. Billett (2012), Annual variability in the radiocarbon age and source of dissolved CO 2 in a peatland stream, *Sci. Total Environ.*, *427–428*, 277–285, doi:10.1016/j.scitotenv.2012.03.087.

Giesler, R., C.-M. Mörth, J. Karlsson, E. J. Lundin, S. W. Lyon, and C. Humborg (2013), Spatiotemporal variations of p CO 2 and δ 13 C-DIC in subarctic streams in northern Sweden, *Global Biogeochem. Cycles*, *27*(1), 176–186, doi:10.1002/gbc.20024.

Holtgrieve, G. W., and D. E. Schindler (2011), Marine-derived nutrients, bioturbation, and ecosystem metabolism: reconsidering the role of salmon in streams., *Ecology*, *92*(2), 373–85.

Holtgrieve, G. W., D. E. Schindler, T. a. Branch, and Z. T. A'mar (2010), Simultaneous quantification of aquatic ecosystem metabolism and reaeration using a Bayesian statistical model of oxygen dynamics, *Limnol. Oceanogr.*, *55*(3), 1047–1062, doi:10.4319/lo.2010.55.3.1047.

Hope, D., S. M. Palmer, M. F. Billett, and J. J. C. Dawson (2004), Variations in dissolved CO2 and CH4 in a first-order stream and catchment: An investigation of soil-stream linkages, *Hydrol. Process.*, *18*(17), 3255–3275, doi:10.1002/hyp.5657.

Hua, Q., M. Barbetti, and A. Z. Rakowski (2013), Atmospheric radiocarbon for the period 1950-2010, *Radiocarbon*, *55*(4), 2059–2072, doi:10.2458/azu_js_rc.v55i2.16177.

Humborg, C., C.-M. Mörth, M. Sundbom, H. Borg, T. Blenckner, R. Giesler, and V. Ittekkot (2010), CO2 supersaturation along the aquatic conduit in Swedish watersheds as

constrained by terrestrial respiration, aquatic respiration and weathering, *Glob. Chang. Biol.*, *16*(7), 1966–1978, doi:10.1111/j.1365-2486.2009.02092.x.

Ishikawa, N. F., F. Hyodo, and I. Tayasu (2013), Use of carbon-13 and carbon-14 natural abundances for stream food web studies, *Ecol. Res.*, *28*(5), 759–769, doi:10.1007/s11284-012-1003-z.

Jankowski, K., D. E. Schindler, and P. J. Lisi (2014), Temperature sensitivity of community respiration rates in streams is associated with watershed geomorphic features, *Ecology*, *95*(10), 2707–2714.

Junk, W. J., P. B. Bayley, and R. E. Sparks (1989), The flood pulse concept in river-floodplain systems, in *Proceedings of the Internation Large River Symposium*, pp. 110–127.

Kling, G. W., G. W. Kipphut, and M. C. Miller (1991), Arctic lakes and streams as gas conduits to the atmosphere: implications for tundra carbon budgets., *Science (80-.).*, *251*(4991), 298–301, doi:10.1126/science.251.4991.298.

Laudon, H., M. Berggren, A. Agren, I. Buffam, K. Bishop, T. Grabs, M. Jansson, and S. Kohler (2011), Patterns and Dynamics of Dissolved Organic Carbon (DOC) in Boreal Streams: The Role of Processes, Connectivity, and Scaling, *Ecosystems*, *14*(6), 880–893, doi:10.1007/s10021-011-9452-8.

Leach, J. A., A. Larsson, M. B. Wallin, M. B. Nilsson, and H. Laudon (2016), Twelve-year interannual and seasonal variability of stream carbon export from a boreal peatland catchment, *J. Geophys. Res. Biogeosciences*, *121*, 1851–1866, doi:10.1002/2016JG003357.

Leith, F. I., M. H. Garnett, K. J. Dinsmore, M. F. Billett, and K. V. Heal (2014), Source and age of dissolved and gaseous carbon in a peatland-riparian-stream continuum: A dual isotope (14C and d13C) analysis, *Biogeochemistry*, *119*(1–3), 415–433, doi:10.1007/s10533-014-

9977-y.

Leopold, L. B., M. G. Wolman and J. P. Miller (1995), Fluvial processes in geomorphology, Dover Publications.

Lewis, E., and D. W. R. Wallace (1998), Program Developed for CO2 System Calculations, ORNL/CDIAC-105, Carbon Dioxide Information Analysis Center, Oak Ridge National Laboratory, U.S. Department of Energy, Oak Ridge,Tennessee.

Lisi, P. J., D. E. Schindler, K. T. Bentley, and G. R. Pess (2013), Association between geomorphic attributes of watersheds, water temperature, and salmon spawn timing in Alaskan streams, *Geomorphology*, *185*, 78–86, doi:10.1016/j.geomorph.2012.12.013.

McGuire, a. D., L. G. Anderson, T. R. Christensen, S. Dallimore, L. Guo, D. J. Hayes, M. Heimann, T. D. Lorenson, R. W. Macdonald, and N. Roulet (2009), Sensitivity of the carbon cycle in the Arctic to climate change, *Ecol. Monogr.*, *79*(4), 523–555, doi:10.1890/08-2025.1.

Olefeldt, D., N. Roulet, R. Giesler, and A. Persson (2013), Total waterborne carbon export and DOC composition from ten nested subarctic peatland catchments-importance of peatland cover, groundwater influence, and inter-annual variability of precipitation patterns, *Hydrol. Process.*, *27*(16), 2280–2294, doi:10.1002/hyp.9358.

Quay, P. D., D. O. Wilbur, J. E. Richey, J. I. Hedges, and A. H. Devol (1992), Carbon cycling in the Amazon River: implications from the d13C compositions of particles and solutes, *Limnol. Oceanogr.*, *37*(4), 857–871.

Raymond, P. A., J. W. McClelland, R. M. Holmes, A. V. Zhulidov, K. Mull, B. J. Peterson, R. G. Striegl, G. R. Aiken, and T. Y. Gurtovaya (2007), Flux and age of dissolved organic carbon exported to the Arctic Ocean: A carbon isotopic study of the five largest arctic

rivers, *Global Biogeochem. Cycles*, *21*(4), n/a-n/a, doi:10.1029/2007GB002934.

Raymond, P. A., C. J. Zappa, D. Butman, T. L. Bott, J. Potter, P. Mulholland, A. E. Laursen, W. H. McDowell, and D. Newbold (2012), Scaling the gas transfer velocity and hydraulic geometry in streams and small rivers, *Limnol. Oceanogr. Fluids Environ.*, *2*(0), 41–53, doi:10.1215/21573689-1597669.

Raymond, P. A., and J. E. Saiers (2010), Event controlled DOC export from forested watersheds, *Biogeochemistry*, *100*(1), 197–209, doi:10.1007/s10533-010-9416-7.

Raymond, P. A., J. E. Saiers, and W. V. Sobczak (2016), Hydrological and biogeochemical controls on watershed dissolved organic matter transport: pulse-shunt concept, *Ecology*, *97*(1), 5–16, doi:10.1890/07-1861.1.

R Core Team (2016), R: A language and environment for statistical computing, R Foundation for Statistical Computing, Vienna, Austria, ISBN 3-900051-07-0, URL http://www.R-project.org/.

Richey, J. E., J. M. Melack, A. K. Aufdenkampe, V. M. Ballester, and L. L. Hess (2002), Outgassing from Amazonian rivers and wetlands as a large tropical source of atmospheric CO2., *Nature*, *416*(6881), 617–20, doi:10.1038/416617a.

Schelker, J., G. A. Singer, A. J. Ulseth, S. Hengsberger, and T. J. Battin (2016), CO2 evasion from a steep, high gradient stream network: Importance of seasonal and diurnal variation in aquatic pCO2 and gas transfer, *Limnol. Oceanogr.*, *2*, 1826–1838, doi:10.1002/lno.10339.

Schindler, D. W., D. R. Lean and E. J. Fee (1975), Nutrient cycling in freshwater ecosystems. National Academy of Sciences, Washington, DC.

Schuur, E. a. G. et al. (2015), Climate change and the permafrost carbon feedback, *Nature*,

520(7546), 171–179, doi:10.1038/nature14338.

Smits, A. P., D. E. Schindler, and M. T. Brett (2015), Geomorphology controls the trophic base of stream food webs in a boreal watershed, *Ecology*, *96*(7), 1775–1782.

Steinmann, P., B. Eilrich, M. Leuenberger, and S. J. Burns (2008), Stable carbon isotope composition and concentrations of CO2 and CH4 in the deep catotelm of a peat bog, *Geochim. Cosmochim. Acta*, *72*(24), 6015–6026, doi:10.1016/j.gca.2008.09.024.

Striegl, R. G., M. M. Dornblaser, C. P. McDonald, J. R. Rover, and E. G. Stets (2012), Carbon dioxide and methane emissions from the Yukon River system, *Global Biogeochem. Cycles*, *26*(4), doi:10.1029/2012GB004306.

Stuiver, M., and H. A. Polach (1977), Reporting of 14C data, *Radiocarbon*, *19*(3), 355–363.

Teodoru, C. R., P. a. Del Giorgio, Y. T. Prairie, and M. Camire (2009), Patterns in pCO2 in boreal streams and rivers of northern Quebec, Canada, *Global Biogeochem. Cycles*, *23*(2), 1–11, doi:10.1029/2008GB003404.

Trumbore, S. E., and J. W. Harden (1997), Accumulation and turnover of carbon in organic and mineral soils of the BOREAS northern study area, *J. Geophys. Res.*, *102*, 28817–28830.

Vannote, R. L., G. W. Minshall, K. W. Cummins, J. R. Sedell, and C. E. Cushing (1980), The river continuum concept, *Can. J. Fish. Aquat. Sci.*, *37*, 130–137.

Wallin, M. B., M. G. Öquist, I. Buffam, M. F. Billett, J. Nisell, and K. H. Bishop (2011), Spatiotemporal variability of the gas transfer coefficient (KCO2) in boreal streams: Implications for large scale estimates of CO2 evasion, *Global Biogeochem. Cycles*, *25*(3), 1–14, doi:10.1029/2010GB003975.

Wallin, M. B., T. Grabs, I. Buffam, H. Laudon, A. Ågren, M. G. Öquist, and K. Bishop (2013), Evasion of CO2 from streams - The dominant component of the carbon export through the

aquatic conduit in a boreal landscape, *Glob. Chang. Biol.*, *19*(3), 785–797, doi:10.1111/gcb.12083.

Wanninkhof, R. (1992), Relationship between wind speed and gas exchange over the ocean, *J. Geophys. Res.*, *97*(92), 7373–7382, doi:10.1029/92JC00188.

Weiss, R. F. (1974), Carbon dioxide in water and seawater: the solubility of a non-ideal gas, *Mar. Chem.*, *2*, 203–215.

Whiticar, M. J., E. Faber, and M. Schoell (1986), Biogenic methane formation in marine and freshwater environments: CO2 reduction vs acetate fermentation - isotope evidence, *Geochim. Cosmochim. Acta*, *50*(5), 693–709, doi:10.1016/0016-7037(86)90346-7.

Zappa, C. J., W. R. McGillis, P. A. Raymond, J. B. Edson, E. J. Hintsa, H. J. Zemmelink, J. W. H. Dacey, and D. T. Ho (2007), Environmental turbulent mixing controls on air-water gas exchange in marine and aquatic systems, *Geophys. Res. Lett.*, *34*(10), 1–6, doi:10.1029/2006GL028790.

Zuur, A., E. N. Ieno, N. Walker, A. A. Saveliev, and G. M. Smith (2009), Mixed effects models and extensions in ecology with R, *Springer Science & Business Media.*

APPENDIX 1. ACKNOWLEDGEMENTS AND COLLABORATORS

Chapter 2:

Co-authors: Daniel E. Schindler, Michael T. Brett

This research was funded by the National Science Foundation and the Harriett Bullitt Professorship. APS was supported by an NSF GRFP. This project is a contribution of the Alaska Salmon Program at University of Washington. We thank M. Conseur, S. Clark and L. Ciepiela for help with sample collection in the field. S. Yeung provided assistance and advice with fatty acid analysis. D. Terracin and C. McCarty prepared samples for analysis.

Chapter 3:

Co-authors: Daniel E. Schindler, Jonathan B. Armstrong, Michael T. Brett, Jackie L. Carter, Bianca S. Santos

Funding for this research was provided by the Gordon and Betty Moore Foundation, the National Science Foundation – CNH program, and the Landscape Conservation Cooperative of Western Alaska. APS was supported by an NSF graduate research fellowship. This research is a contribution of the Alaska Salmon Program at University of Washington. We thank J. Ching and many others for assistance in the field, and S. Yeung for help with chemical methods.

Chapter 4:

Co-authors: Daniel E. Schindler, Gordon W. Holtgrieve, KathiJo Jankowski

This research was funded by the National Science Foundation and the Harriett Bullitt Professorship. A. P. Smits was supported by an NSF GRFP. This project is a contribution of the Alaska Salmon Program at the University of Washington. We thank D. Yiu, J. Carter, J. Ching,

B. Smith, and L. Smith for help with sample collection in the field. A. T. Ellis helped prepare samples for isotopic analysis. We thank P. Quay for access to laboratory equipment, and J. Stutsman for advice and assistance with DIC extractions. We thank Dr. U. Zoppi (in memorium) for radiocarbon analysis of our samples, D. Butman for helpful discussions on gas transfer velocity and carbon isotopes, and D. French for making the map figure.